Hydrodynamic Model Development Report: Sacramento-San Joaquin River Delta and Suisun Bay (Water Year 2016)

A. King, Z. Zhang, & D. Senn
San Francisco Estuary Institute

December 13, 2019

SFEI Contribution #964

Acknowledgements

The work presented in this report received support from several sources, carried out as part of a broader, multi-year cooperatively funded project related to Delta-Suisun numerical model development and application. Funding for the bulk of the hydrodynamic model development work came primarily from the State Water Board (secured by Central Valley and San Francisco Bay Regional Water Quality Control Boards); the Delta Regional Monitoring Program; and the San Francisco Bay Nutrient Management Strategy. Other funding sources supported model development at earlier stages, including capacity-building that directly contributed to this project (e.g., initial work on database building): Delta Science Program; Regional San; Central Contra Costa Sanitation District; and San Francisco Bay Nutrient Management Strategy. Throughout this project, we received generous technical support from L. Lucas (USGS), N. Knowles (USGS), M. van der Wegen (Deltares, UNESCO-IHE), and K. Nederhoff (Deltares-USA). Thanks to J. Cook and M. Howard (CVRWQCB) for project management and collaboration on aligning management goals and science/model-development goals; and to M. Heberger (SFEI; DRMP) and J. Hunt (SFEI) for project/financial/contract management.

Multiple regulators and stakeholders generously contributed time for planning, prioritization, and project update meetings for the broader Delta-Suisun model development work: L. Thompson (Regional San), L. Schechtel (CCCSD), J. Cook (CVRWQCB), D. Stern (DSP), M. Esparza, L. Smith (MWD), and M. Howard (CVRWQCB)

1 Introduction

This report describes work related to hydrodynamic model development for the San Francisco Bay-Delta Estuary, undertaken as part of a broader effort to develop and apply coupled biogeochemical-hydrodynamic models to inform nutrient management decisions. The primary intended application of the hydrodynamic model output is for use as input to an offline-coupled biogeochemical model to simulate a wide range of state variables and processes, including: advective and dispersive transport, nutrient transformations, phytoplankton production, benthic and pelagic grazing, sediment diagenesis, and oxygen cycling.

The project's primary goals included:

- Simulate hydrodynamics, salinity, and temperature for Water Year 2016 (WY2016) by updating/refining an existing public-domain/open-source Bay-Delta hydrodynamic model (Martyr-Koller et al., 2017; Vroom et al., 2017), including:
  - build boundary condition (e.g., tides, freshwater flows) and external forcing datasets (e.g., wind, other meteorological data);
  - refine representation of gate operations and other water management forcings.
- Validate WY2016 hydrodynamic model output by comparing model predictions with field observations for discharge, water elevation, salinity, and temperature.
- Pursue the above concrete goals in ways that build capacity for simulating and validating additional water years, including flexible or generalizable utilities (e.g., scripts) and data resources that allow for efficient model set-up/launch and analysis/validation of model output.

Section 2 describes model set-up, including the origin of the starting model, model platform and performance, grid, boundary conditions, initial conditions, structures and model parameters. Section 3 discusses the development of the database that supports model set-up and validation for both hydrodynamic and biogeochemical models. Section 4 covers the model results, including validation statistics and a discussion of model performance. Finally, in Section 5 we discuss potential next steps to improve hydrodynamic model performance.

2 Model Setup

2.1 Background

This work builds on the CASCaDE (USGS, 2018) and San Francisco Bay-Delta Community Model (Community Model, 2019) projects. The three-dimensional hydrodynamic model of the San Francisco Bay and Sacramento-San Joaquin River Delta developed by Martyr-Koller et al. (2017) and Vroom et al. (2017) for WY2011 and WY2012 as part of CASCaDE II serves as the basis for SFEI's biogeochemical model of the same system. The biogeochemical model was applied to WY2011, and results were presented at the March 2019 Delta-Suisun modeling progress update to the California Water Board Region 5. The hydrodynamic model is built on Delft3D-FM (DFM), and the biogeochemical model is built on Delta Water Quality (DWAQ) – both of these are open-source modeling platforms developed and maintained by Deltares of the Netherlands. WY2011 was a relatively wet year, and to develop a model capable of handling a wider range of hydrological forcing, it was decided to extend the model to WY2016, a year with more moderate inflows. This report describes extension of the DFM hydrodynamic model to WY2016. We have developed the model set-up scripts, validation scripts, and supporting database so that application of the hydrodynamic model to additional water years, between WY2000 and present, is fairly straightforward – at this point, each additional water year should take only a couple of weeks to set up and validate.

2.2 Model Platform and Performance

The hydrodynamic model platform is Delft3D-FM (DFM), the flexible-mesh three-dimensional hydrodynamic model from Deltares. The model revision number used for these simulations is 64634, and the model is compiled from source code using GCC on a Linux workstation running Ubuntu 16.04LTS. The simulation is run in parallel using 16 cores (Intel Xeon E5-2680 2.40 GHz) communicating over MPI. The simulation is initialized on August 1, 2015 and run through September 30, 2016, spanning water year 2016 (WY2016: October 1, 2015 through September 30, 2016) with two months of spin-up time and requires four days to run to completion.

2.3 Bathymetry and Model Grid

Our grid is the CASCaDE II model grid, version r18cee. This grid is identical to the one used in Martyr-Koller et al. (2017) and Vroom et al. (2017) with one exception: the ocean boundary has been straightened in order to eliminate a spurious plume that emanated from the curvy boundary in the original grid. The new grid is plotted in Figures 1 and 2.

2.4 Boundary Conditions

Boundary conditions are specified for the tidal ocean boundary, tributary inflows, withdrawals (i.e., pumps), the wind field, and surface heat exchange. Figure 4 shows the loca-

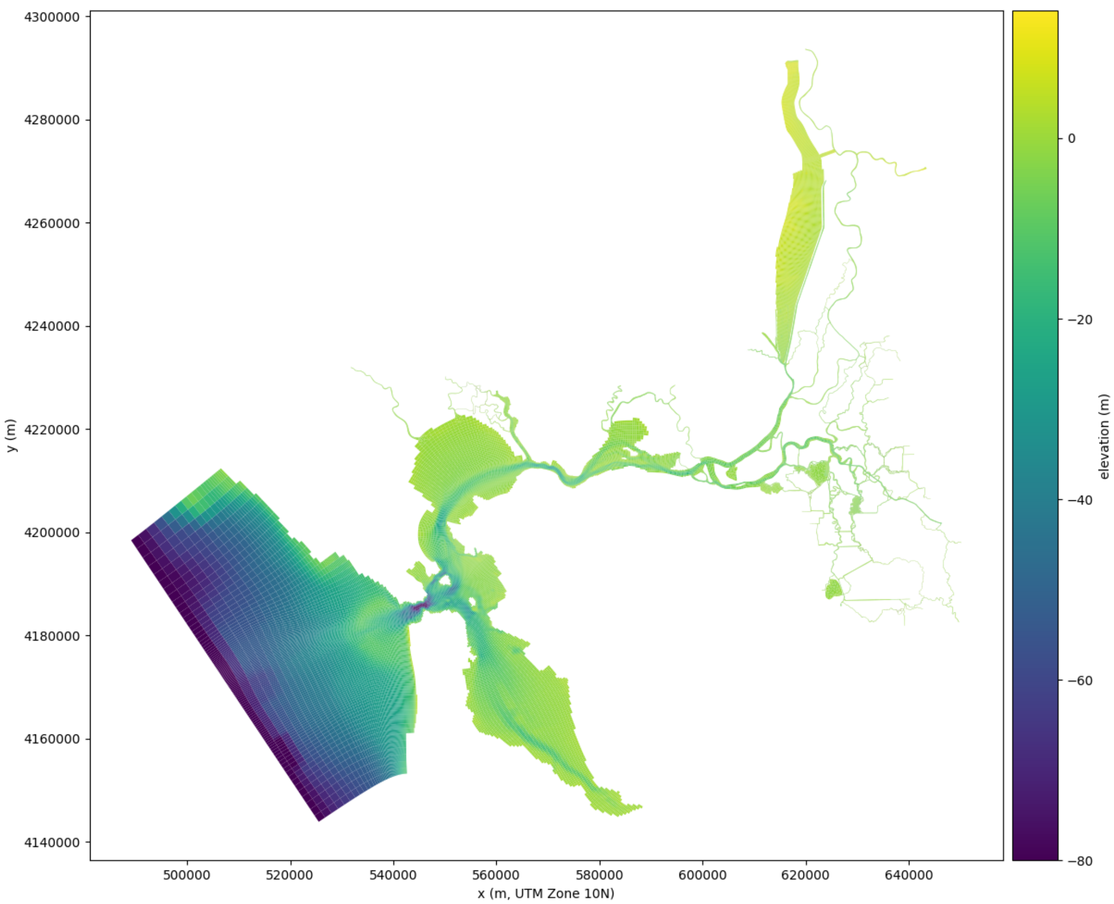

Figure 1: Model grid. Elevations are relative to MLLW.

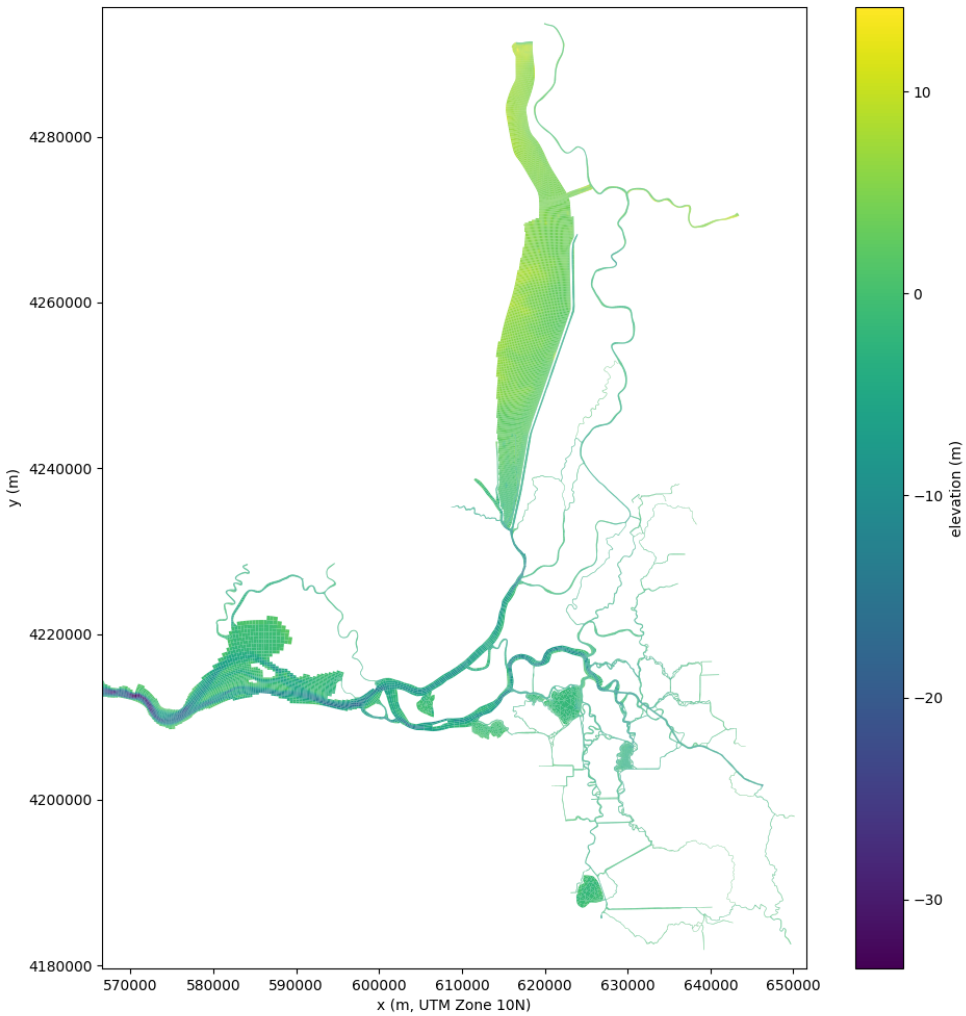

Figure 2: Delta-Suisun portion of the model grid. Elevations are relative to MLLW.

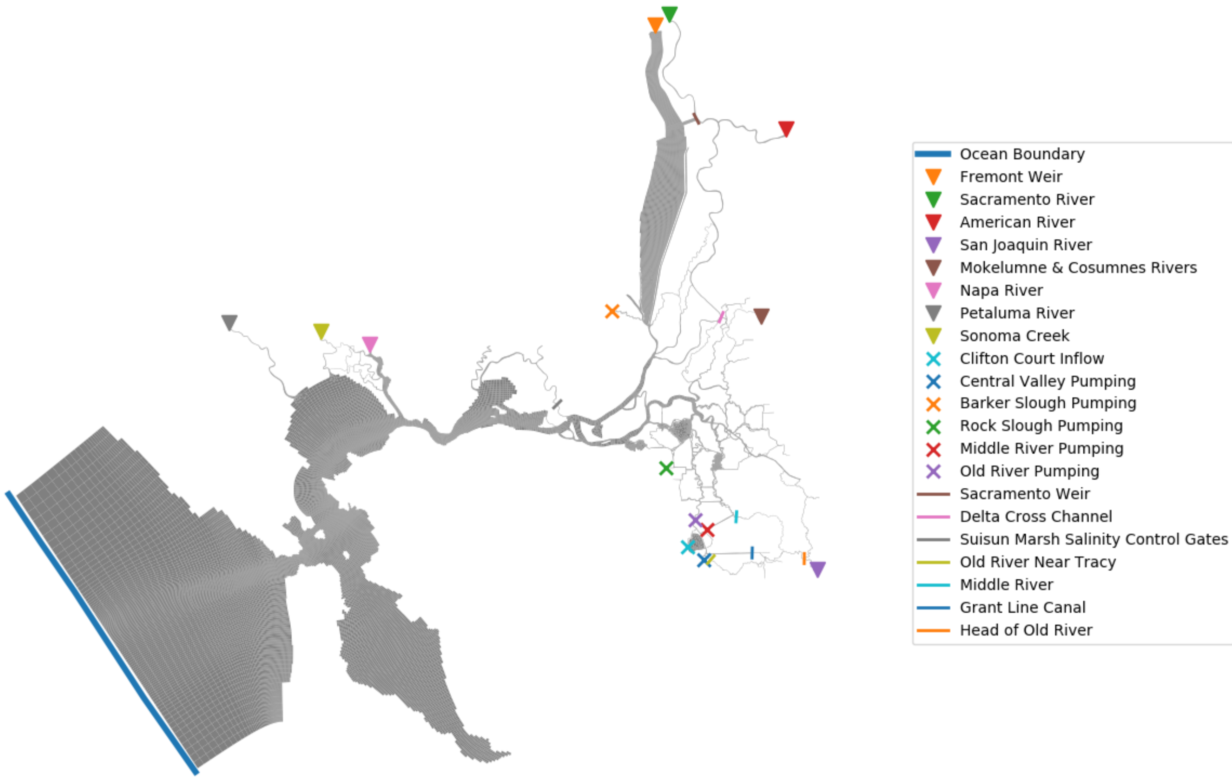

Figure 3: Boundary conditions and structures. The water surface elevation boundary at the ocean is plotted as a thick line; inflow boundaries are plotted as downward-pointing triangles; withdrawals are plotted with an "x"; gates and temporary barriers are plotted as thin lines.

tions of the ocean boundary, tributary inflows, and withdrawals (also showing the locations of structures discussed in Section 2.6).

2.4.1 Tidal Ocean Boundary

Water level, salinity, temperature, and momentum are specified at the ocean boundary. The location of the ocean boundary is shown in Figure 4. Water levels are based on hourly mesurements at NOAA CO-OPS Station 9415020 (Point Reyes). Salinity is based on daily measurements at the Farallon Islands Shore Stations Program (2019). Temperature is based on a data set derived from ROMS simulations and assimilated measurements along the California Coast (Neveu et al., 2016) as described in Vroom et al. (2017). Simulated temperatures were averaged on a daily basis over the period 1980-2010 to arrive at a temperature time history exhibiting typical seasonal patterns and appropriate for use in any water year. A zero-momentum boundary condition is imposed at the ocean boundary to suppress spurious currents.

2.4.2 Inflows

Locations of the inflow boundaries are shown in Figure 4 and data sources are given in Table 1. Flow rate, salinity, and temperature are specified at 15-minute intervals. While most inflows are based on gaged discharge, some inflow temperatures are not measured near the boundary, so temperature from a nearby tributary is used as a proxy. The only inflow for which nearby salinity measurements are available is the San Joaquin River – salinity is set to zero at all of the other inflow boundaries.

Table 1: Inflow boundary conditions. Prefix of model input files associated with each boundary condition is given in parentheses. Source of data for inflow, temperautre, and salinity is given by station code or 0 where value is set to zero. Station codes are defined in Table 3.

Inflow Boundary	Parameter	Data Source
Fremont Weir (fremontweir)	inflow temperature salinity	YBY (CCY when YBY <1000 m^3/s) VON 0
Sacramento River (sacverona)	inflow temperature salinity	VON VON 0
American River (amriv)	inflow temperature salinity	AFO AWB 0
San Joaquin River (sanjoa)	inflow temperature salinity	VNS MSD MSD
Mokelumne & Consumnes Rivers (mok)	inflow temperature salinity	MOKW + MHB SMR (gaps filled with VON) 0
Napa River (napa)	inflow temperature salinity	NAP VON 0
Petaluma River (pet)	inflow temperature salinity	PETA VON 0
Sonoma Creek (sonoma)	inflow temperature salinity	AGUA VON 0

2.4.3 Withdrawals

Five pumping stations are included in the model as withdrawals as illustrated in Figure 4. Daily average pumping rates were either obtained from DAYFLOW or from correspondence with Stacy Smith at United States Bureau of Reclamation. Data sources are specified in Table 2. Smith provided QA/QC'd daily data corresponding to the CDEC stations listed in Table 2.

Table 2: Withdrawals. Prefix of model input files associated with each withdrawal is given in parentheses.

Withdrawal	Data Source
Clifton Court Inflow (CC)	DAYFLOW–SWP
Central Valley Pumping (tracy)	DAYFLOW–CVP
Barker Slough Pumping (nbaq)	DAYFLOW–NBAQ
Rock Slough Pumping (rock)	CDEC/USBR–INB
Middle River Pumping (ccwd)	CDEC/USBR–CCW
Old River Pumping (idbpump)	CDEC/USBR–IDB

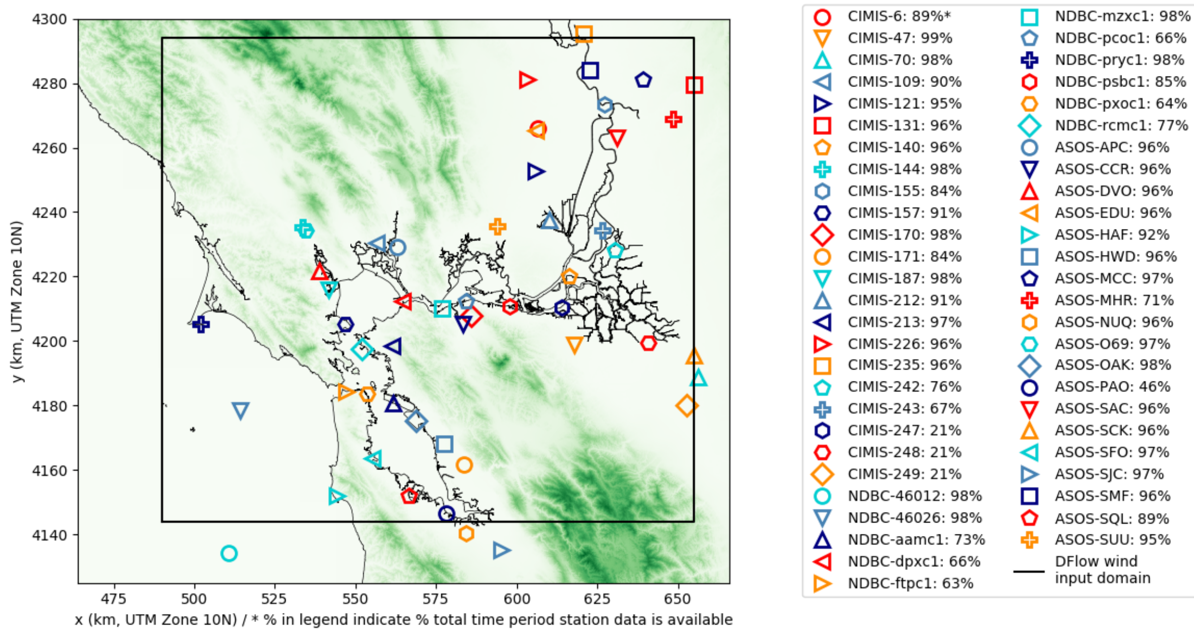

Figure 4: Locations of 52 wind stations used to interpolate 10-m wind speeds onto the 1.5 km $\times$ 1.5 km grid. Extent of the grid is plotted as a black box. Percentage of WY2016 in which wind speeds were available from each station is shown in the legend.

2.4.4 Wind Field

Wind stress over the water surface is calculated within DFlow3D-FM from 10-m wind speeds, which we specify hourly on a 1.5 km $\times$ 1.5 km grid spanning the Bay and Delta. The CASCaDE II project utilized the Ludwig wind model (Ludwig et al., 1991; Ludwig and Sinton, 2000) to generate these 10-m winds. We have instead used the SFEI_Wind package documented in King (2019). SFEI_Wind interpolates winds measured at 52 stations around the Bay and Delta and improves predictions of wind speed by $\sim$ 30% compared to the Ludwig model.

2.4.5 Surface Heat Exchange

The heat flux model within DFlow3D-FM calculates heat exchange from relative humidity, air temperature, and cloudiness. For our model, these quantities are specified hourly on a 5 km $\times$ 5 km grid. Vroom et al. (2017) used the gridMET/METDATA reanalysis product (Abatzoglou, 2011) and the Livneh temperature data set (Livneh et al., 2015) to estimate these quantities. We also use the gridMET data set, but since the Livneh data set ends in 2013, we instead used air temperatures measured at the 52 wind stations in the SFEI_Wind package. gridMET gives daily average specific humidity and solar radiation at the earth surface across the contiguous United States. gridMET and air temperature data are interpolated onto the 5 km × 5 km grid using the natural neighbor method.

To estimate cloudiness (C) from solar radiation (Q), we invert the formula used in Delft3D-FM to compute solar radiation from cloudiness, arriving at:

$$C = \frac{-0.4 + \sqrt{1.68 - 1.52\frac{Q_s}{Q_{cs}}}}{0.76} \times 100\% \tag{1}$$

where Q_{cs} is clear sky solar radiation. Q_{cs} is calculated following the Delft3D-FM User Manual (Deltares, 2019, Section 11.2). We compute relative humidity (RH) from specific humidity (q) and air temperature (T_a) using the formula

$$RH = 0.263\, P_{atm}\, q \exp\left(-\frac{17.67\, T_a}{T_a + 243.5}\right) \tag{2}$$

where atmospheric pressure is set to $P_{atm} = 101300$ Pa. Relative humidity is bounded to the range $0\% \leq RH \leq 100\%$. Note our formula for cloudiness is different from the Vroom et al. (2017) formula for cloudiness, which was incorrect.

2.5 Initial Conditions

Initial conditions are identical to those described in Martyr-Koller et al. (2017). Spatially varying top and bottom salinity are specified based on historical measurements, and temperatures are initialized at 15^oC.

2.6 Structures

2.6.1 Permanent Structures

Three permanent structures are included in the model: Sacramento Weir, Delta Cross Channel, and the Suisun Marsh Salinity Control Gates. Locations of these structures are shown in Figure 4. These structures are implemented as "damlevel"'s within DFlow3D-FM. A thin dam spans the width of the channel, and its height is specified as a function of time. When the structure is open, the dam height is set to the minimum elevation along the open structure. When the structure is closed, the dam height is set to a level comfortably higher than the water level.

The damlevel implementation is not ideal as it will result in incorrect transient behavior, but provided the dam height when open is equal to the lowest point along the open structure, the steady-state solution will be correct. In future versions of the model, implementation of the permaent structures may be improved by use of the “general structure” in DFlow3D-FM, which would allow us to tune the hydraulic behavior to a rating curve.

For Sacramento Weir and Delta Cross Channel, it is possible to see if the weir/gates are open by observing discharge measurements downstream of the structure (station SWTY for Sacramento Weir and station DLC for Delta Cross Channel). When discharge measurements are available, the structure is set to the open position, and when discharge measurements are not available, the structure is set to the closed position.

For Suisun Gates, operations are more complicated. When in operation, the gates are used as a salinity pump – they are closed on flood tide and openend on ebb tide (Enright, 2008), allowing fresh water into Montezuma Slough and blocking salty water from entering. The operations log for the gates is published online by CA Department of Water Resources: each of the three gates is listed as either “open”, “closed”, or “operational” on a given date. Additionally the stop logs may be “in” or “out”. However, when the gates are operational, the details of the operations are not given. In order to simulate operations during operational periods, we use the gage height measured at station CSE (Collinsville), near the entrance to Montezuma Slough, removing the tidally filtered signal to obtain the tidal residual gage height. The gates are opened when the tidal residual gage height is negative and closed when tidal residual gage height is positive. Since high tide and flood tide are correlated at CSE, this effectively closes the gates on flood tide and opens the gates on ebb tide. N. Knowles and L. Lucas of USGS are credited with developing this scheme.

2.6.2 Temporary Barriers

In addition to the permanent structures, there are four temporary barriers included in the model. These are shown in Figure 4. The temporary barriers are implemented by CA Department of Water Resources and their operating schedule is published online. The barriers are a mix of permanent structures and piles of rocks that are moved between the channel and shore seasonally. Like the permanent structures, the temporary barriers are implemented as “damlevel”’s in Delft3D-FM, with the open height set to the lowest point along the strucutre at a given time. As there are a mix of flashboard structures, culverts, and gaps in the piles of rocks, this elevation changes with the specifics of operations. Engineering drawings (CA Department of Water Resources, 2018) were used to evaluate elevations corresponding to different operational states, with input from Jacob McQuirk (DWR).

2.7 Bed Friction

The main result of the CASCaDE II WY2011-WY2012 calibration conducted by Martyr-Koller et al. (2017) was a spatially varying Manning coefficient used as input to the Delft3D-FM model. The calibration period was March 1, 2000 through September 30, 2000. By decreasing the Manning coefficient in the main channel, Martyr-Koller et al. (2017) was able to better predict vertical salinity stratification in Suisun Bay, San Pablo Bay, and Central Bay. A map of the spatially varying Manning coefficient can be found in Martyr-Koller et al. (2017, Figure A.10).

3 Building Observation Database for Model Set-up and Validation

In the Delta and San Francisco Bay there are more than 80 stations where continuous high-frequency (15 min to 1 hour) data are collected by various organizations including United States Geological Survey (USGS), California Department of Water Resources (DWR), National Oceanic and Atmospheric Administration (NOAA), and United States Bureau of Reclamation (USBR). Parameters measured at these sites include those relevant to hydrodynamics (e.g., discharge, gage height, temperature, and conductivity/salinity) as well as water quality parameters (e.g., dissolved oxygen, nitrate and nitrite, pH, turbidity/specific conductivity, and fluorescence from chlorophyll, pyhcocyanin, and dissolved organic matter). These abundant data resources are useful for model development, but utilizing all of these data comes with significant data management overhead. To streamline the data management process, we incorporated hydrodynamic and water quality data from USGS and DWR into a SQL database. Continuous data were originally loaded into the database in a batch from 2000 through mid-2018 and subsequently have been automatically updated nightly. In Table 3 we list stations where hydrodynamic parameters are measured. The station locations are shown in Figures 5 and 6.

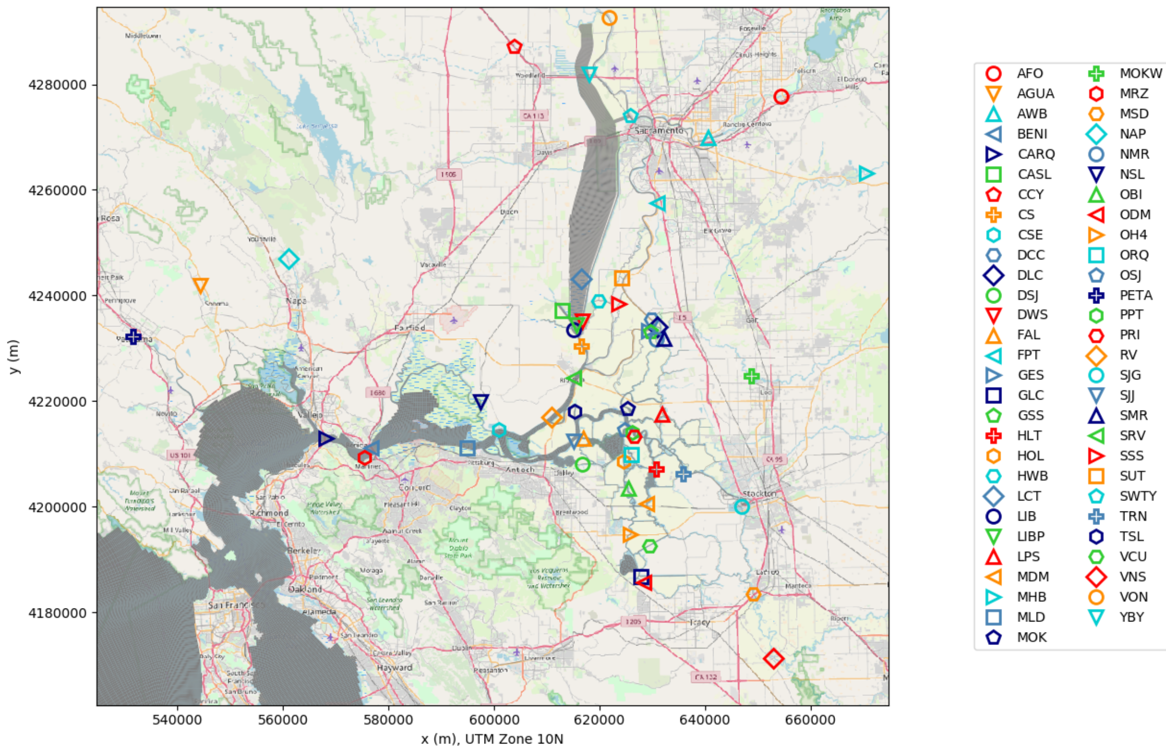

Figure 5: Data stations.

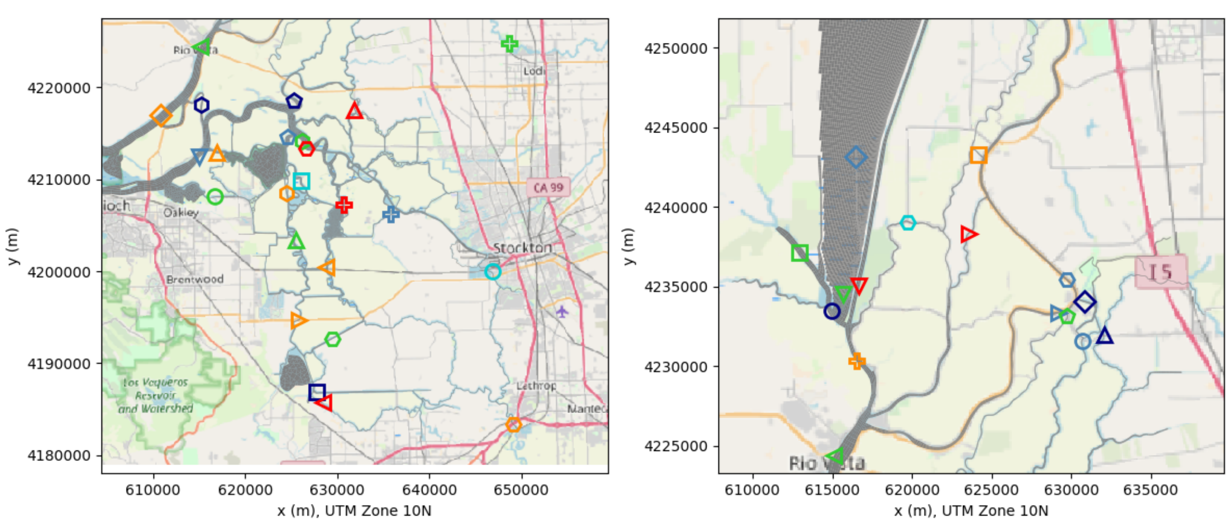

Figure 6: Data stations – zoomed in.

Table 3: List of stations in the SQL database. Parameters include discharge (D), gage height (G), specific conductivity (S), and temperature (T). Station coordinates (x, y) are in UTM Zone 10N, WGS84.

Station Code	Site Description	Organization	Station Code	x (m)	y (m)	Parameters
AFO	American R A Fair Oaks	USGS-NWIS	11446500	654346	4277827	D, G, T
AGUA	Sonoma C A Agua Caliente	USGS-NWIS	11458500	544288	4241811	D, G
AWB	American R BL Watt Ave Bridge	USGS-NWIS	11446980	640504	4269985	T
BENI	Suisun Bay A Benicia Bridge Nr Benicia	USGS-NWIS	11455780	576727	4211168	S, T
CARQ	Carquinez Strait A Carquinez Br Nr Crockett	USGS-NWIS	11455820	568035	4212910	S, T
CASL	Cache Slough Nr Hastings Tract Nr Rio Vista	USGS-NWIS	11455280	612908	4237177	S, T
CCY	Cache Creek at Yolo	USGS-NWIS	11452500	603778	4287183	D, G
CS	Cache Slough	USGS-Biogeo	11455350	616506	4230353	D, G, S, T
CSE	Sacramento River at Mallard Island	DWR	CSE	600858	4214649	G, S, T
DCC	Delta Cross Channel	USGS-Biogeo	11447890	629730	4235456	D, G, S, T
DLC	Delta Cross Channel Btw Sac R & Snodgras	USGS-NWIS	11336600	630822	4234055	D, G, S
DSJ	Dutch Slough At Jersey Island	USGS-NWIS	11313433	616664	4208090	D, G, S, T
DWS	Deep Water Shipping Channel	USGS-NWIS	11455335	616657	4235072	D, G, T
		USGS-Biogeo	11455142	616657	4235072	S
FAL	False River Near Oakley	USGS-NWIS	11313440	616947	4212867	D, G
FPT	Sacramento River at Freeport	USGS-Biogeo	11447650	630855	4257488	D, G, S, T
GES	Sacramento River Below Georgiana Slough	USGS-NWIS	11447905	629223	4233352	D, G, S, T
GLC	Grantline Canal	USGS-NWIS	11313240	627796	4186837	D, G
GSS	Georgiana Slough At Sacramento River	USGS-NWIS	11447903	629699	4233149	D, G, S, T
HLT	Middle River Near Holt	USGS-NWIS	11312685	630728	4207193	D, G
HOL	Holland Cut Near Bethel Island	USGS-NWIS	11313431	624472	4208538	D, G
HWB	Miner Slough At Hwy 84 Bridge	USGS-NWIS	11455165	619737	4239067	D, G, S, T
LCT	Liberty Cut	USGS-Biogeo	11455146	616465	4243142	D, S, T
LIB	Cache Slough at Liberty Island	USGS-Biogeo	11455315	614977	4233506	D, G, S, T
LIBP	Liberty Island Nr Prospect Island Nr Rio Vista	USGS-NWIS	381504121404001	615693	4234503	S, T
LPS	Little Potato Slough at Terminous	USGS-NWIS	11336790	631878	4217534	D, G, S, T
MDM	Middle River at Middle River	USGS-NWIS	11312676	628813	4200504	D, G
MHB	Cosumnes R A Michigan Bar	USGS-NWIS	11335000	670551	4263137	D, G, T
MLD	Mallard Island	DWR	MAL	594840	4211112	S, T
MOK	Mokelumne R @ San Joaquin River	USGS-NWIS	11336930	625284	4218540	D, G
MOKW	Mokelumne R A Woodbridge	USGS-NWIS	11325500	648719	4224774	D
MRZ	Martinez	DWR	MRZ	575435	4209230	S, T
MSD	Mossdale	DWR	MSD	649165	4183423	S, T
NAP	Napa R Nr Napa	USGS-NWIS	11458000	560955	4246913	D, G
NMR	North Mokelumne R at W Walnut Grove Rd	USGS-NWIS	11336685	630686	4231611	D, G, S, T
NSL	Montezuma Slough at National Steel	DWR	NSL	597456	4219938	D, T
OBI	Old River at Bacon Island	USGS-NWIS	11313405	625516	4203449	D, G
ODM	Old River at Delta Mendota Canal	USGS-NWIS	11312968	628429	4185737	D, G
OH4	Old River at Highway 4	USGS-NWIS	11313315	625826	4194686	D, G
ORQ	Old River @ Quimbly Is Near Bethel Is	USGS-NWIS	11313434	626033	4209783	D, G
OSJ	Old River at Franks Tract Near Terminous	USGS-NWIS	11313452	624642	4214645	D, G
PETA	Petaluma R A Copland Pumping Station A Petaluma	USGS-NWIS	11459150	531577	4232320	D, G
PPT	Prisoner Point	DWR	PPT	626142	4214114	S, T
PRI	San Joaquin R at Prisoners Pt Nr Termino	USGS-NWIS	11313460	626593	4213344	D, G, S, T
RV	Rio Vista at Decker Island	USGS-Biogeo	11455478	610827	4216924	G, S, T
SJG	San Joaquin R Bl Garwood Bridge a Stockton Ca	USGS-NWIS	11304810	646828	4199981	D, G, S, T
SJJ	San Joaquin River at Jersey Point	USGS-NWIS	11337190	615023	4212395	D, G, S, T
SMR	South Mokelumne R at W Walnut Grove Rd	USGS-NWIS	11336680	632082	4231967	D, S, T
SRV	Sacramento River at Rio Vista	USGS-NWIS	11455420	615116	4224383	D, G, S, T
SSS	Steamboat Slough Nr Walnut Grove	USGS-NWIS	11447850	623608	4238350	D, G, S, T
SUT	Sutter Slough A Courtland	USGS-NWIS	11447830	624188	4243292	D, G, T
SWTY	Sacramento Weir Spill to Yolo Bypass	USGS-NWIS	11426000	625889	4274151	D
TRN	Turner Cut Near Holt	USGS-NWIS	11311300	635751	4206165	D, G
TSL	Threemile Slough at San Joaquin River	USGS-NWIS	11337080	615206	4218058	D, G
VCU	Victoria Canal Near Byron	USGS-NWIS	11312672	629465	4192634	D, G
VNS	San Joaquin R Nr Vernalis	USGS-NWIS	11303500	652977	4171295	D, G, T
VON	Sacramento R A Verona	USGS-NWIS	11425500	621856	4292680	D, G, S, T
YBY	Yolo Bypass Nr Woodland	USGS-NWIS	11453000	618033	4281894	D, G, T

4 Results

4.1 Validation Statistics

The model is validated by comparing time series of modeled and observed discharge, gage height, salinity, and temperature at measurement stations across the Delta and Suisun Bay. At this point we do not show results for gage height because we are still in the process of determining the vertical datum at all of the stations.

Let o_i denote an observed value at time i, and let m_i denote the corresponding modeled value at time i. Let an overbar indicate the mean over all time, e.g., $\bar{o}$ is the mean observed signal. We define the following validation statistics:

Lag is the time shift by which the best correlation between observed and modeled data is obtained. A positive lag indicates the model is behind the observations, and a negative lag indicates the model is ahead of the observations. We limit the lag to $\pm$ 6 hours. The lag-corrected model signal is denoted m_i'.

Bias is defined as $\overline{m_i - o_i}$, the mean difference between modeled and observed data.

RMSE is the abbreviation for "root mean square error" and is here defined as

$$\sqrt{\overline{(m_i' - o_i - \overline{m_i' - o_i})^2}},$$

equal to the square root of the variance of the difference between modeled and observed data, where the modeled data has been corrected for lag.

Skill is calculated according to the formula proposed by Willmott (1981):

$$1 - \frac{\sum_i (m_i' - o_i)^2}{\sum_i (|m_i' - \bar{o}| + |o_i - \bar{o}|)^2}.$$

Note the modeled data are corrected for lag before computing skill.

R2 is defined as the coefficient of determination for the best-fit line between o_i and m_i', i.e. between the observed signal and the lag-corrected modeled signal.

Tidal Amplitude Ratio is defined as the slope of the best-fit line between the observed and lag-corrected modeled signal, where the tidally filtered component of both signals has been removed.

To obtain the tidally filtered signal, we use a 6th order low-pass Butterworth filter with a cutoff frequency of 30 hours. A tidally averaged signal is obtained by resampling the tidally filtered signal on a daily basis. Validation statistics are also calculated for the tidally averaged observed and modeled signal, and in this case no lag correction is performed, and neither lag nor tidal amplitude ratio is reported.

In Tables 4 through 9 we present validation statistics for unfiltered and tidally averaged discharge, salinity, and temperature at stations across the Delta, Suisun Bay, and Carquinez Strait. In Figures 7 through 12 we show maps of these same statistics.

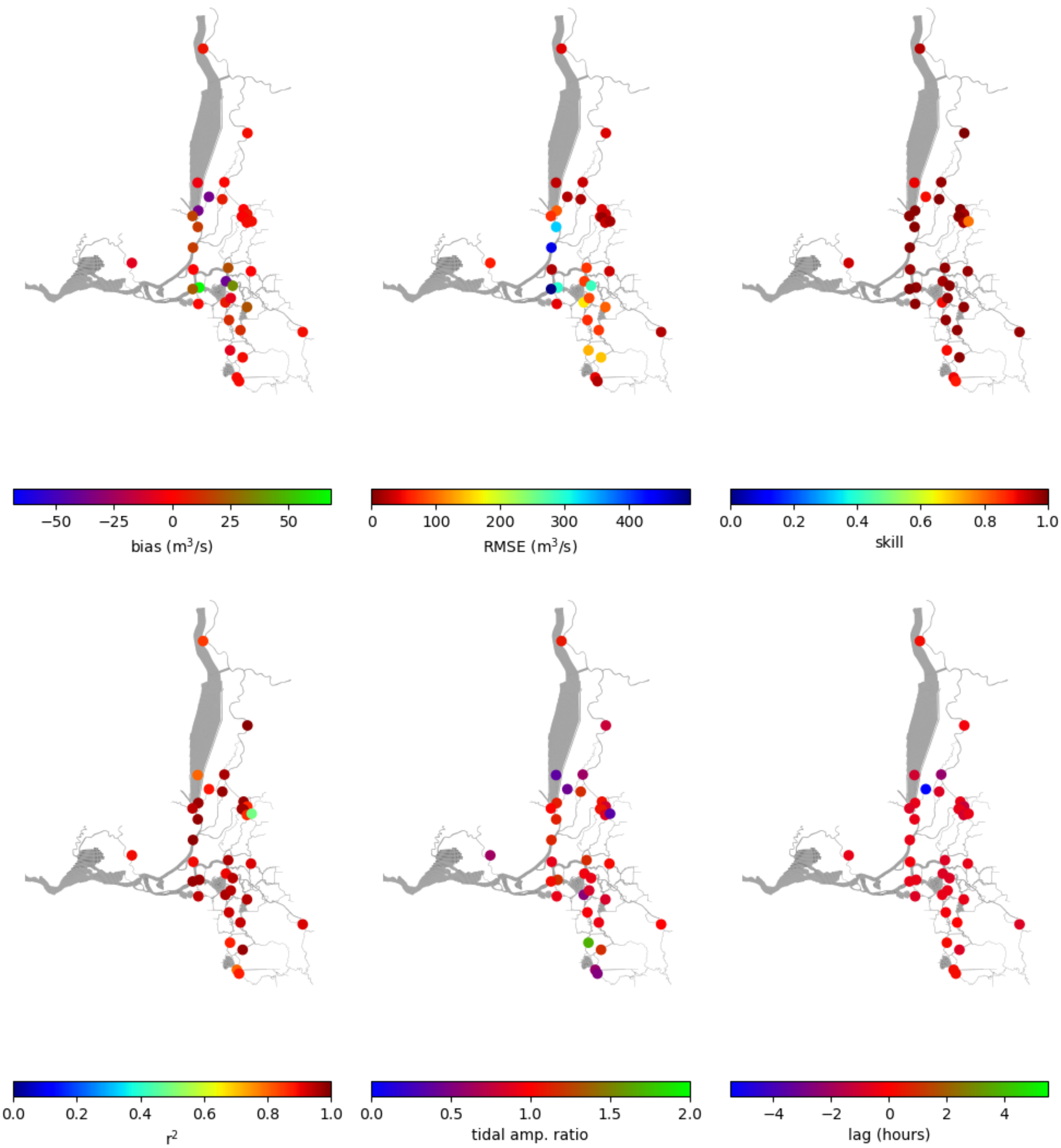

Figure 7: Validation statistics for unfiltered discharge.

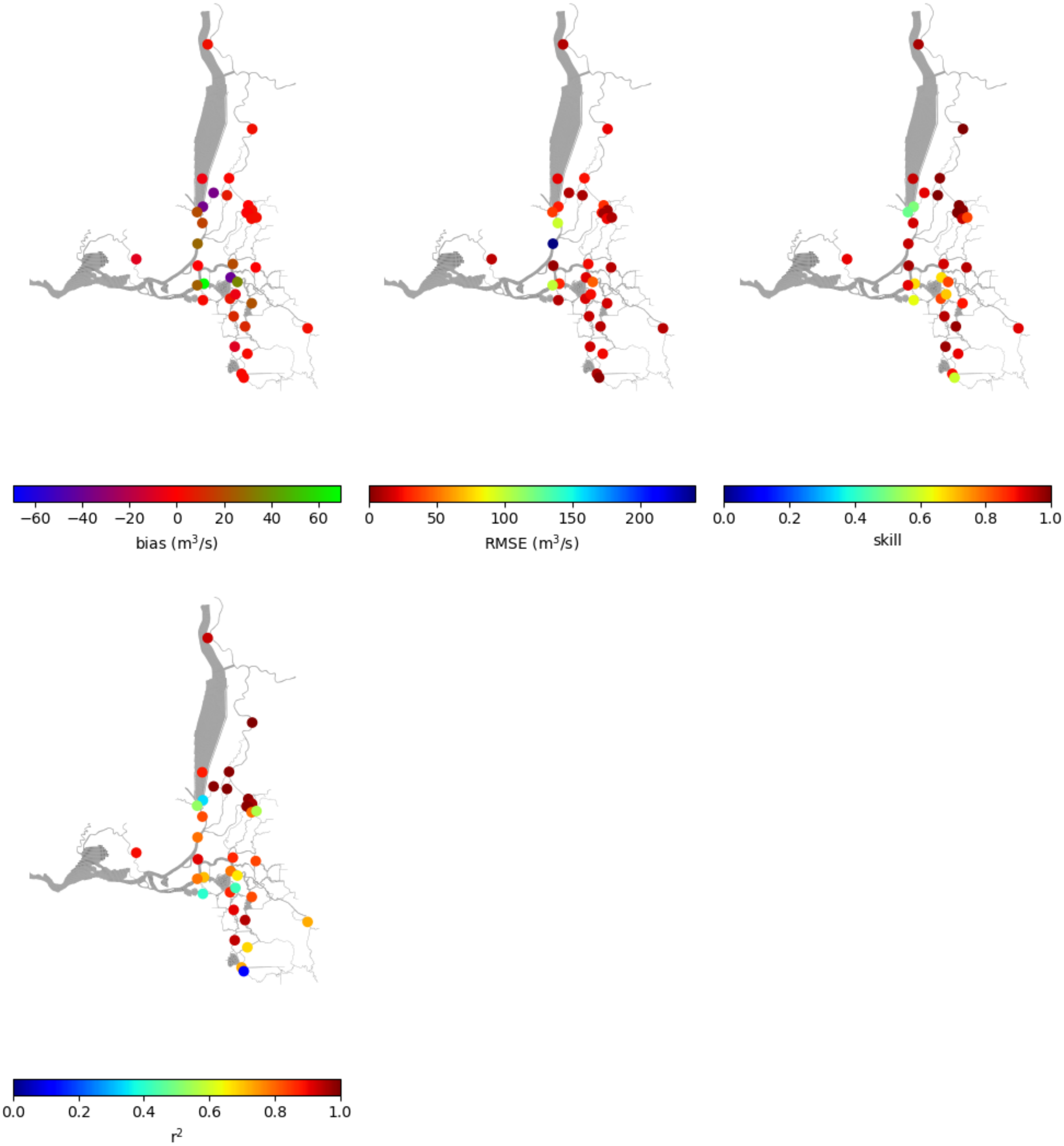

Figure 8: Validation statistics for tidally averaged discharge.

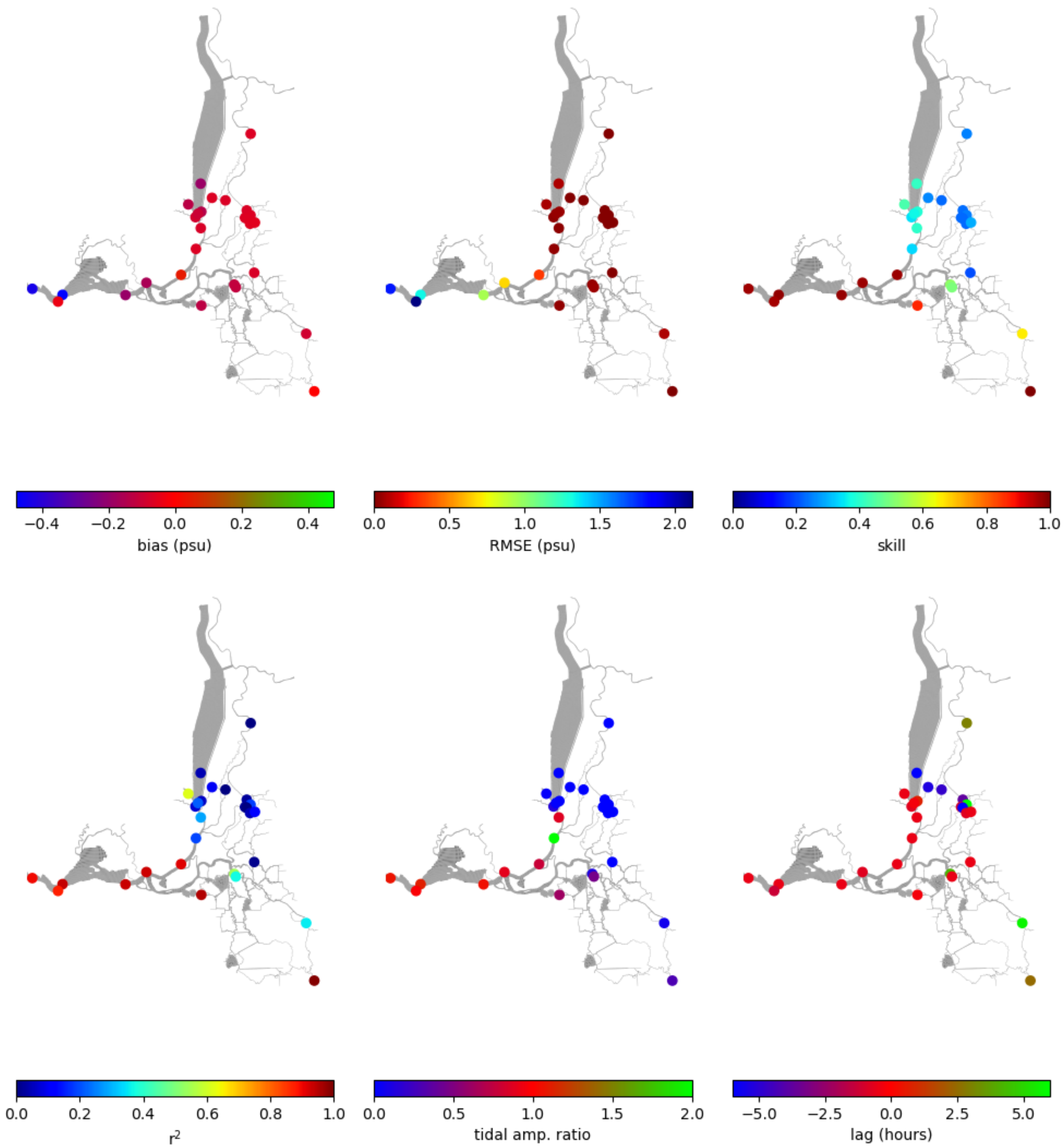

Figure 9: Validation statistics for unfiltered salinity.

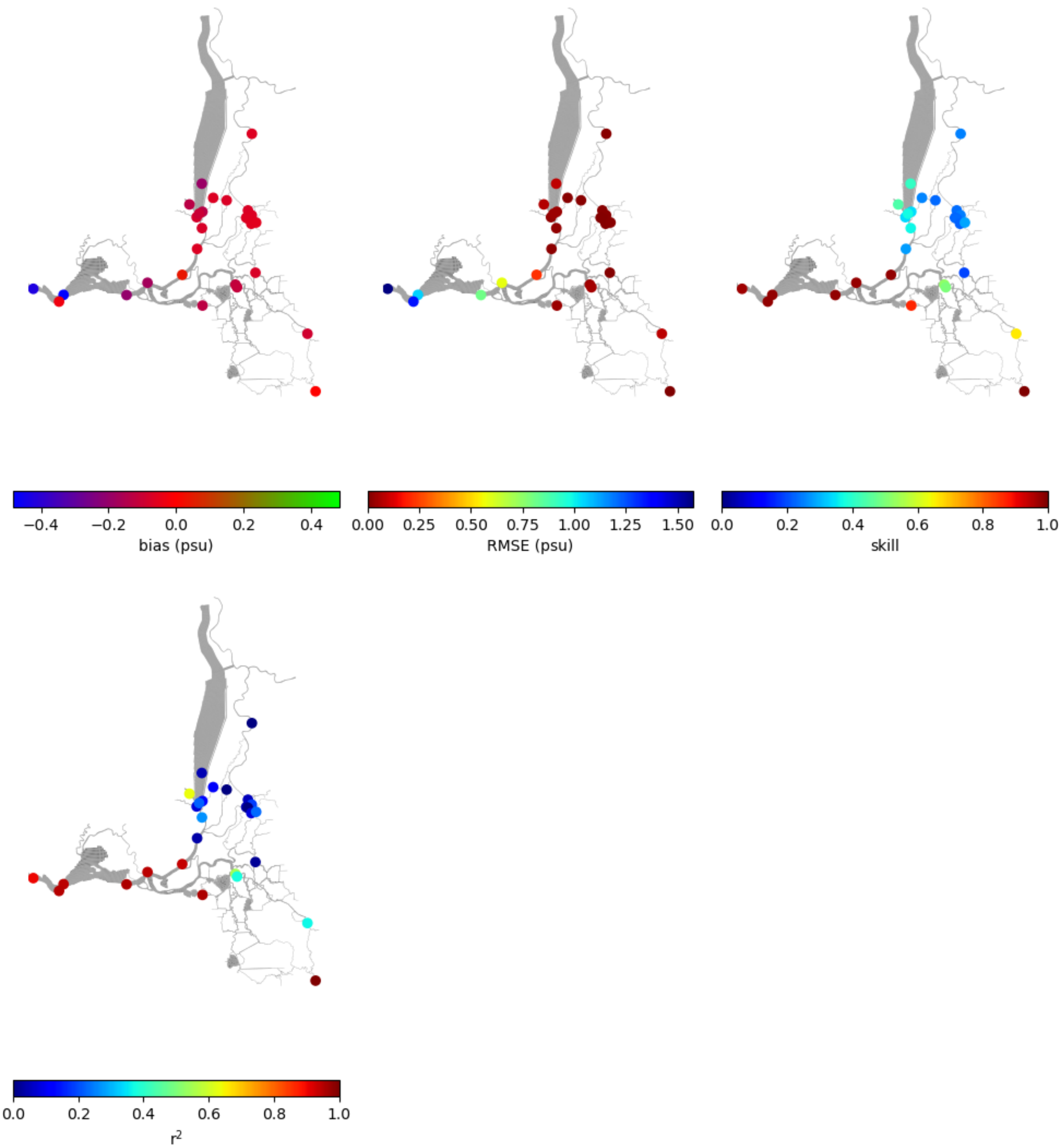

Figure 10: Validation statistics for tidally averaged salinity.

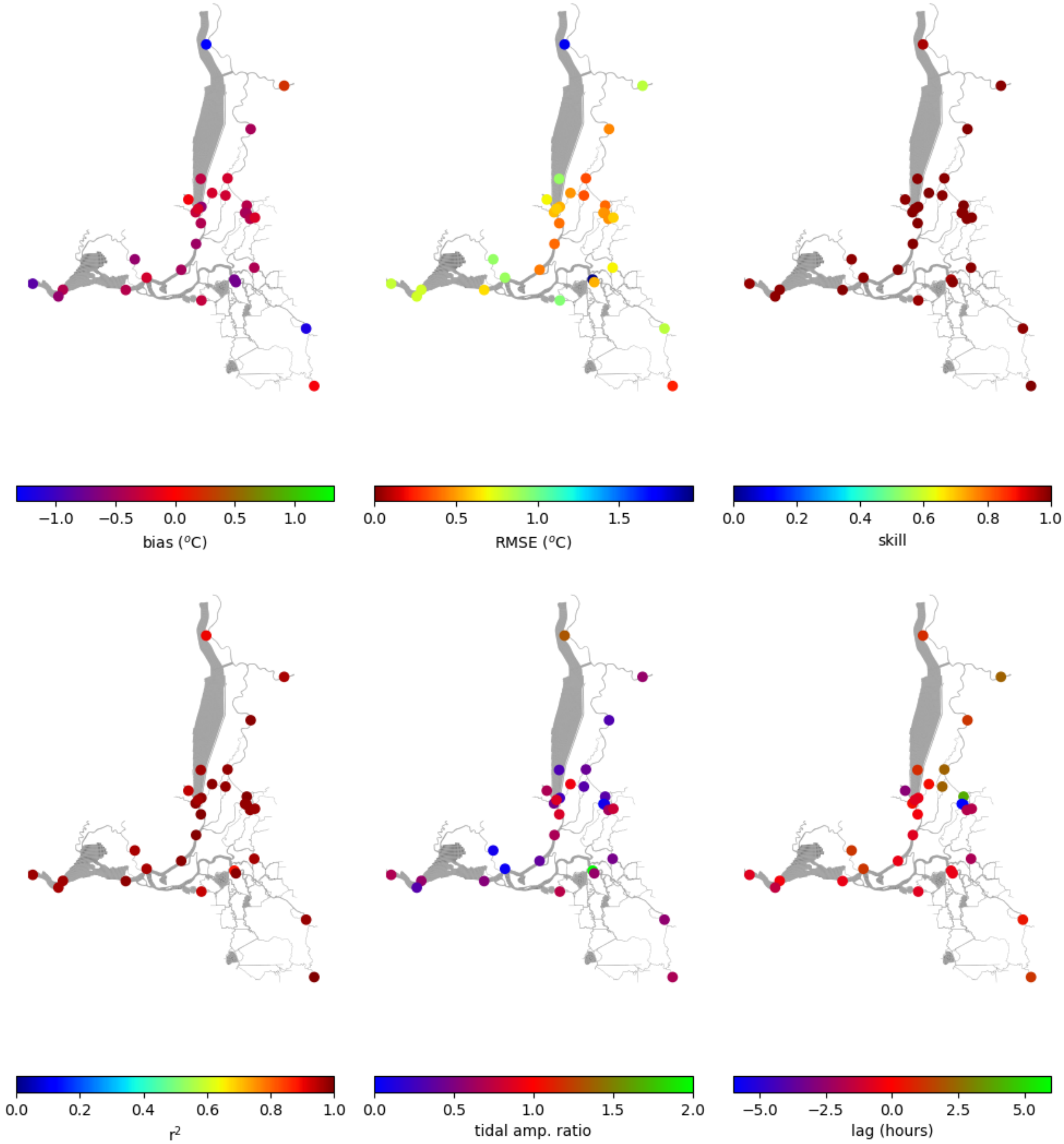

Figure 11: Validation statistics for unfiltered temperature.

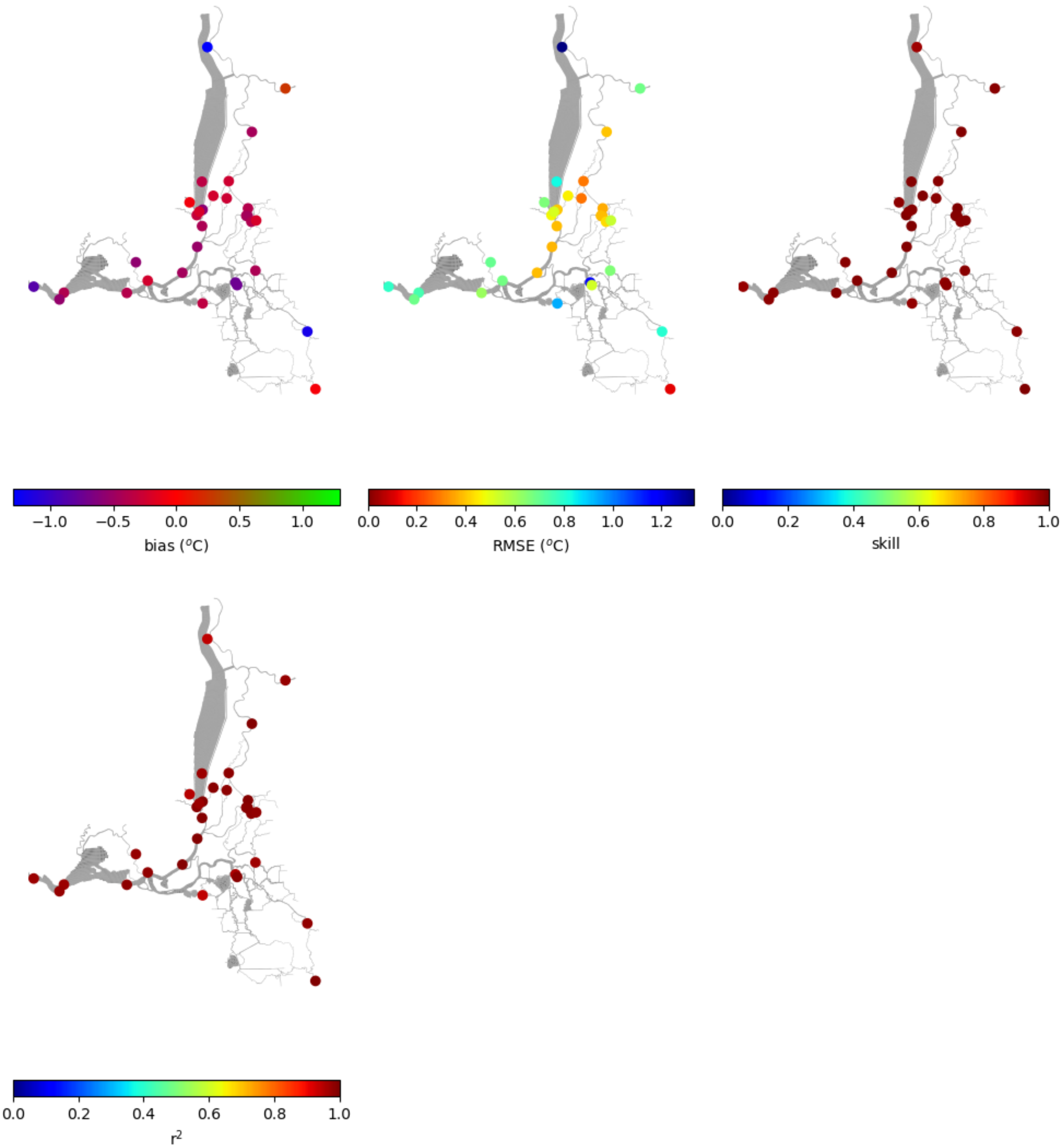

Figure 12: Validation statistics for tidally averaged temperature.

Table 4: Validation statistics for unfiltered discharge.

Station	Mean Obs. (m^3/s)	Mean Mod. (m^3/s)	St. Dev. Obs. (m^3/s)	Bias (m^3/s)	RMSE (m^3/s)	Skill	R2	Lag (min)	Tidal Amp. Ratio
CS	67	52	1767	15.3	332.7	0.99	0.98	-30	1.12
DCC	326	326	242	-0.2	38.8	0.99	0.98	-30	1.06
DLC	112	107	92	4.9	33.4	0.96	0.87	-75	0.82
DSJ	-3	-5	180	1.4	42.5	0.98	0.94	-45	0.92
DWS	-0	36	442	-36.3	91.9	0.99	0.97	-30	1.10
FAL	14	-54	1109	68.3	298.0	0.98	0.97	-30	1.19
FPT	539	536	426	3.6	38.7	1.00	0.99	-15	0.79
GES	174	178	226	-3.2	42.7	0.99	0.97	-45	1.01
GLC	15	14	91	1.8	45.7	0.91	0.80	15	0.59
GSS	98	99	65	-0.9	11.2	0.99	0.97	-30	1.09
HLT	-51	-73	389	22.1	95.7	0.98	0.95	-30	0.84
HOL	-11	-17	348	6.0	167.4	0.90	0.96	-30	0.53
HWB	46	84	62	-37.1	22.8	0.90	0.89	-330	0.44
LCT	5	10	58	-4.1	28.5	0.91	0.80	-60	0.37
LIB	-16	-33	290	17.1	69.0	0.99	0.95	-45	1.01
LPS	51	52	110	-0.7	32.9	0.98	0.92	-30	1.03
MDM	-64	-76	293	11.2	72.1	0.98	0.94	0	0.92
MOK	118	98	266	20.3	71.6	0.98	0.96	-45	1.16
NMR	59	56	83	3.1	30.4	0.96	0.86	-60	0.87
NSL	9	17	137	-8.0	57.9	0.93	0.90	-30	0.63
OBI	-40	-51	257	11.5	67.4	0.98	0.93	-15	0.96
ODM	5	2	43	2.2	22.2	0.88	0.88	15	0.52
OH4	-81	-73	159	-7.7	137.6	0.90	0.88	15	1.69
ORQ	-29	-22	318	-7.1	80.4	0.98	0.95	-30	0.84
OSJ	-36	3	242	-39.0	75.2	0.97	0.90	-45	0.95
PRI	-22	-60	1278	37.8	286.3	0.99	0.95	-45	0.92
SJG	11	8	74	3.3	21.7	0.98	0.92	-45	1.00
SJJ	109	86	3064	23.5	494.0	0.99	0.98	-30	1.05
SMR	21	18	27	3.5	19.2	0.79	0.49	-30	0.35
SRV	429	413	2248	15.8	448.1	0.99	0.99	-30	1.14
SSS	105	98	112	7.0	19.9	0.99	0.98	-45	1.17
SUT	124	123	99	1.2	31.3	0.98	0.96	-135	0.62
TRN	-21	-21	62	-0.5	19.5	0.97	0.90	-15	0.90
TSL	-43	-46	603	2.9	148.2	0.99	0.98	-45	1.17
VCU	-39	-44	95	4.9	41.6	0.96	0.85	15	1.09
YBY	28	28	180	-0.0	4.7	1.00	1.00	240	0.47

Table 5: Validation statistics for tidally averaged discharge.

Station	Mean Obs. (m^3/s)	Mean Mod. (m^3/s)	St. Dev. Obs. (m^3/s)	Bias (m^3/s)	RMSE (m^3/s)	Skill	R2
CS	69	52	160	17.4	97.4	0.93	0.83
DCC	326	326	222	-0.1	33.1	0.99	0.99
DLC	113	108	37	4.4	6.9	0.99	0.97
DSJ	-4	-6	14	2.3	11.1	0.63	0.40
DWS	1	38	35	-37.6	29.1	0.50	0.34
FAL	14	-55	57	69.1	30.7	0.68	0.71
FPT	540	535	414	4.1	22.6	1.00	1.00
GES	175	178	183	-2.8	27.6	0.99	0.99
GLC	16	14	19	1.7	10.2	0.89	0.73
GSS	98	98	63	-0.7	7.4	1.00	0.99
HLT	-50	-72	41	21.6	17.0	0.89	0.83
HOL	-10	-16	31	5.7	18.0	0.84	0.87
HWB	47	83	57	-36.4	10.6	0.91	0.99
LCT	5	9	52	-3.9	21.5	0.94	0.88
LIB	-17	-37	43	20.4	37.2	0.48	0.53
LPS	51	52	28	-0.7	11.5	0.95	0.84
MDM	-64	-74	55	10.5	11.7	0.98	0.96
MOK	118	98	64	20.3	23.9	0.93	0.87
NMR	57	54	49	2.8	22.9	0.94	0.79
NSL	9	16	30	-7.6	13.2	0.91	0.90
OBI	-39	-50	47	11.1	14.9	0.95	0.91
ODM	5	3	3	1.8	3.5	0.60	0.11
OH4	-81	-72	55	-8.7	16.5	0.98	0.94
ORQ	-32	-27	33	-5.0	25.2	0.70	0.42
OSJ	-36	5	38	-40.5	20.0	0.67	0.79
PRI	-21	-58	79	36.3	45.9	0.84	0.66
SJG	11	8	23	3.6	12.2	0.92	0.73
SJJ	113	87	207	25.6	100.6	0.91	0.79
SMR	21	17	15	3.7	9.9	0.84	0.56
SRV	419	391	524	28.0	241.0	0.94	0.79
SSS	105	98	94	7.2	9.3	1.00	0.99
SUT	124	122	96	1.6	26.2	0.99	0.99
TRN	-21	-20	15	-0.9	4.8	0.97	0.92
TSL	-43	-45	41	2.2	24.0	0.91	0.68
VCU	-39	-43	35	4.2	11.2	0.96	0.94
YBY	28	28	179	-0.1	18.4	1.00	0.99

Table 6: Validation statistics for unfiltered salinity.

Station	Mean Obs. (psu)	Mean Mod. (psu)	St. Dev. Obs. (psu)	Bias (psu)	RMSE (psu)	Skill	R2	Lag (min)	Tidal Amp. Ratio
BENI	12.78	13.25	5.36	-0.48	1.33	0.98	0.94	-30	1.12
CARQ	18.61	19.04	5.64	-0.43	1.80	0.97	0.90	-30	1.08
CASL	0.00	0.13	0.08	-0.13	0.07	0.44	0.62	-30	0.02
CS	0.01	0.09	0.03	-0.07	0.03	0.40	0.29	-30	0.87
CSE	2.15	2.31	2.39	-0.16	0.67	0.98	0.93	-45	0.90
DCC	0.00	0.07	0.01	-0.07	0.01	0.23	0.02	-225	0.00
DLC	0.00	0.06	0.01	-0.06	0.01	0.25	0.19	360	0.00
DSJ	0.13	0.25	0.18	-0.13	0.04	0.87	0.95	-15	0.62
DWS	0.01	0.14	0.06	-0.13	0.05	0.39	0.06	45	0.00
FPT	0.00	0.06	0.01	-0.06	0.01	0.25	0.00	180	0.00
GES	0.00	0.06	0.01	-0.06	0.01	0.23	0.03	-60	0.00
GSS	0.00	0.06	0.01	-0.06	0.01	0.23	0.00	-360	0.00
HWB	0.00	0.07	0.01	-0.07	0.01	0.26	0.10	-315	0.01
LCT	0.01	0.20	0.09	-0.19	0.09	0.41	0.04	-360	0.00
LIB	0.01	0.09	0.03	-0.08	0.03	0.35	0.07	-45	0.14
LIBP	0.00	0.10	0.04	-0.10	0.04	0.37	0.22	-15	0.01
LPS	0.00	0.07	0.01	-0.07	0.01	0.20	0.01	-30	0.00
MLD	4.15	4.34	3.63	-0.19	0.94	0.98	0.94	-30	1.05
MRZ	12.95	12.98	6.00	-0.03	2.11	0.97	0.88	-75	0.98
MSD	0.29	0.29	0.11	-0.00	0.01	1.00	1.00	150	0.30
NMR	0.00	0.06	0.01	-0.06	0.01	0.23	0.05	-45	0.00
PPT	0.04	0.16	0.07	-0.11	0.05	0.53	0.54	255	0.12
PRI	0.04	0.15	0.06	-0.11	0.05	0.50	0.37	-30	0.46
RV	0.69	0.64	1.09	0.05	0.32	0.98	0.92	-30	0.78
SJG	0.21	0.29	0.10	-0.09	0.09	0.66	0.36	345	0.07
SMR	0.00	0.05	0.01	-0.05	0.01	0.29	0.11	-30	0.00
SRV	0.01	0.08	0.02	-0.06	0.04	0.34	0.19	-30	2.70
SSS	0.00	0.07	0.01	-0.07	0.01	0.23	0.00	-285	0.00

Table 7: Validation statistics for tidally averaged salinity.

Station	Mean Obs. (psu)	Mean Mod. (psu)	St. Dev. Obs. (psu)	Bias (psu)	RMSE (psu)	Skill	R2
BENI	12.79	13.27	4.61	-0.48	1.06	0.98	0.95
CARQ	18.60	19.02	5.09	-0.42	1.58	0.97	0.90
CASL	0.00	0.13	0.08	-0.13	0.07	0.44	0.63
CS	0.01	0.09	0.02	-0.07	0.03	0.37	0.27
CSE	2.14	2.31	2.24	-0.17	0.58	0.98	0.95
DCC	0.00	0.07	0.01	-0.07	0.01	0.23	0.05
DLC	0.00	0.06	0.01	-0.06	0.01	0.25	0.18
DSJ	0.13	0.25	0.18	-0.13	0.04	0.87	0.96
DWS	0.01	0.14	0.04	-0.13	0.04	0.34	0.12
FPT	0.00	0.06	0.01	-0.06	0.01	0.25	0.00
GES	0.00	0.06	0.01	-0.06	0.01	0.23	0.05
GSS	0.00	0.06	0.01	-0.06	0.01	0.23	0.00
HWB	0.00	0.07	0.01	-0.07	0.01	0.26	0.11
LCT	0.01	0.20	0.09	-0.19	0.09	0.41	0.05
LIB	0.01	0.09	0.02	-0.08	0.03	0.34	0.08
LIBP	0.00	0.10	0.04	-0.10	0.04	0.37	0.22
LPS	0.00	0.07	0.01	-0.07	0.01	0.19	0.02
MLD	4.15	4.35	3.38	-0.20	0.81	0.98	0.96
MRZ	12.95	12.98	5.35	-0.03	1.35	0.98	0.95
MSD	0.29	0.29	0.10	0.00	0.00	1.00	1.00
NMR	0.00	0.06	0.01	-0.06	0.01	0.22	0.08
PPT	0.04	0.16	0.07	-0.11	0.05	0.53	0.55
PRI	0.04	0.15	0.06	-0.11	0.05	0.50	0.38
RV	0.68	0.64	0.89	0.04	0.22	0.98	0.94
SJG	0.21	0.29	0.10	-0.09	0.08	0.66	0.37
SMR	0.00	0.05	0.01	-0.05	0.01	0.29	0.23
SRV	0.01	0.08	0.01	-0.06	0.02	0.28	0.04
SSS	-0.00	0.07	0.01	-0.07	0.01	0.23	0.00

Table 8: Validation statistics for unfiltered temperature.

Station	Mean Obs. (^oC)	Mean Mod. (^oC)	St. Dev. Obs. (^oC)	Bias (^oC)	RMSE (^oC)	Skill	R2	Lag (min)	Tidal Amp. Ratio
AWB	14.9	14.7	4.0	0.2	0.8	0.99	0.96	135	0.59
BENI	16.2	16.6	3.6	-0.4	0.8	0.99	0.97	-15	0.59
CARQ	14.8	15.7	3.7	-0.9	0.8	0.98	0.97	-45	0.68
CASL	18.9	19.0	2.9	-0.1	0.7	0.99	0.94	-165	0.67
CS	16.4	16.8	4.7	-0.4	0.4	1.00	0.99	-15	0.85
CSE	16.3	16.6	4.4	-0.2	0.9	0.99	0.96	75	0.04
DCC	16.0	16.4	4.6	-0.4	0.4	1.00	0.99	240	0.35
DSJ	19.7	20.0	3.4	-0.3	1.0	0.98	0.94	-45	0.72
DWS	16.6	17.2	4.7	-0.6	0.5	0.99	0.99	-30	0.25
FPT	15.8	16.3	4.5	-0.4	0.5	0.99	0.99	75	0.32
GES	17.9	18.4	3.6	-0.4	0.5	0.99	0.98	-360	0.03
GSS	17.9	18.4	3.6	-0.5	0.5	0.99	0.98	-360	0.09
HWB	16.2	16.4	4.7	-0.2	0.5	1.00	0.99	15	0.94
LCT	16.9	17.3	5.2	-0.3	0.9	0.99	0.97	60	0.30
LIB	16.5	16.8	4.7	-0.3	0.6	1.00	0.99	15	0.45
LIBP	18.7	18.9	3.2	-0.2	0.6	0.99	0.97	-45	0.86
LPS	19.2	19.6	3.8	-0.4	0.7	0.99	0.97	-120	0.47
MLD	16.3	16.6	4.2	-0.4	0.6	0.99	0.99	-30	0.53
MRZ	15.9	16.5	3.8	-0.6	0.8	0.99	0.97	-90	0.33
MSD	18.3	18.3	5.8	-0.0	0.2	1.00	1.00	75	0.67
NMR	18.6	19.0	3.4	-0.4	0.5	0.99	0.98	-105	0.65
NSL	16.2	16.7	4.7	-0.6	0.9	0.99	0.96	75	0.07
PPT	16.7	17.4	5.0	-0.7	2.0	0.96	0.89	-30	4.66
PRI	16.7	17.4	5.0	-0.7	0.5	0.99	0.99	-30	0.59
RV	16.3	16.8	4.6	-0.5	0.4	1.00	0.99	-30	0.38
SJG	17.4	18.6	5.8	-1.2	0.8	0.98	0.98	30	0.57
SMR	18.8	19.0	3.6	-0.2	0.6	0.99	0.98	-105	0.80
SRV	16.3	16.8	4.7	-0.5	0.4	1.00	0.99	-45	0.67
SSS	14.0	14.3	2.2	-0.3	0.3	0.99	0.98	135	0.34
SUT	14.0	14.2	2.2	-0.2	0.3	0.99	0.98	135	0.42
YBY	16.1	17.5	5.6	-1.3	1.8	0.96	0.90	60	1.33

Table 9: Validation statistics for tidally averaged temperature.

Station	Mean Obs. (^{o}C)	Mean Mod. (^{o}C)	St. Dev. Obs. (^{o}C)	Bias (^{o}C)	RMSE (^{o}C)	Skill	R2
AWB	14.9	14.6	4.0	0.3	0.7	0.99	0.98
BENI	16.2	16.6	3.6	-0.4	0.8	0.99	0.97
CARQ	14.9	15.7	3.7	-0.9	0.8	0.98	0.98
CASL	18.9	19.0	2.9	-0.1	0.7	0.99	0.95
CS	16.4	16.8	4.7	-0.4	0.4	1.00	0.99
CSE	16.3	16.6	4.3	-0.2	0.7	0.99	0.98
DCC	16.0	16.4	4.6	-0.4	0.4	1.00	0.99
DSJ	19.6	20.0	3.4	-0.3	0.9	0.98	0.94
DWS	16.6	17.2	4.7	-0.6	0.4	0.99	0.99
FPT	15.8	16.3	4.5	-0.5	0.4	1.00	0.99
GES	17.9	18.4	3.6	-0.4	0.4	0.99	0.99
GSS	17.9	18.4	3.6	-0.5	0.4	0.99	0.99
HWB	16.2	16.4	4.7	-0.2	0.5	1.00	0.99
LCT	17.0	17.3	5.2	-0.3	0.8	0.99	0.97
LIB	16.5	16.8	4.7	-0.3	0.5	1.00	0.99
LIBP	18.7	18.9	3.1	-0.2	0.5	0.99	0.97
LPS	19.2	19.6	3.8	-0.4	0.7	0.99	0.97
MLD	16.3	16.7	4.1	-0.4	0.6	0.99	0.99
MRZ	15.9	16.5	3.8	-0.5	0.7	0.99	0.98
MSD	18.3	18.4	5.8	-0.0	0.1	1.00	1.00
NMR	18.6	19.0	3.4	-0.4	0.4	0.99	0.99
NSL	16.2	16.7	4.7	-0.6	0.7	0.99	0.98
PPT	16.7	17.4	5.0	-0.7	1.2	0.98	0.96
PRI	16.7	17.5	5.0	-0.7	0.5	0.99	0.99
RV	16.3	16.8	4.6	-0.5	0.4	1.00	0.99
SJG	17.4	18.6	5.8	-1.2	0.8	0.98	0.98
SMR	18.7	19.0	3.6	-0.2	0.5	0.99	0.98
SRV	16.3	16.8	4.7	-0.5	0.4	1.00	0.99
SSS	14.0	14.3	2.2	-0.3	0.3	0.99	0.99
SUT	14.0	14.2	2.2	-0.2	0.3	0.99	0.99
YBY	16.2	17.5	5.5	-1.3	1.3	0.97	0.94

4.2 Model Performance

For unfiltered discharge, model skill is high throughout the Suisun-Delta system, and for the most part, lag between the model and observations is small. There are two exceptions with respect to lag: stations YBY and HWB. Tides do not appear to influence station YBY, thus lag is not meaningful here. At station HWB, on the other hand, the modeled discharge signal exhibits oscillations near twice the tidal frequency, suggesting a possible numerical instability or resonance at this station. Tidal amplitude ratio is close to 1 throughout the Suisun-Delta system except at YBY (where again, since there is no tidal influence, tidal amplitude ratio is not meaningfyl), at HWB (where the same resonance/instability issue is likely to blame), and at LCT, HOL, SMR, OH4, GLC, ODM, and NSL. Errors in tidal amplitidue at these stations could be due to errors in bathymetry and/or friction. Errors in the vicinity of the permanent gates/weirs and temporary barriers could be due to our rough parameterization of these structures.

Model predictions of tidally averaged discharge are overall good. While model skill and R2 are lower than for unfiltered discharge, this is due to the smaller variance in the tidal average time series compared to the unfiltered time series. The main model weaknesses for tidally averaged flow are in the Yolo Bypass, where boundary inflows are not well-characterized, and in the central Delta, where the absence of consumptive use is a likely source of error.

The model predicts both unfiltered and tidally averaged discharge fairly well downstream of the Delta Cross Channel (site DLC) and the Suisun Marsh Salinity Control Gates (site NSL), but there is room for improvement, which could be accomplished by better parameterization of these structures. In WY2016, the Sacramento Weir was not opened, so we do not have the opportunity to evaluate performance of this structure using the model results from WY2016.

For both unfiltered and tidally averaged salinity, model skill is high through Suisun Bay and the confluence of the Sacramento and San Joaquin Rivers, but skill drops to zero moving deeper into the Delta. This is because salinity is set to zero at all tributary inflows except the San Joaquin River. Errors in salinity are small in an absolute sense (several psu) throughout the domain. Where model skill is high, there is no lag in the modeled tidal signal and the tidal amplitude ratio is close to one; where skill is low, these statistics are not meaningful as the model does not capture the signal.

Model skill for unfiltered and tidally averaged temperature is high throughout the entire Suisun-Delta system. Vroom et al. (2017) found that surface heat exchange is the primary driver of temperature in the Delta, and tides play a more minor role, so what we call "tidal amplitude ratio" here is actually the amplitdue ratio for daily flucutations in temperature due to surface heating and cooling.

5 Next Steps

Next steps in model development will be driven by performance of the biogeochemical model. If biogeochemical model performance is weak in a particular region, we will investigate whether limitations of the the hydrodynamic model are a potentially important cause and could be improved in a way that would substantially improve biogeochemical model skill. Examples of potential hydrodynamic model improvements include:

1. Consumptive use is currently neglected in the hydrodynamic model and could be added. As a first step, estimates from DAYFLOW could be used.

2. In several regions of the Delta, additional bathymetry datasets are available that represent improvements over the bathymetry used in the current WY2016 simulation. In addition, the grid could be refined in some regions to address numerical artifacts (e.g., excessive numerical dispersion) or improve computational efficiency. With potential bathymetry and grid changes, this could quickly turn into a very large and time-consuming undertaking, and the potential gains need to be weighed against the necessary effort (dollars or time).

3. Improved parameterization of the permanent structures and temporary barriers, possibly using the "general structure" feature of Delft3D-FM, could improve model performance, particulary in the vicinity of these structures.

4. The spatially varying Manning coefficient used in the current WY2016 simulation is based on the Martyr-Koller et al. (2017) calibration, which focused on optimizing vertical salinity stratification in Suisun, San Pablo, and Central Bays in WY2000. Optimizing for discharge, with a focus on tidal amplitudes and lags, could produce a different optimal friction field. Furthermore, friction is likely to vary from year-to-year, due to the increasing prevalence of aquatic vegetation communities throughout the Delta. While vegetation friction due to submerged vegetation is better parameterized with a water column drag coefficient, a properly tuned Manning coefficient could capture the effects to first order. These various approaches to fine-tuning drag could improve predictions of tidal dispersion.

5. Including submerged aquatic vegetation (SAV) using water-column drag, instead of a Manning coefficient, and including floating vegetation (FAV) as high drag at the water surface, could improve predictions of vertical mixing, which is an important control on clam grazing rate in the biogeochemical model. Hyperspectral flyover data has been used to map density of SAV and both density and species distribution of FAV in the

Delta in recent years (Khanna et al., 2018) and this data could be used to generate water colum drag distributions.

6. Investigating and remedying the instability or resonance in discharge at site HWB. As net discharge is predicted fairly well at this station despite the numerical issue, correcting this is not critical, but could improve local predictions of tidal dispersion.

References

Abatzoglou, J. T. (2011). Development of gridded surface meteorological data for ecological applications and modelling. *International Journal of Climatology*. doi: 10.1002/joc.3413.

CA Department of Water Resources (2018). Envineering Drawings: South Delta Faciliites: Middle River, Old River and Grant Line Canal Temporary Rock Barriers - 2019, 2020 and 2021. State of California Natural Resources Agency Department of Water Resources Division of Engineering.

Community Model (2019). San Francisco Bay-Delta Community Model. http://www.d3d-baydelta.org/.

Deltares (2019). *D-Flow Flexible Mesh User Manual*. Version 1.5.0. SVN Revision: 62704. July 19, 2019.

Enright, C. (2008). Suisun Marsh Salinity Control Gate: Purpose, operation, and hydrodynamics/salinity transport effect. Presentation given at the California Water and Environmental Modeling Forum, Folsom, CA. Retrieved from http://www.cwemf.org/Asilomar/ChrisEnright.pdf.

Khanna, S., Conrad, J. L., Caudill, J., Christman, M., Darin, G., Ellis, D., Gilbert, P., Hartman, R., Kayfetz, K., Pratt, W., Tobias, V., and Wasserman, A. (2018). Framework for Aquatic Vegetation Monitoring in the Delta. Technical report. Interagency Ecological Program Technical Report 92.

King, A. (2019). Wind over San Francisco Bay and the Sacramento-San Joaquin River Delta: Forcing for hydrodynamic models. Technical report, San Francisco Estuary Institute, Richmond, CA. SFEI Contribution No. 937.

Livneh, B., Bohn, T. J., Pierce, D. W., Munoz-Arriola, F., Nijssen, B., Vose, R., Cayan, D. R., and Brekke, L. (2015). A spatially comprehensive, meteorological data set for

Mexico, the U.S., and southern Canada (NCEI Accession 0129374). version 1.1. Retrieved from https://doi.org/10.7289/V5X34VF6; https://doi.org/10.1038/sdata.2015.42.

Ludwig, F. L., Livingston, J. M., and Endlich, R. M. (1991). Use of mass conservation and critical dividing streamline concepts for efficient objective analysis of winds in complex terrain. *J. Appl. Meteor.*, 30:1490–1499.

Ludwig, F. L. and Sinton, D. (2000). Evaluating an objective wind analysis technique with a long record of routinely collected data. *J. Appl. Meteor.*, 39:335–348.

Martyr-Koller, R. C., Kernkamp, H. W. J., van Dam, A., van der Wegen, M., Lucas, L. V., Knowles, N., Jaffe, B., and Fregoso, T. A. (2017). Application of an unstructured 3D finite volume numerical model to flows and salinity dynamics in the San Francisco Bay-Delta. *Estuarine, Coastal and Shelf Science*, 192:86–107.

Neveu, E., Moore, A. M., Edwards, C. A., Fiechter, J., Drake, P., Crawford, W. J., Jacox, M. G., and Nuss, E. (2016). An historical analysis of the California Current circulation using ROMS 4D-Var: System configuration and diagnostics. *Ocean Modelling*, 99:133–151.

Shore Stations Program (2019). Farallon Islands measurements collected by Point Blue Conservation Science. Data provided by the Shore Stations Program sponsored at Scripps Institution of Oceanography by California State Parks, Division of Boating and Waterways. Contact: shorestation@ucsd.edu.

USGS (2018). CASCaDE: Computational Assessments of Scenarios of Change for the Delta Ecosystem. https://cascade.wr.usgs.gov/.

Vroom, J., van der Wegen, M., MartyrKoller, R. C., and Lucas, L. V. (2017). What determines water temperature dynamics in the San Francisco Bay-Delta system? *Water Resources Research*, 53:9901–9921.

Willmott, C. J. (1981). On the validation of models. *Physical Geography*, 2:184–194.

A Validation Plots: Discharge

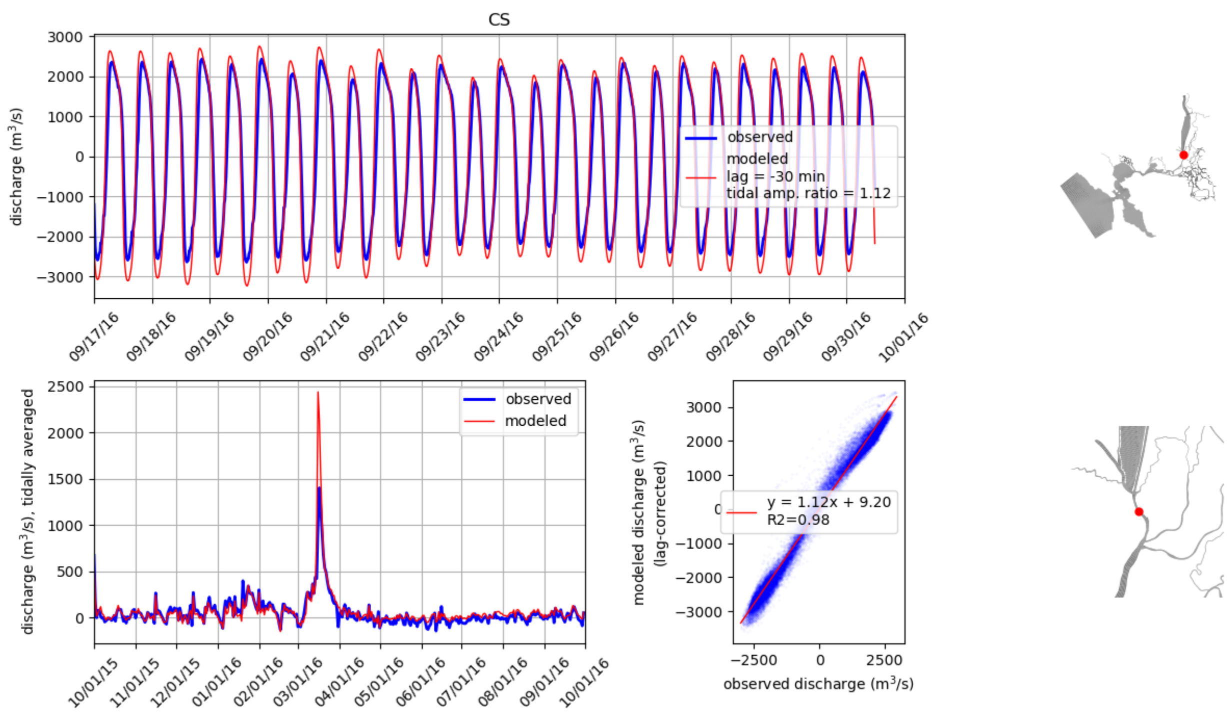

Figure 13: Comparison of modeled and observed flow rates at station CS. Tidally averaged signals are compared over the water year in lower left panel. Unfiltered signals are compared over a two-week period in the upper panel. Lower right panel compares unfiltered signals where modeled signal has been corrected for lag. On the right, the station location is shown on the model grid.

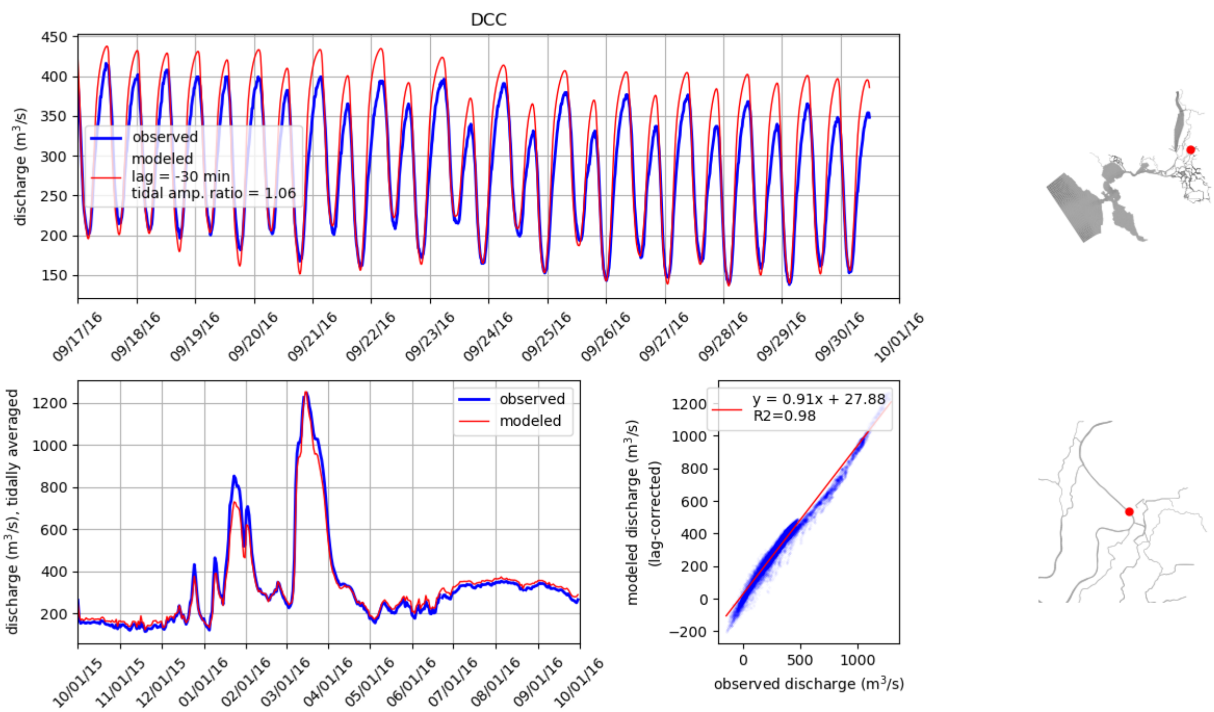

Figure 14: Comparison of modeled and observed flow rates at station DCC. Tidally averaged signals are compared over the water year in lower left panel. Unfiltered signals are compared over a two-week period in the upper panel. Lower right panel compares unfiltered signals where modeled signal has been corrected for lag. On the right, the station location is shown on the model grid.

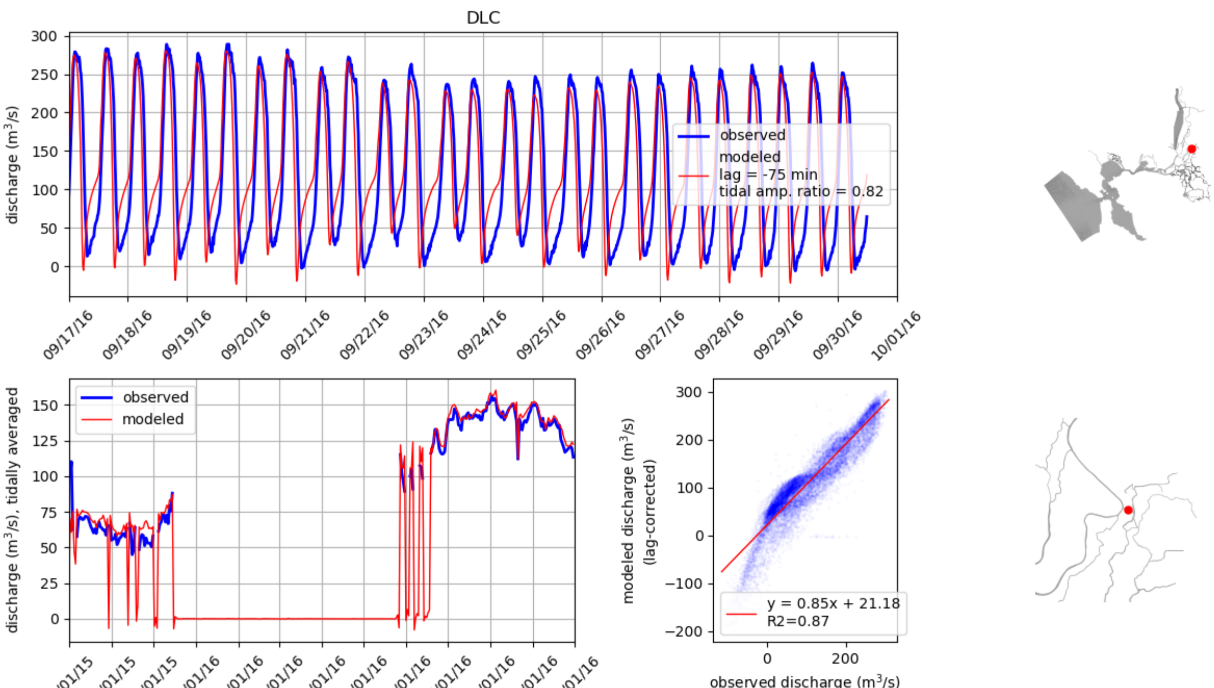

Figure 15: Comparison of modeled and observed flow rates at station DLC. Tidally averaged signals are compared over the water year in lower left panel. Unfiltered signals are compared over a two-week period in the upper panel. Lower right panel compares unfiltered signals where modeled signal has been corrected for lag. On the right, the station location is shown on the model grid.

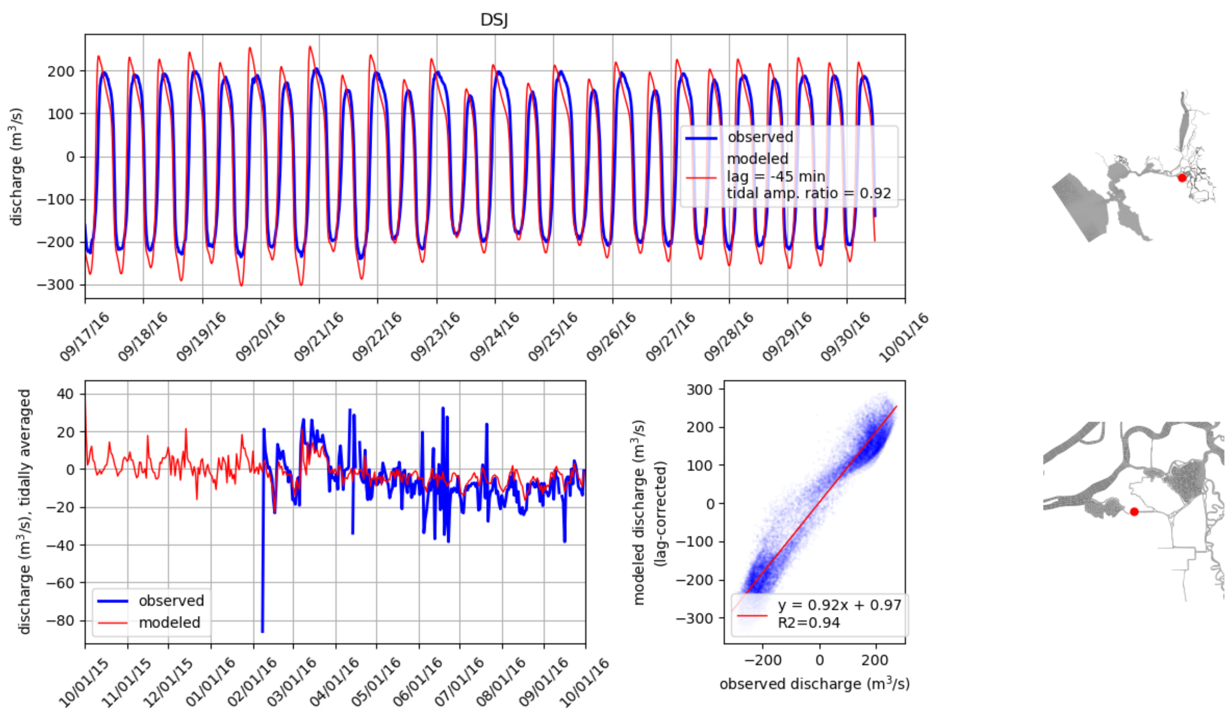

Figure 16: Comparison of modeled and observed flow rates at station DSJ. Tidally averaged signals are compared over the water year in lower left panel. Unfiltered signals are compared over a two-week period in the upper panel. Lower right panel compares unfiltered signals where modeled signal has been corrected for lag. On the right, the station location is shown on the model grid.

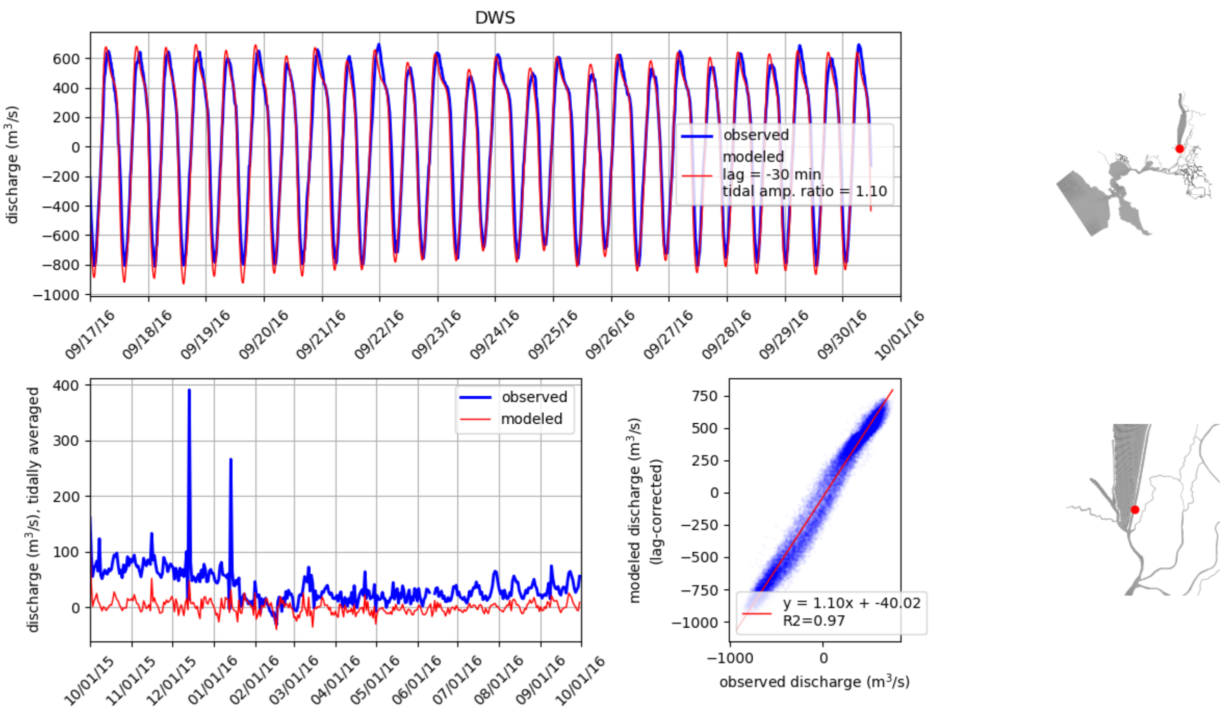

Figure 17: Comparison of modeled and observed flow rates at station DWS. Tidally averaged signals are compared over the water year in lower left panel. Unfiltered signals are compared over a two-week period in the upper panel. Lower right panel compares unfiltered signals where modeled signal has been corrected for lag. On the right, the station location is shown on the model grid.

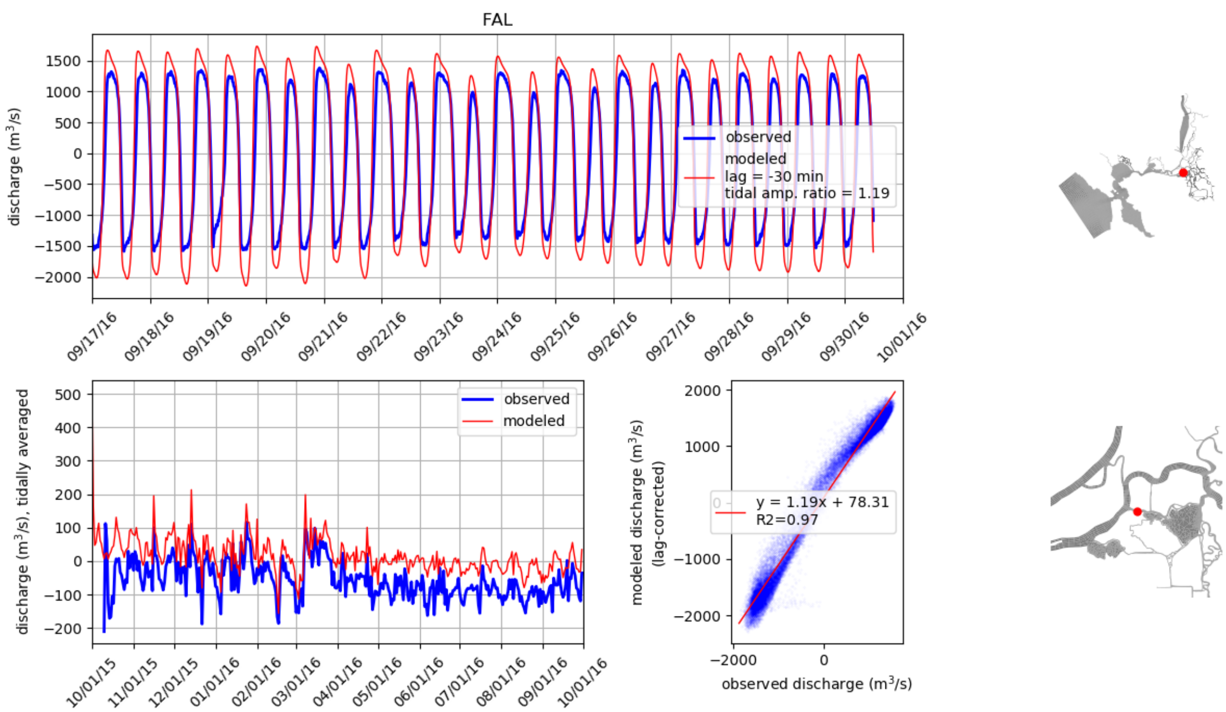

Figure 18: Comparison of modeled and observed flow rates at station FAL. Tidally averaged signals are compared over the water year in lower left panel. Unfiltered signals are compared over a two-week period in the upper panel. Lower right panel compares unfiltered signals where modeled signal has been corrected for lag. On the right, the station location is shown on the model grid.

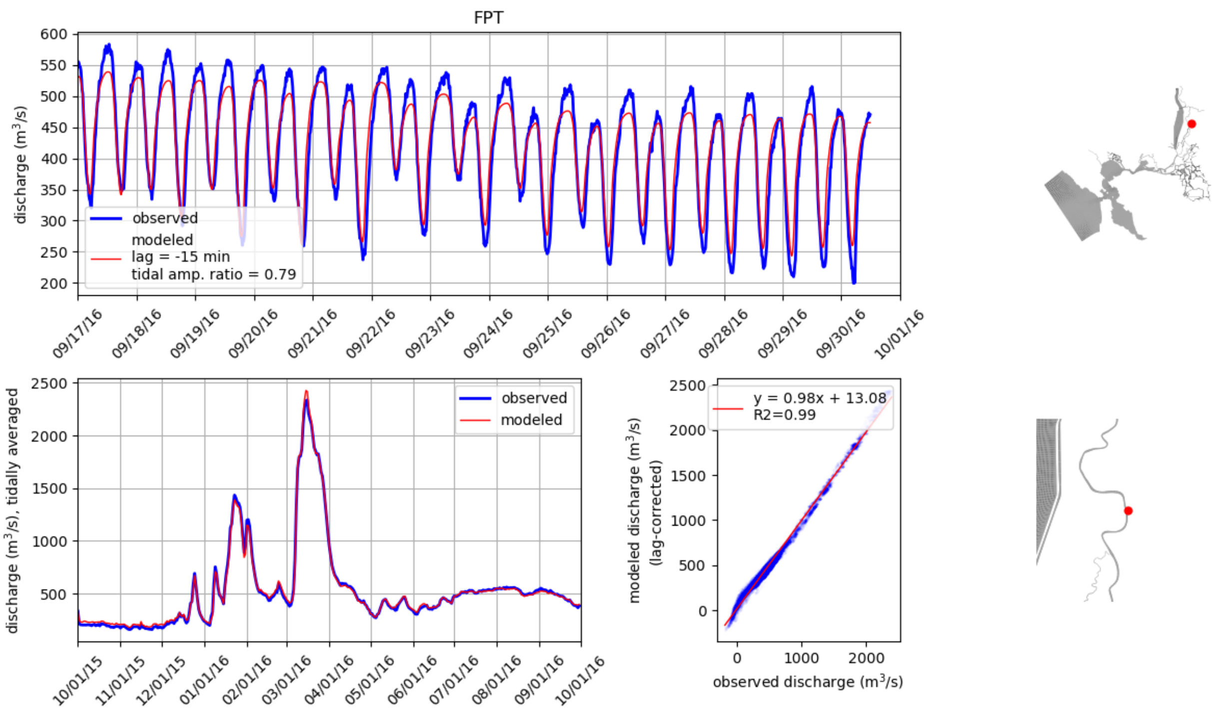

Figure 19: Comparison of modeled and observed flow rates at station FPT. Tidally averaged signals are compared over the water year in lower left panel. Unfiltered signals are compared over a two-week period in the upper panel. Lower right panel compares unfiltered signals where modeled signal has been corrected for lag. On the right, the station location is shown on the model grid.

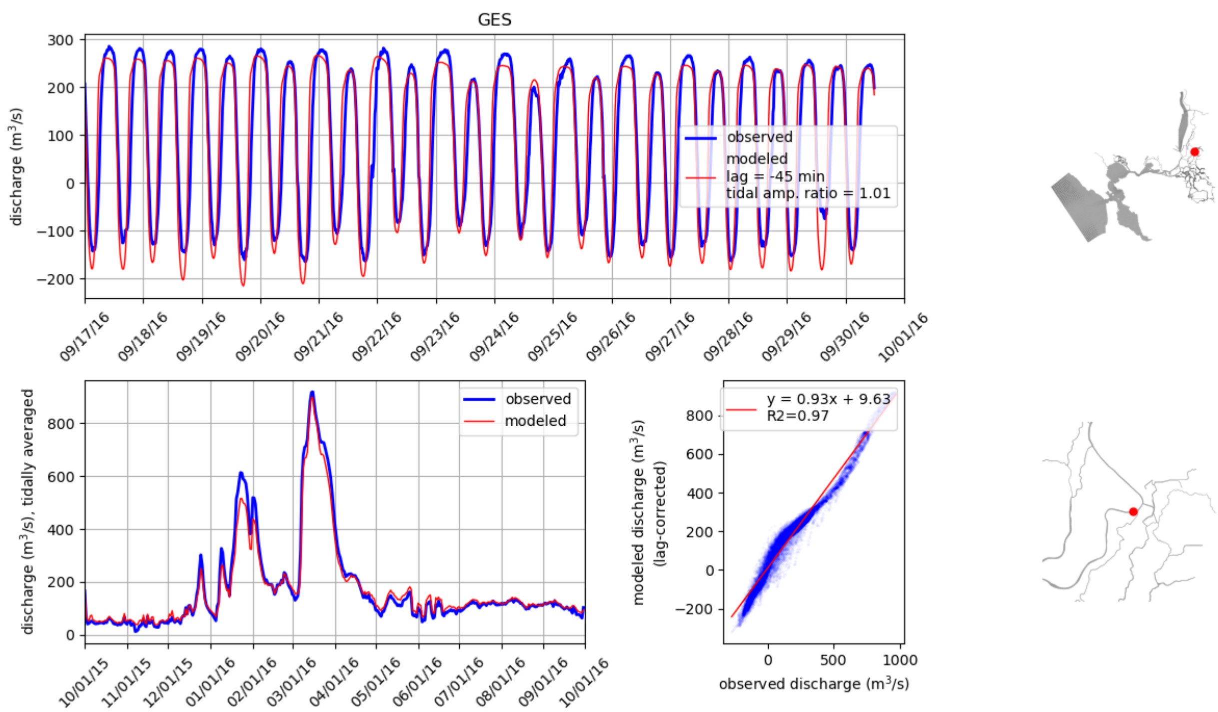

Figure 20: Comparison of modeled and observed flow rates at station GES. Tidally averaged signals are compared over the water year in lower left panel. Unfiltered signals are compared over a two-week period in the upper panel. Lower right panel compares unfiltered signals where modeled signal has been corrected for lag. On the right, the station location is shown on the model grid.

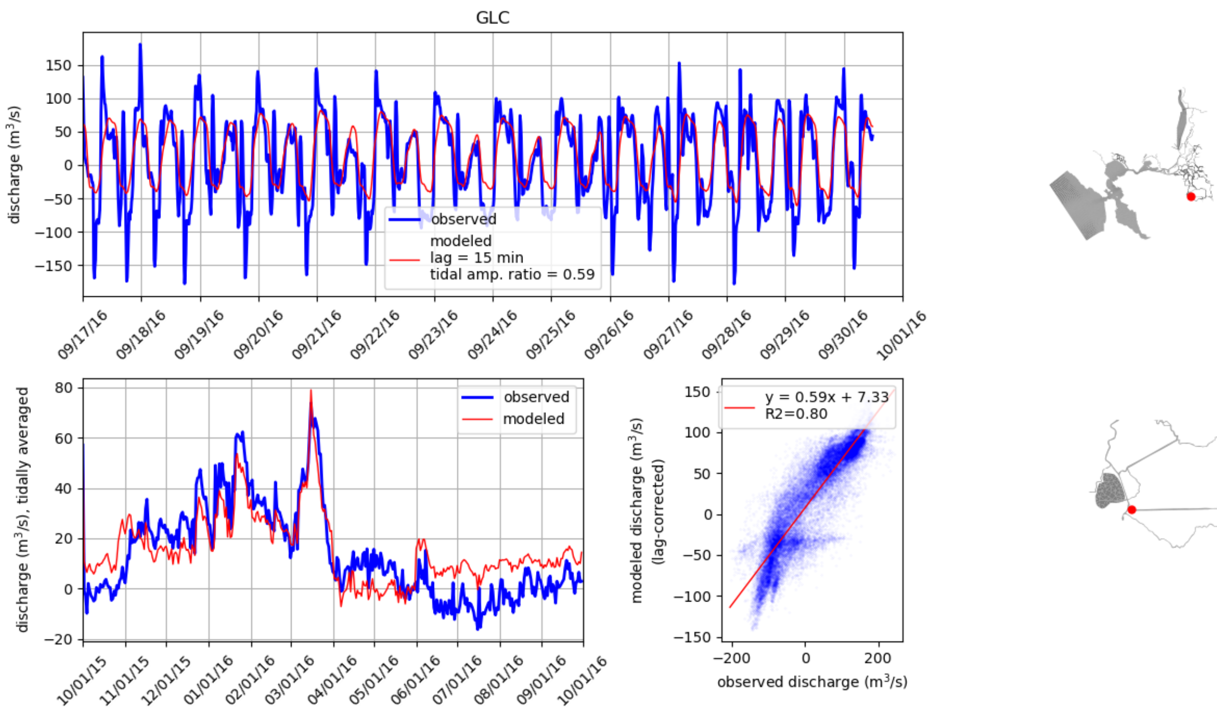

Figure 21: Comparison of modeled and observed flow rates at station GLC. Tidally averaged signals are compared over the water year in lower left panel. Unfiltered signals are compared over a two-week period in the upper panel. Lower right panel compares unfiltered signals where modeled signal has been corrected for lag. On the right, the station location is shown on the model grid.

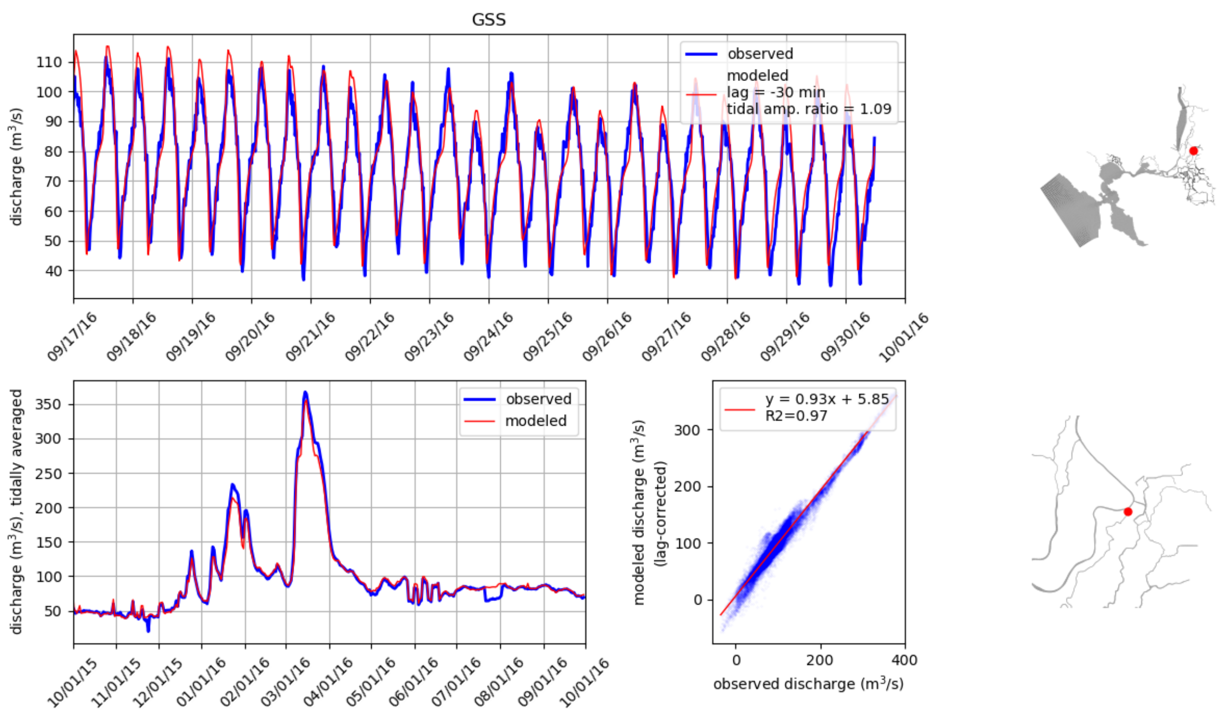

Figure 22: Comparison of modeled and observed flow rates at station GSS. Tidally averaged signals are compared over the water year in lower left panel. Unfiltered signals are compared over a two-week period in the upper panel. Lower right panel compares unfiltered signals where modeled signal has been corrected for lag. On the right, the station location is shown on the model grid.

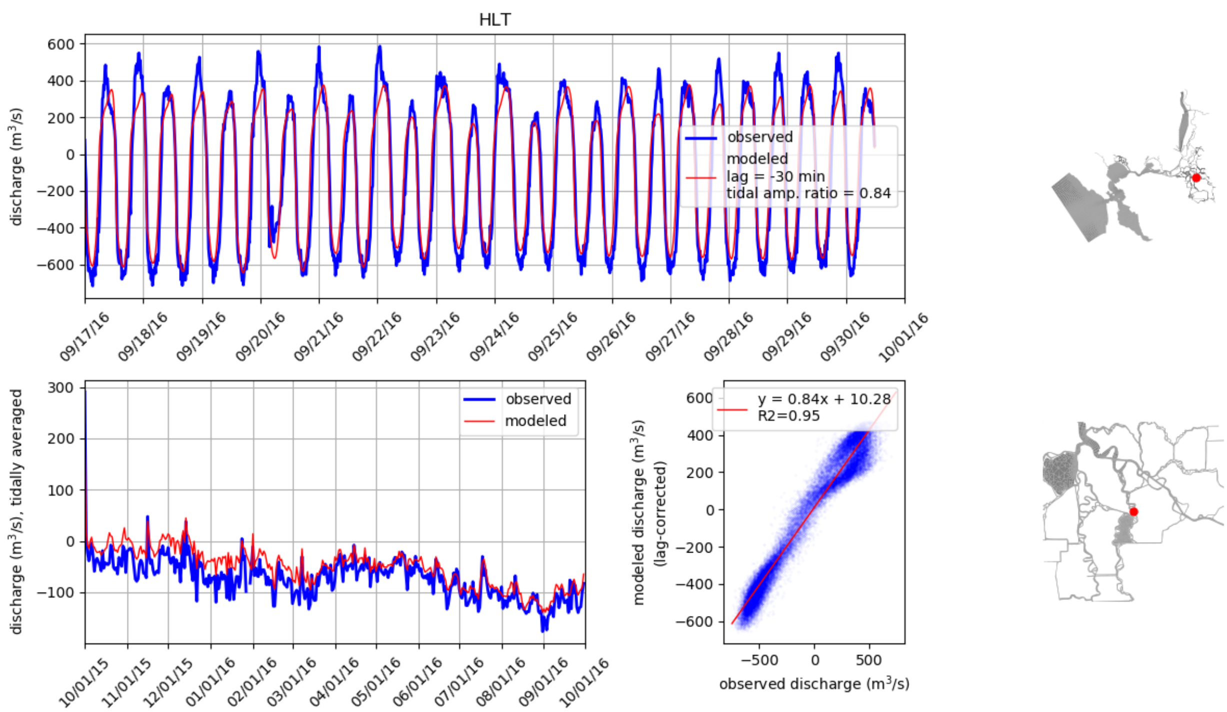

Figure 23: Comparison of modeled and observed flow rates at station HLT. Tidally averaged signals are compared over the water year in lower left panel. Unfiltered signals are compared over a two-week period in the upper panel. Lower right panel compares unfiltered signals where modeled signal has been corrected for lag. On the right, the station location is shown on the model grid.

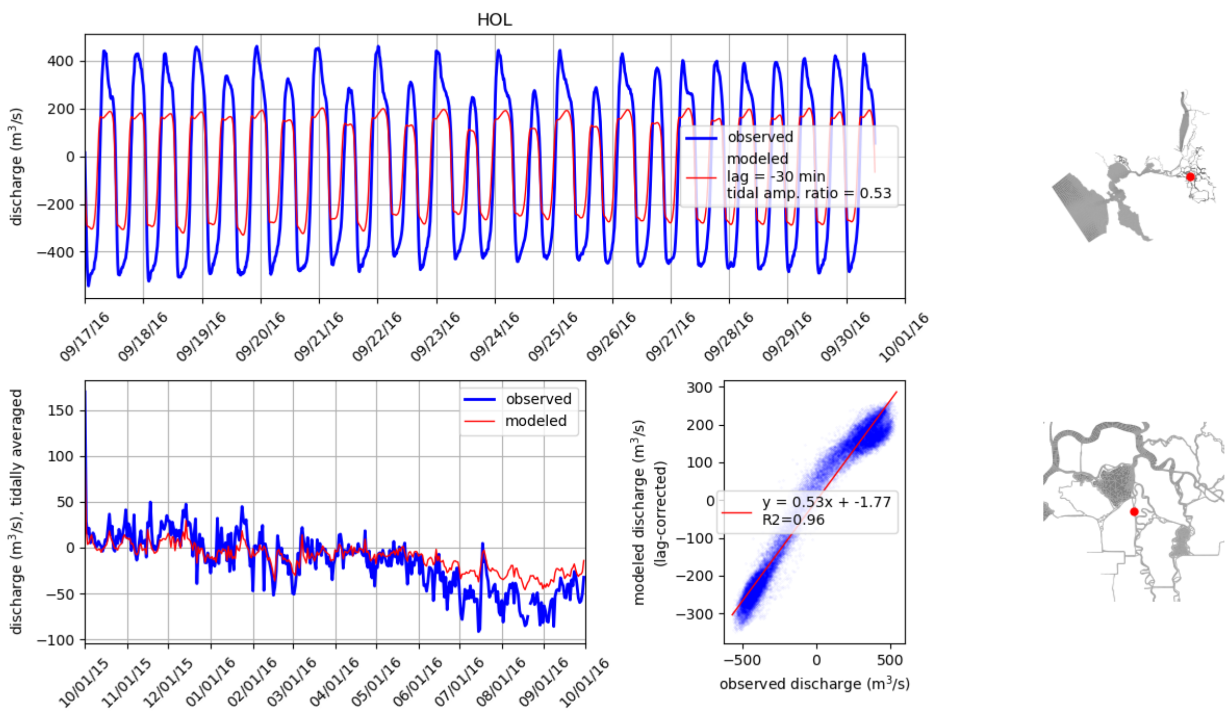

Figure 24: Comparison of modeled and observed flow rates at station HOL. Tidally averaged signals are compared over the water year in lower left panel. Unfiltered signals are compared over a two-week period in the upper panel. Lower right panel compares unfiltered signals where modeled signal has been corrected for lag. On the right, the station location is shown on the model grid.

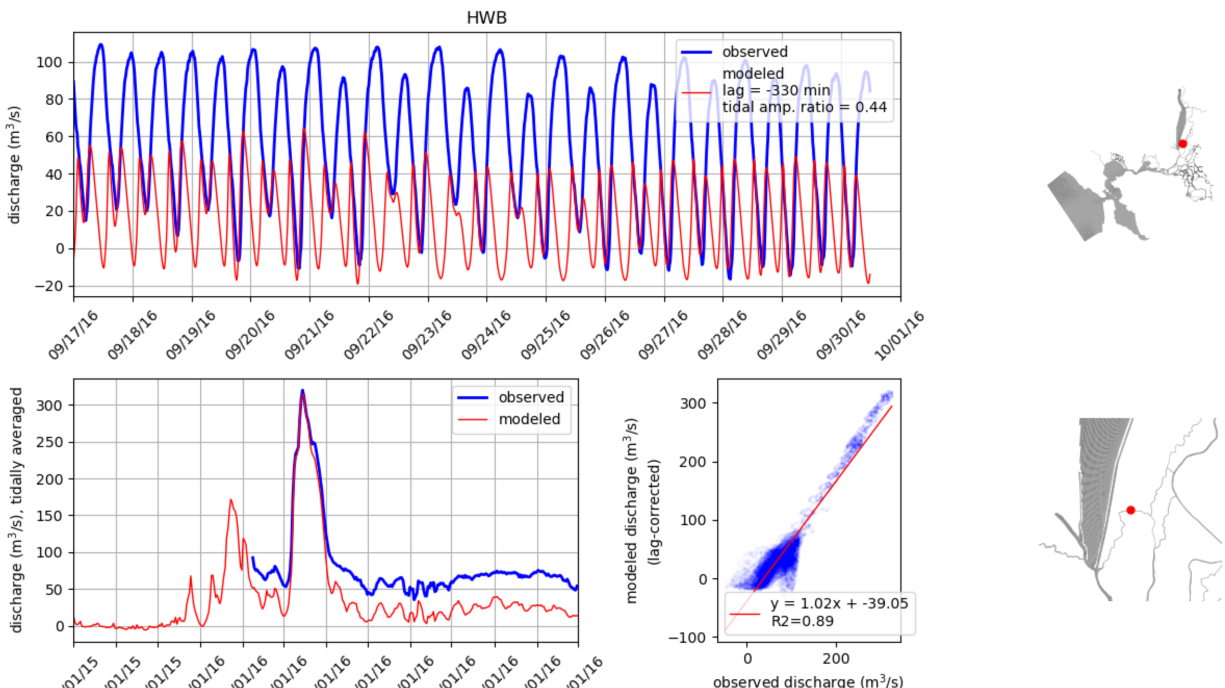

Figure 25: Comparison of modeled and observed flow rates at station HWB. Tidally averaged signals are compared over the water year in lower left panel. Unfiltered signals are compared over a two-week period in the upper panel. Lower right panel compares unfiltered signals where modeled signal has been corrected for lag. On the right, the station location is shown on the model grid.

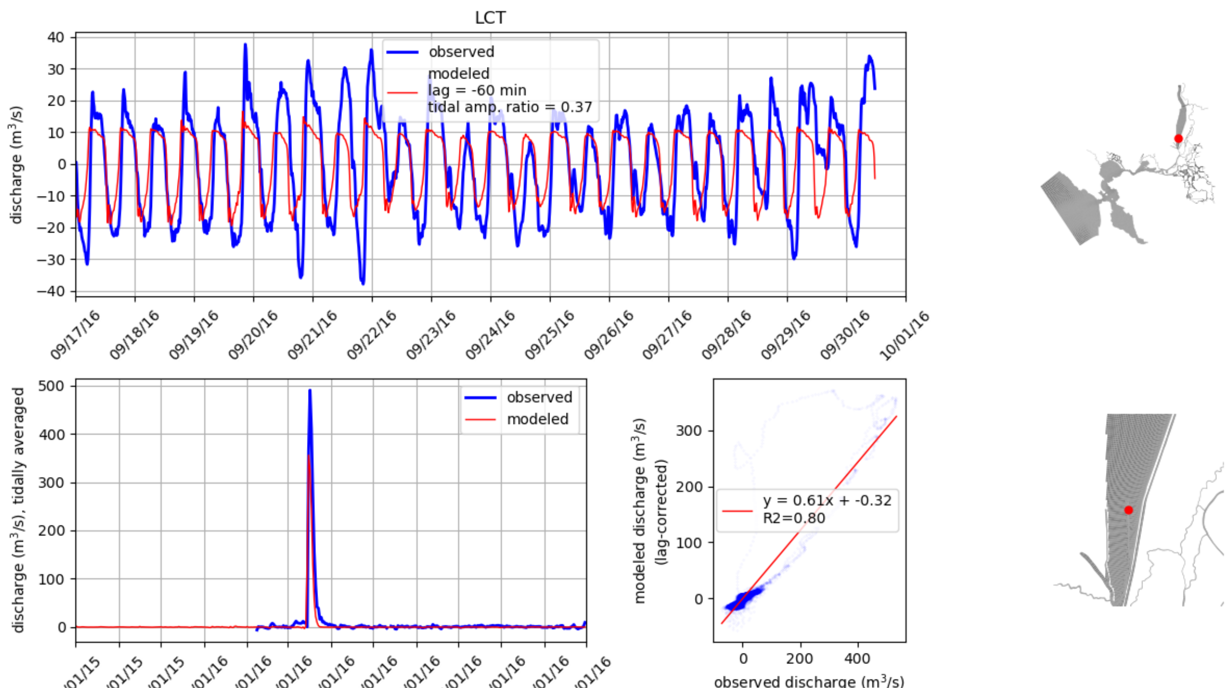

Figure 26: Comparison of modeled and observed flow rates at station LCT. Tidally averaged signals are compared over the water year in lower left panel. Unfiltered signals are compared over a two-week period in the upper panel. Lower right panel compares unfiltered signals where modeled signal has been corrected for lag. On the right, the station location is shown on the model grid.

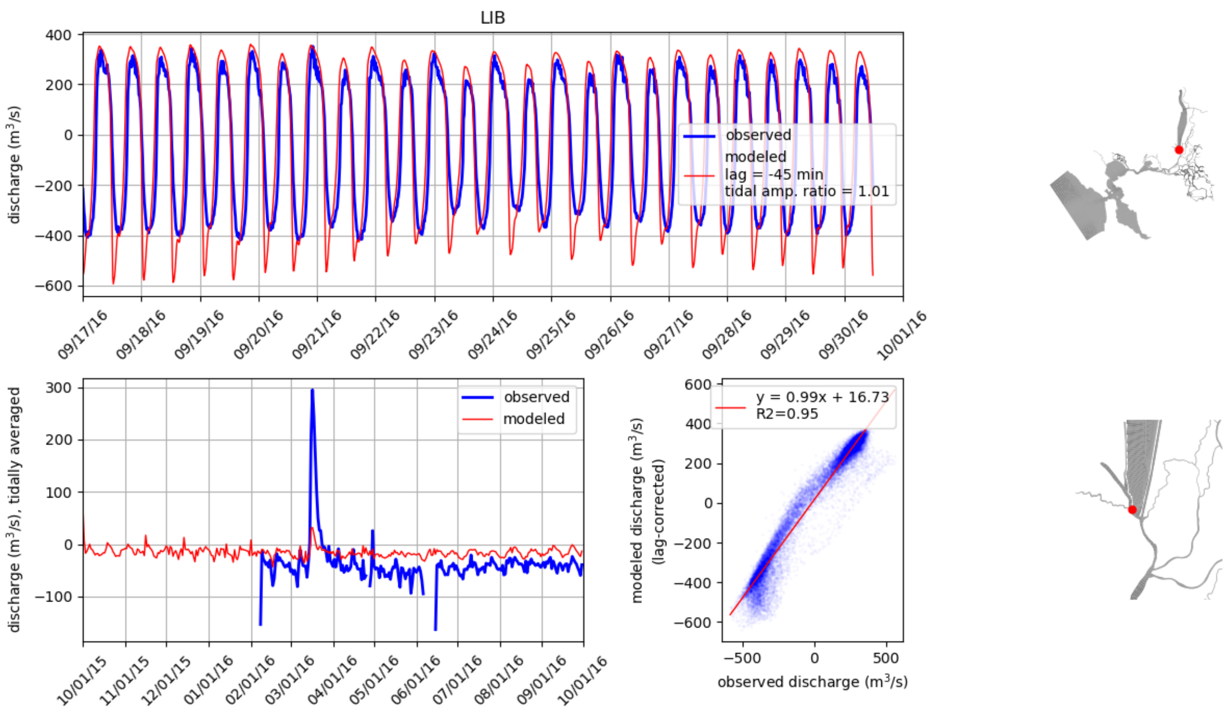

Figure 27: Comparison of modeled and observed flow rates at station LIB. Tidally averaged signals are compared over the water year in lower left panel. Unfiltered signals are compared over a two-week period in the upper panel. Lower right panel compares unfiltered signals where modeled signal has been corrected for lag. On the right, the station location is shown on the model grid.

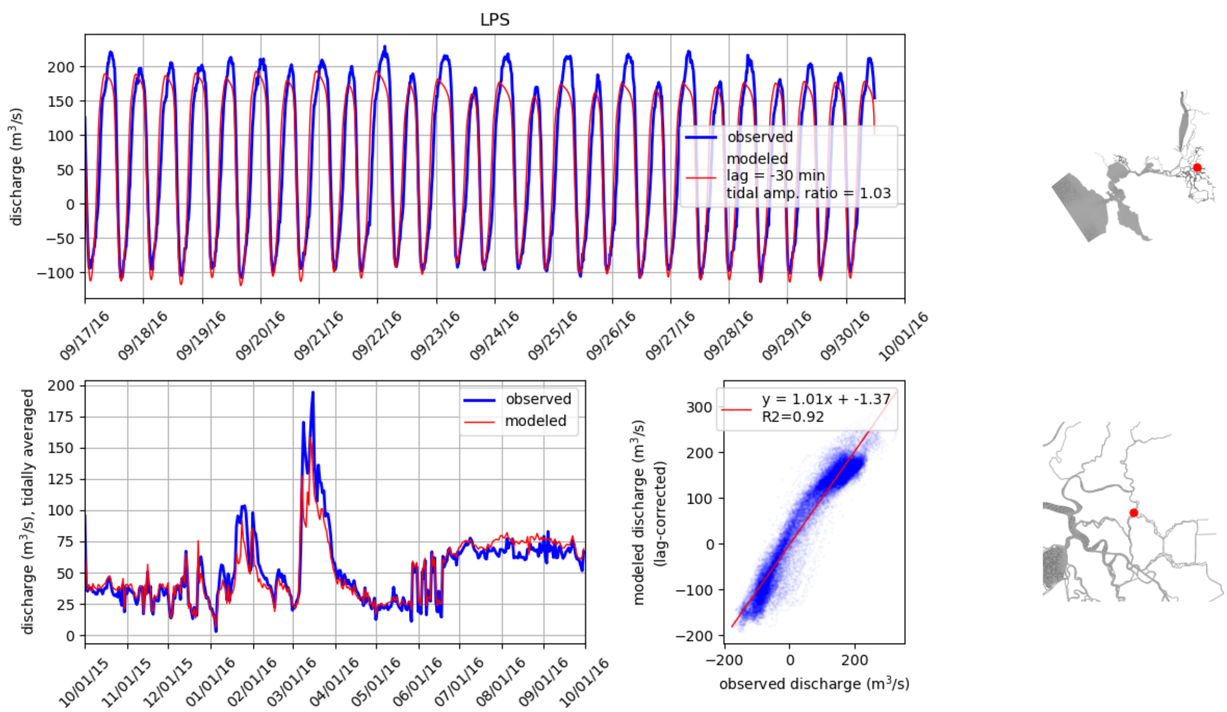

Figure 28: Comparison of modeled and observed flow rates at station LPS. Tidally averaged signals are compared over the water year in lower left panel. Unfiltered signals are compared over a two-week period in the upper panel. Lower right panel compares unfiltered signals where modeled signal has been corrected for lag. On the right, the station location is shown on the model grid.

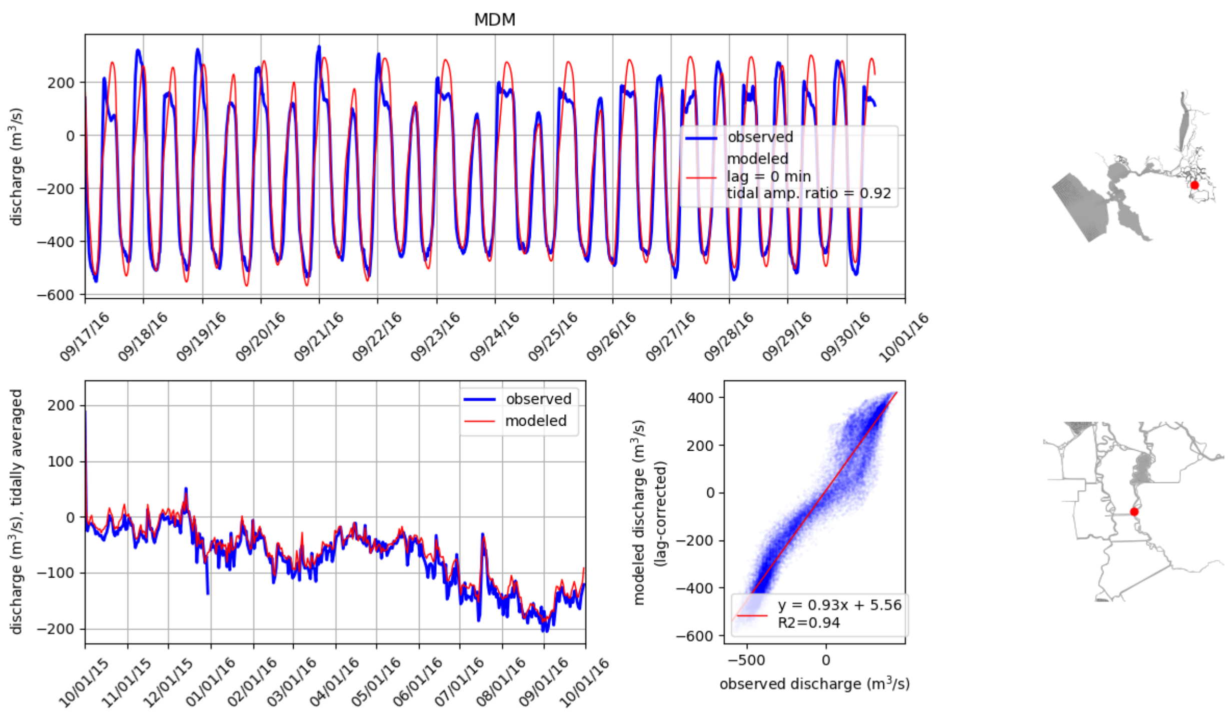

Figure 29: Comparison of modeled and observed flow rates at station MDM. Tidally averaged signals are compared over the water year in lower left panel. Unfiltered signals are compared over a two-week period in the upper panel. Lower right panel compares unfiltered signals where modeled signal has been corrected for lag. On the right, the station location is shown on the model grid.

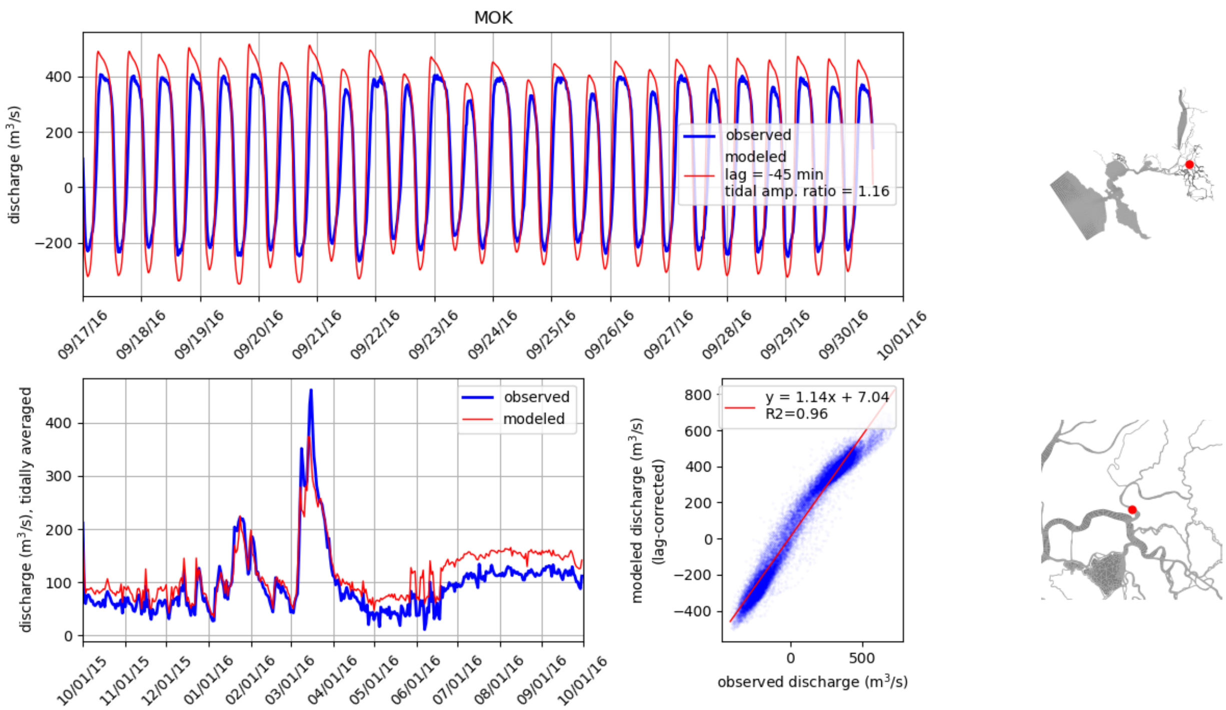

Figure 30: Comparison of modeled and observed flow rates at station MOK. Tidally averaged signals are compared over the water year in lower left panel. Unfiltered signals are compared over a two-week period in the upper panel. Lower right panel compares unfiltered signals where modeled signal has been corrected for lag. On the right, the station location is shown on the model grid.

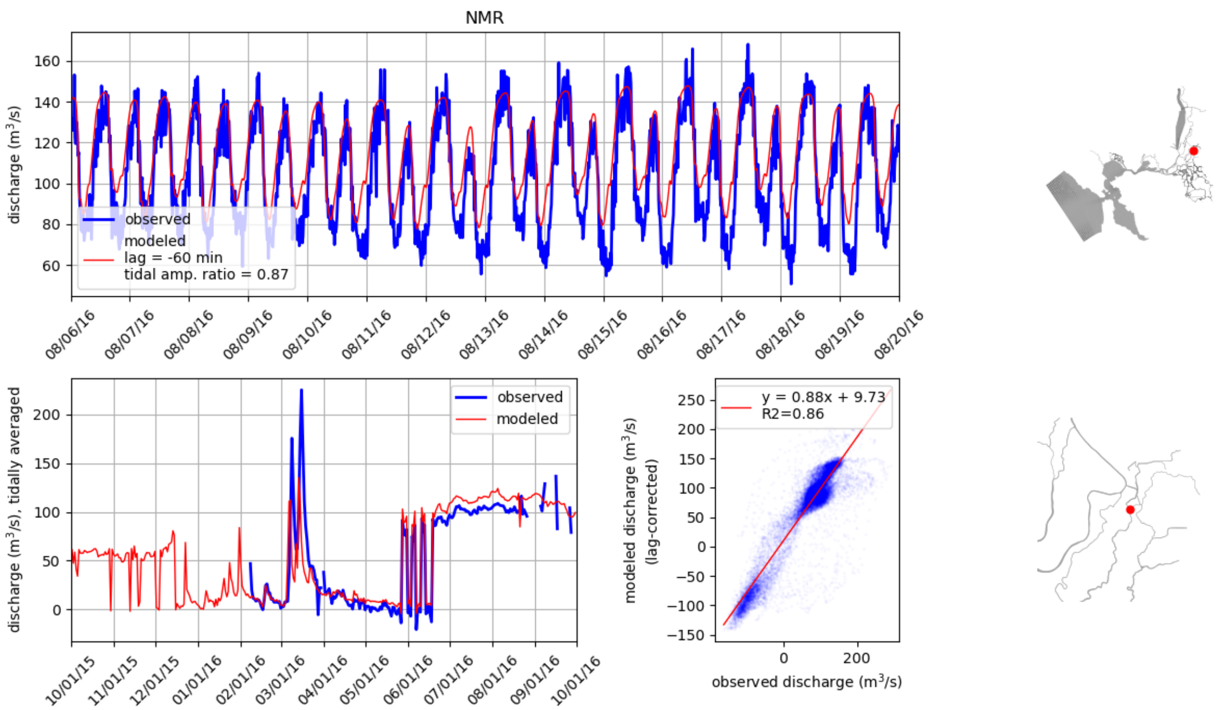

Figure 31: Comparison of modeled and observed flow rates at station NMR. Tidally averaged signals are compared over the water year in lower left panel. Unfiltered signals are compared over a two-week period in the upper panel. Lower right panel compares unfiltered signals where modeled signal has been corrected for lag. On the right, the station location is shown on the model grid.

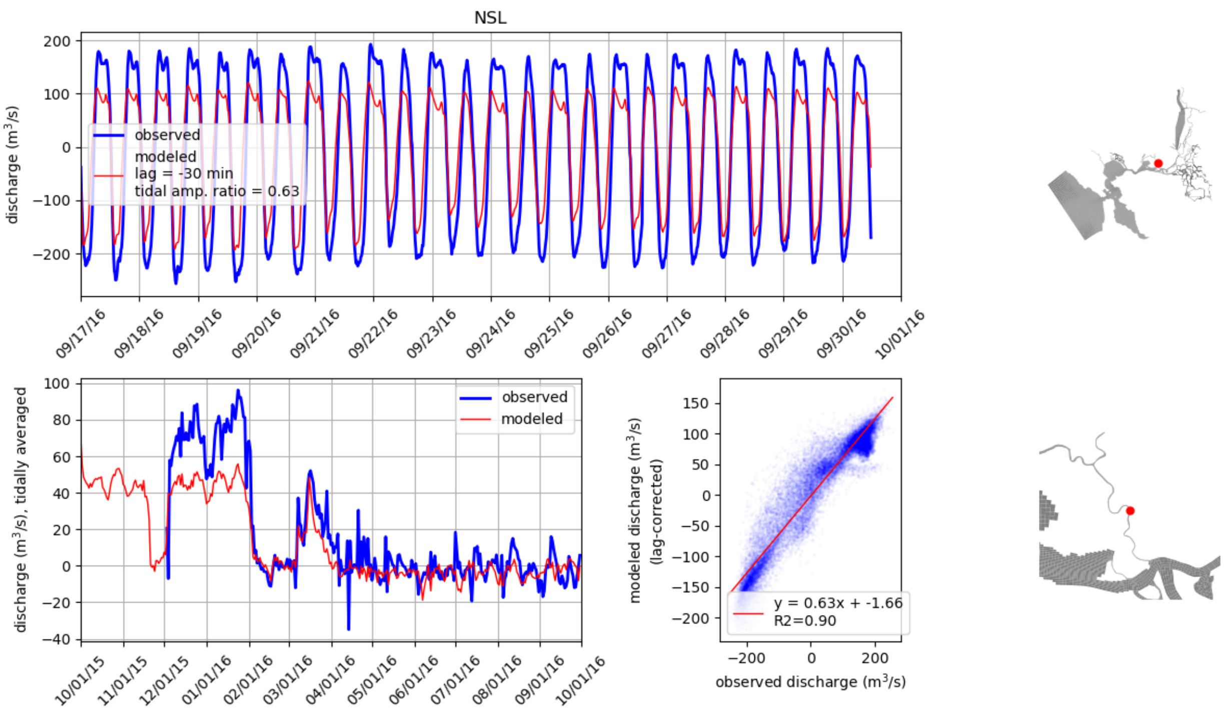

Figure 32: Comparison of modeled and observed flow rates at station NSL. Tidally averaged signals are compared over the water year in lower left panel. Unfiltered signals are compared over a two-week period in the upper panel. Lower right panel compares unfiltered signals where modeled signal has been corrected for lag. On the right, the station location is shown on the model grid.

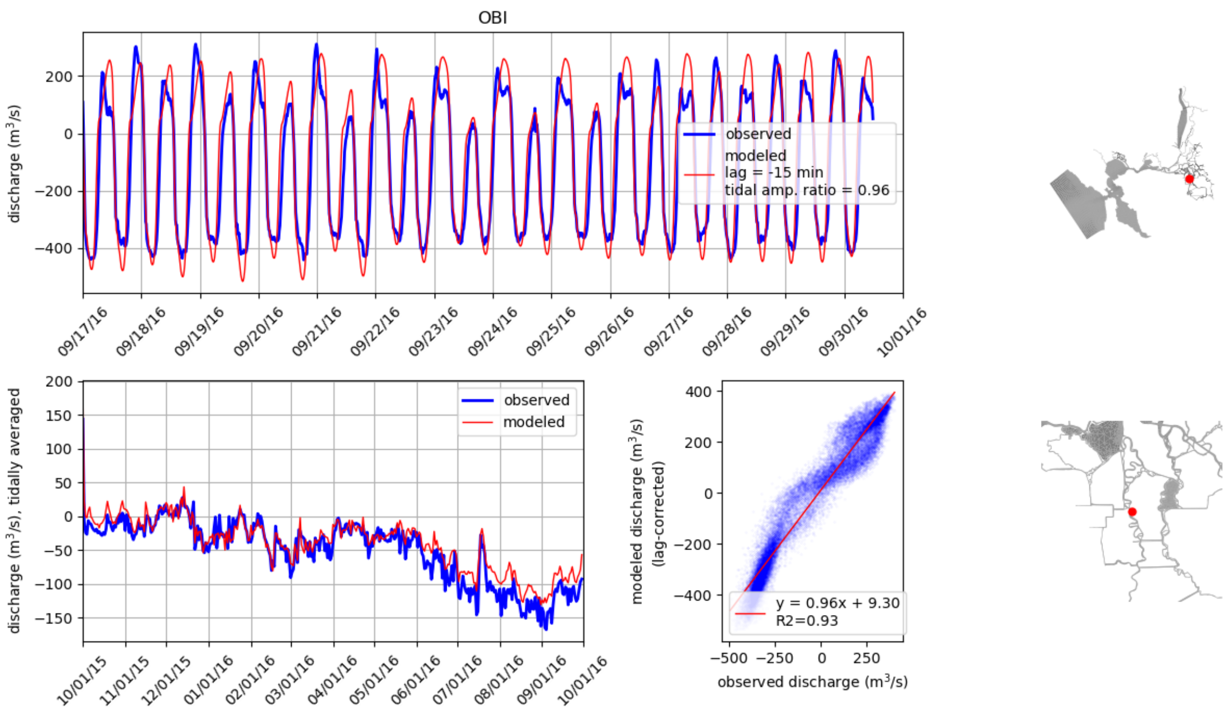

Figure 33: Comparison of modeled and observed flow rates at station OBI. Tidally averaged signals are compared over the water year in lower left panel. Unfiltered signals are compared over a two-week period in the upper panel. Lower right panel compares unfiltered signals where modeled signal has been corrected for lag. On the right, the station location is shown on the model grid.

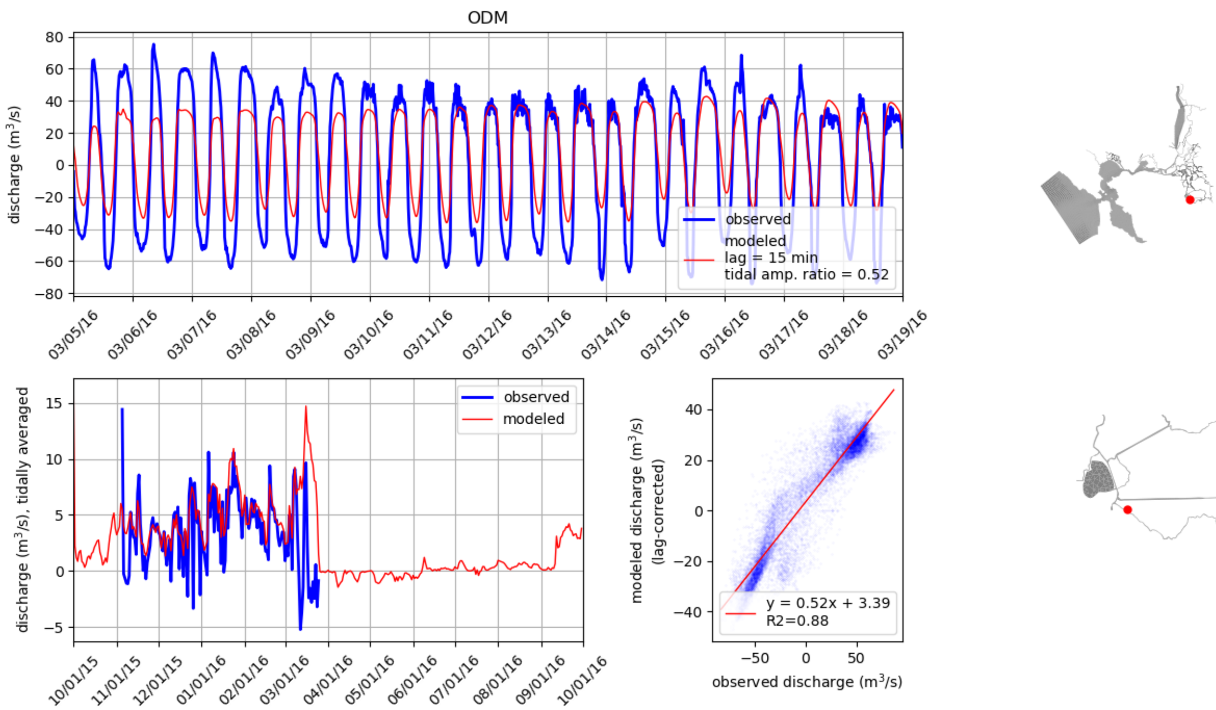

Figure 34: Comparison of modeled and observed flow rates at station ODM. Tidally averaged signals are compared over the water year in lower left panel. Unfiltered signals are compared over a two-week period in the upper panel. Lower right panel compares unfiltered signals where modeled signal has been corrected for lag. On the right, the station location is shown on the model grid.

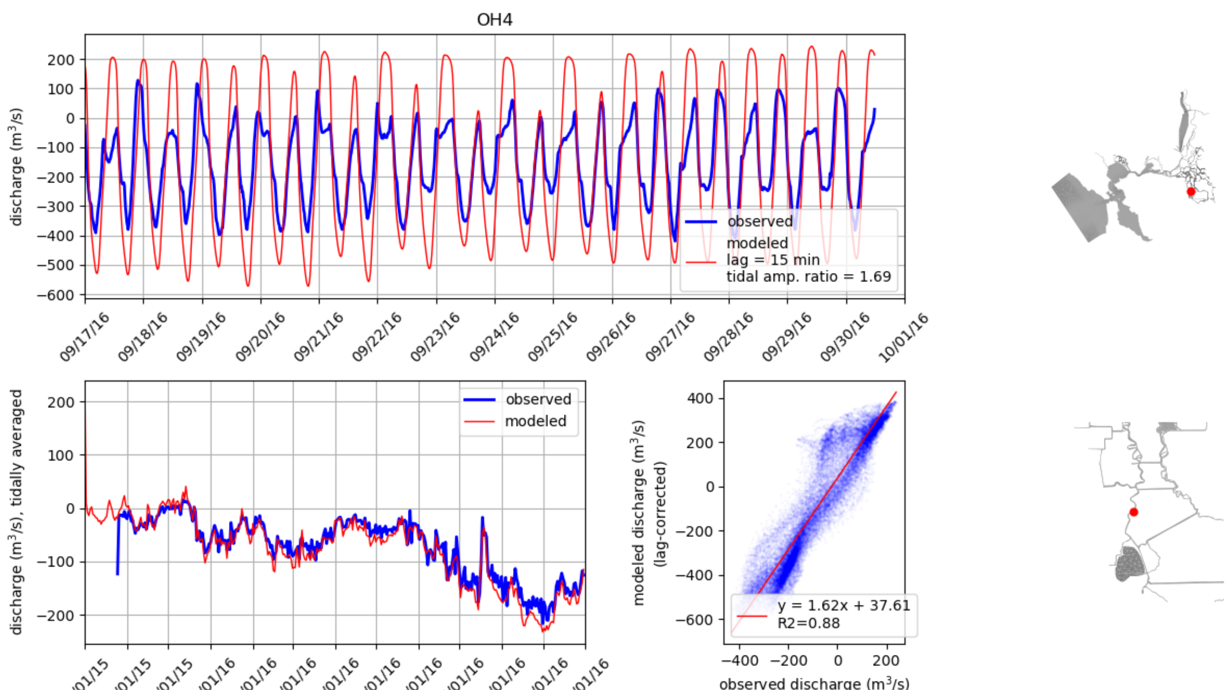

Figure 35: Comparison of modeled and observed flow rates at station OH4. Tidally averaged signals are compared over the water year in lower left panel. Unfiltered signals are compared over a two-week period in the upper panel. Lower right panel compares unfiltered signals where modeled signal has been corrected for lag. On the right, the station location is shown on the model grid.

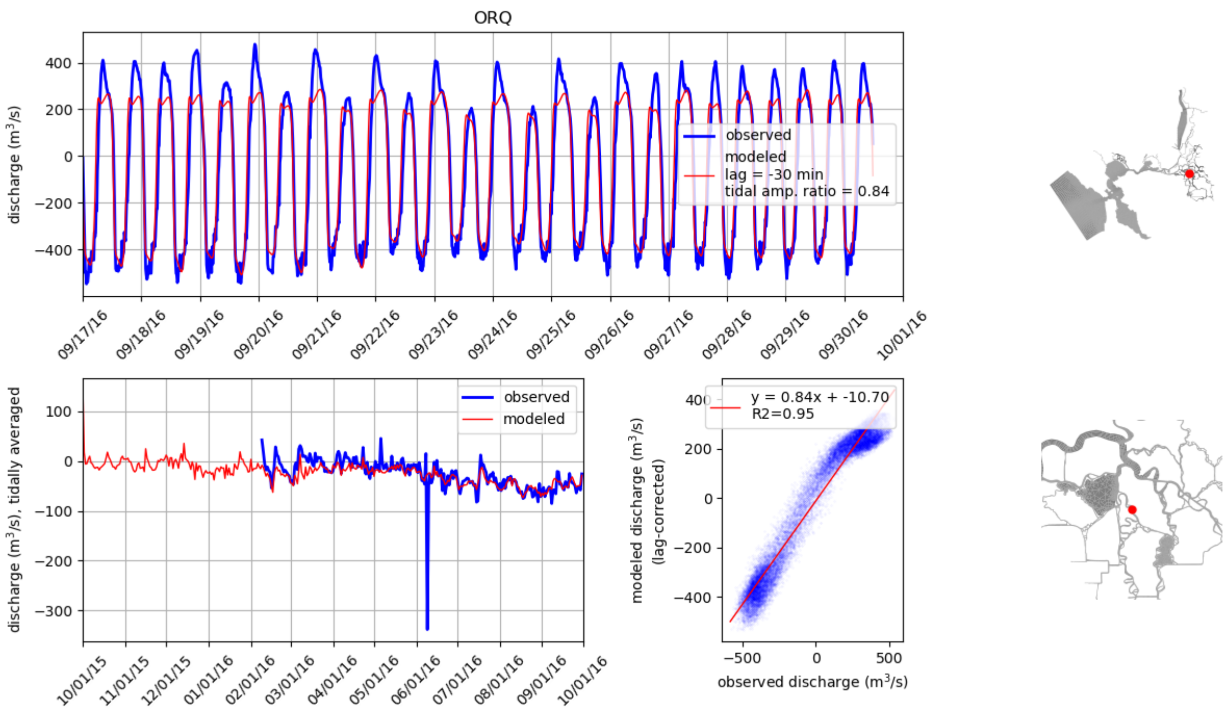

Figure 36: Comparison of modeled and observed flow rates at station ORQ. Tidally averaged signals are compared over the water year in lower left panel. Unfiltered signals are compared over a two-week period in the upper panel. Lower right panel compares unfiltered signals where modeled signal has been corrected for lag. On the right, the station location is shown on the model grid.

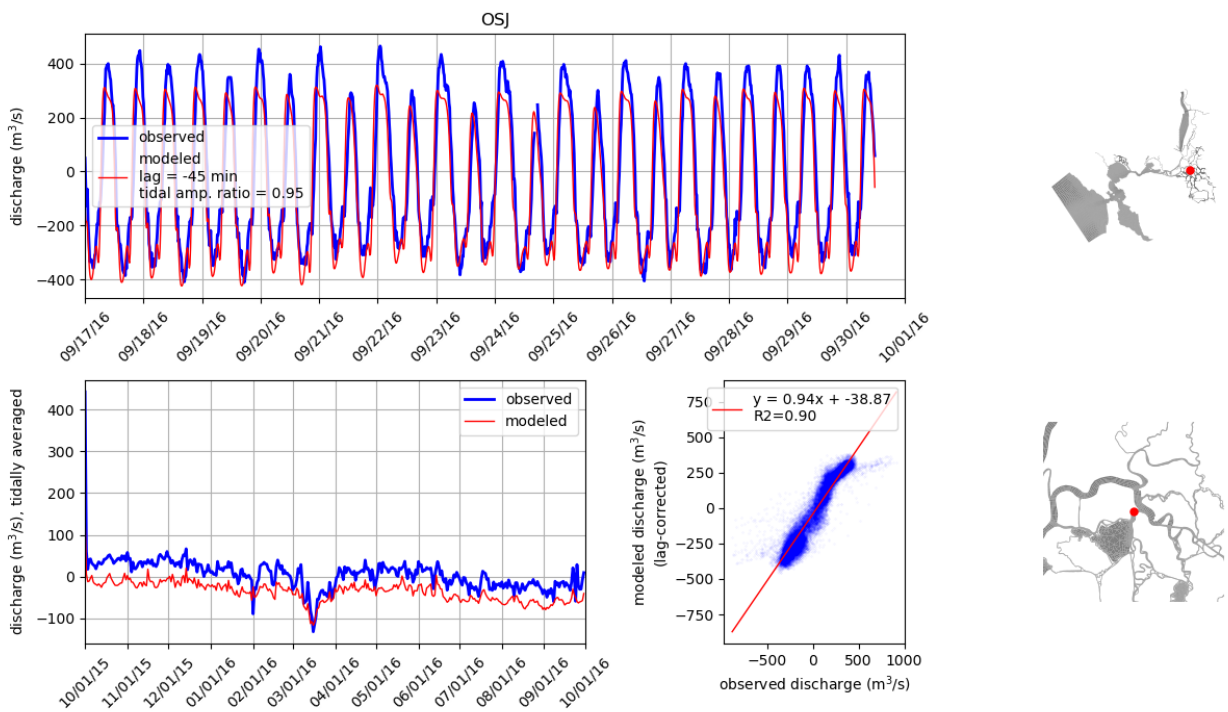

Figure 37: Comparison of modeled and observed flow rates at station OSJ. Tidally averaged signals are compared over the water year in lower left panel. Unfiltered signals are compared over a two-week period in the upper panel. Lower right panel compares unfiltered signals where modeled signal has been corrected for lag. On the right, the station location is shown on the model grid.

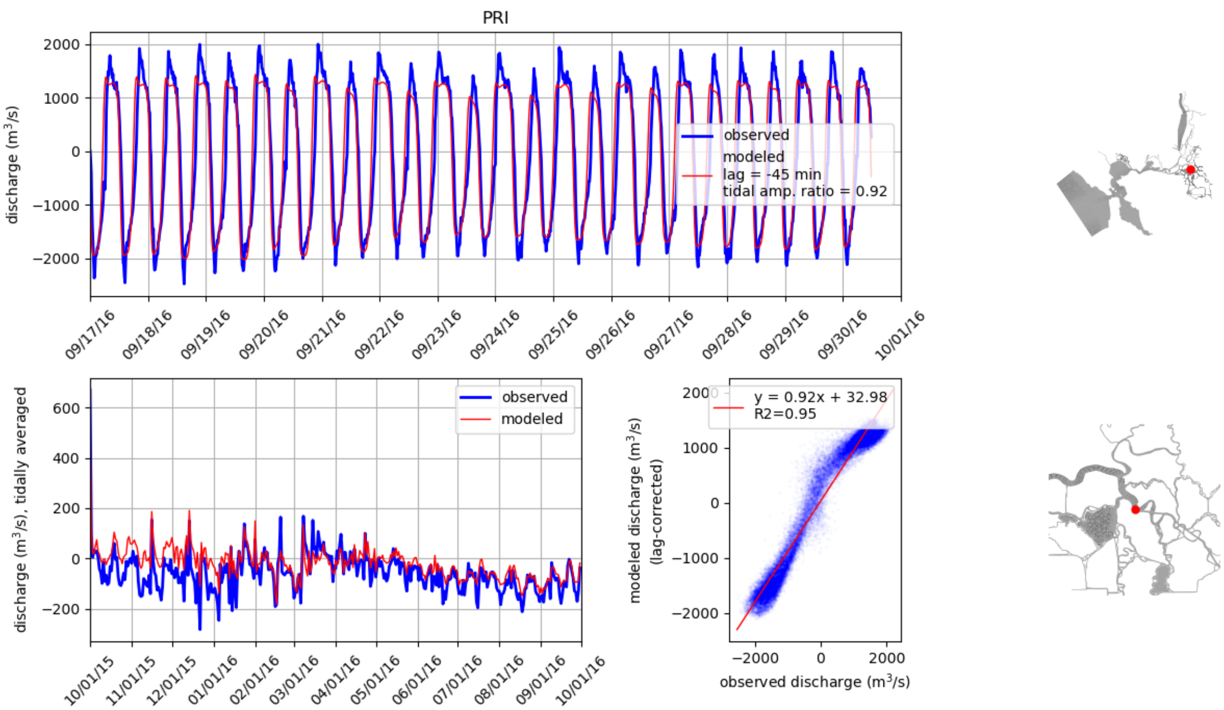

Figure 38: Comparison of modeled and observed flow rates at station PRI. Tidally averaged signals are compared over the water year in lower left panel. Unfiltered signals are compared over a two-week period in the upper panel. Lower right panel compares unfiltered signals where modeled signal has been corrected for lag. On the right, the station location is shown on the model grid.

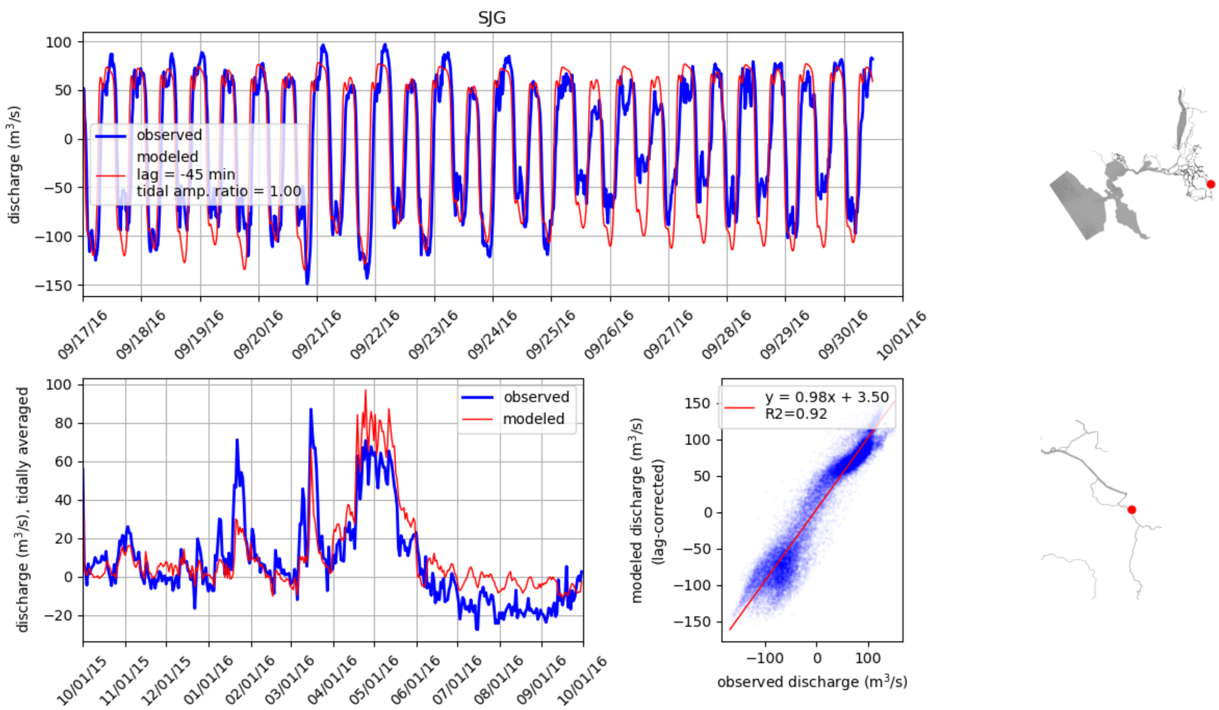

Figure 39: Comparison of modeled and observed flow rates at station SJG. Tidally averaged signals are compared over the water year in lower left panel. Unfiltered signals are compared over a two-week period in the upper panel. Lower right panel compares unfiltered signals where modeled signal has been corrected for lag. On the right, the station location is shown on the model grid.

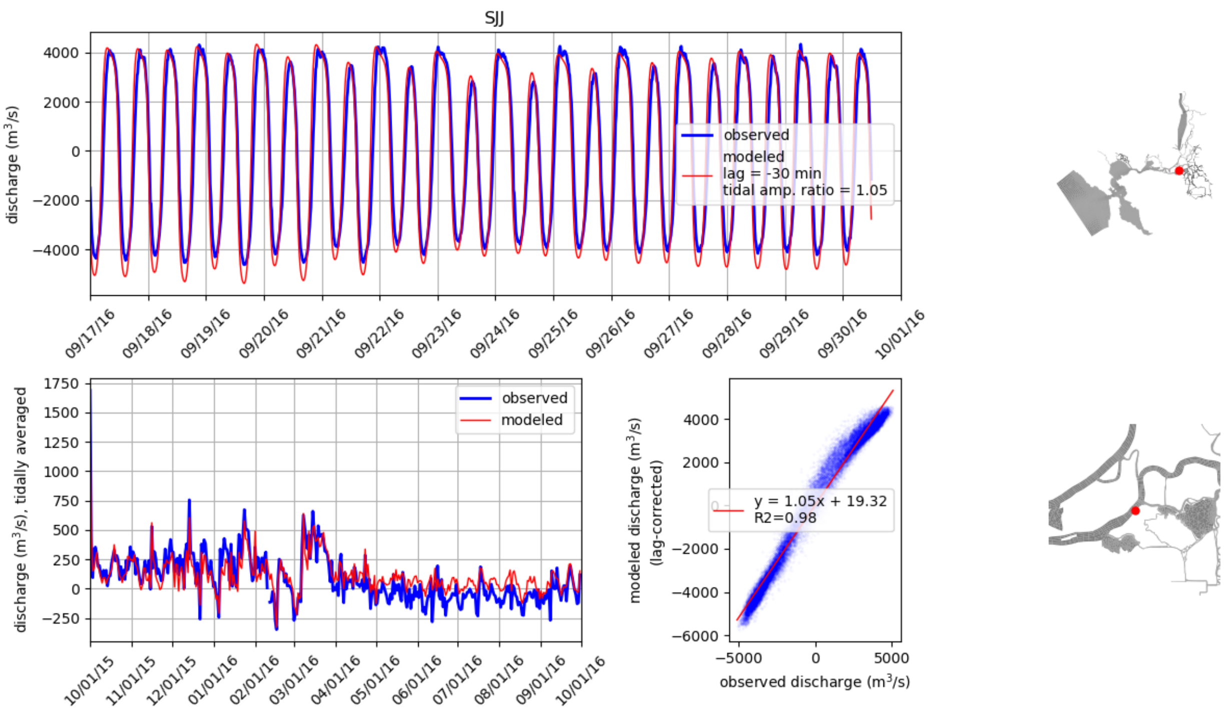

Figure 40: Comparison of modeled and observed flow rates at station SJJ. Tidally averaged signals are compared over the water year in lower left panel. Unfiltered signals are compared over a two-week period in the upper panel. Lower right panel compares unfiltered signals where modeled signal has been corrected for lag. On the right, the station location is shown on the model grid.

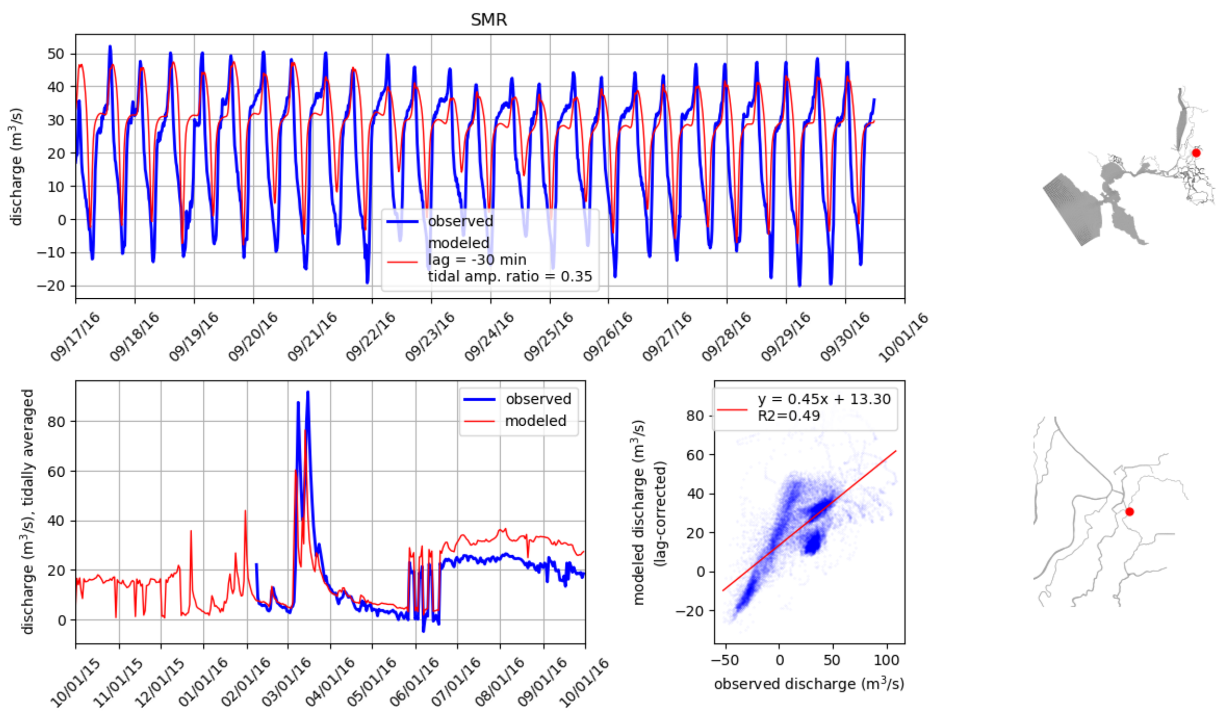

Figure 41: Comparison of modeled and observed flow rates at station SMR. Tidally averaged signals are compared over the water year in lower left panel. Unfiltered signals are compared over a two-week period in the upper panel. Lower right panel compares unfiltered signals where modeled signal has been corrected for lag. On the right, the station location is shown on the model grid.

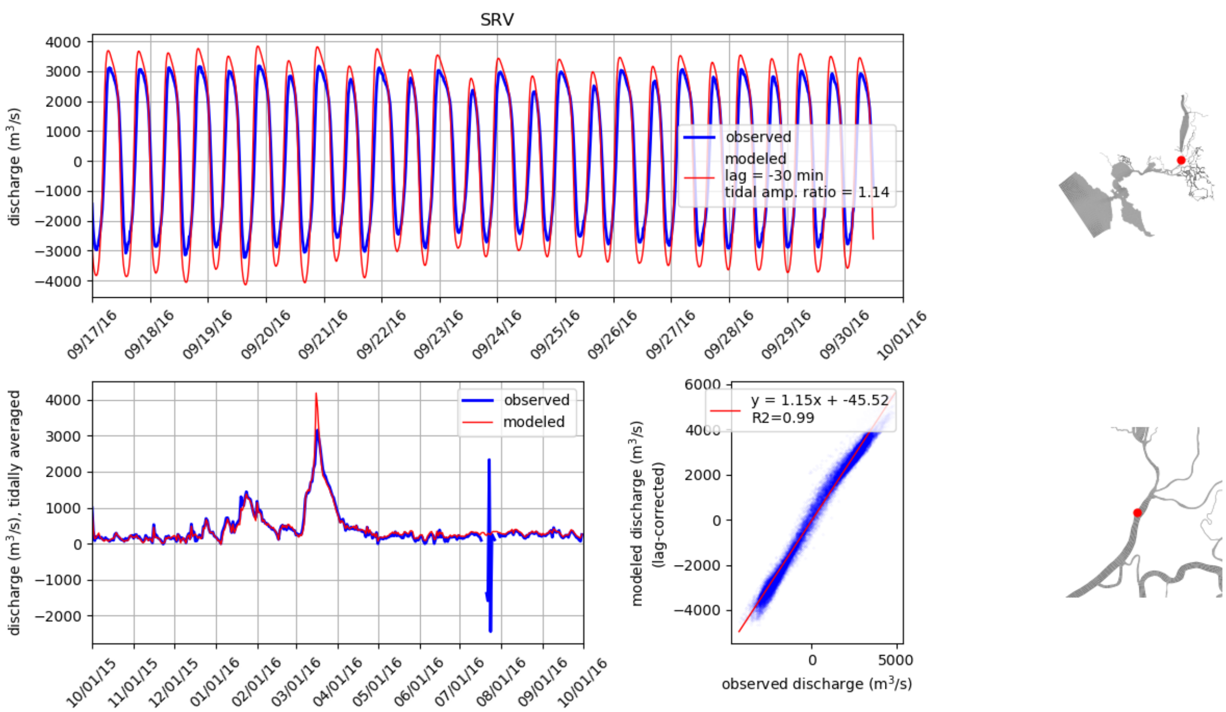

Figure 42: Comparison of modeled and observed flow rates at station SRV. Tidally averaged signals are compared over the water year in lower left panel. Unfiltered signals are compared over a two-week period in the upper panel. Lower right panel compares unfiltered signals where modeled signal has been corrected for lag. On the right, the station location is shown on the model grid.

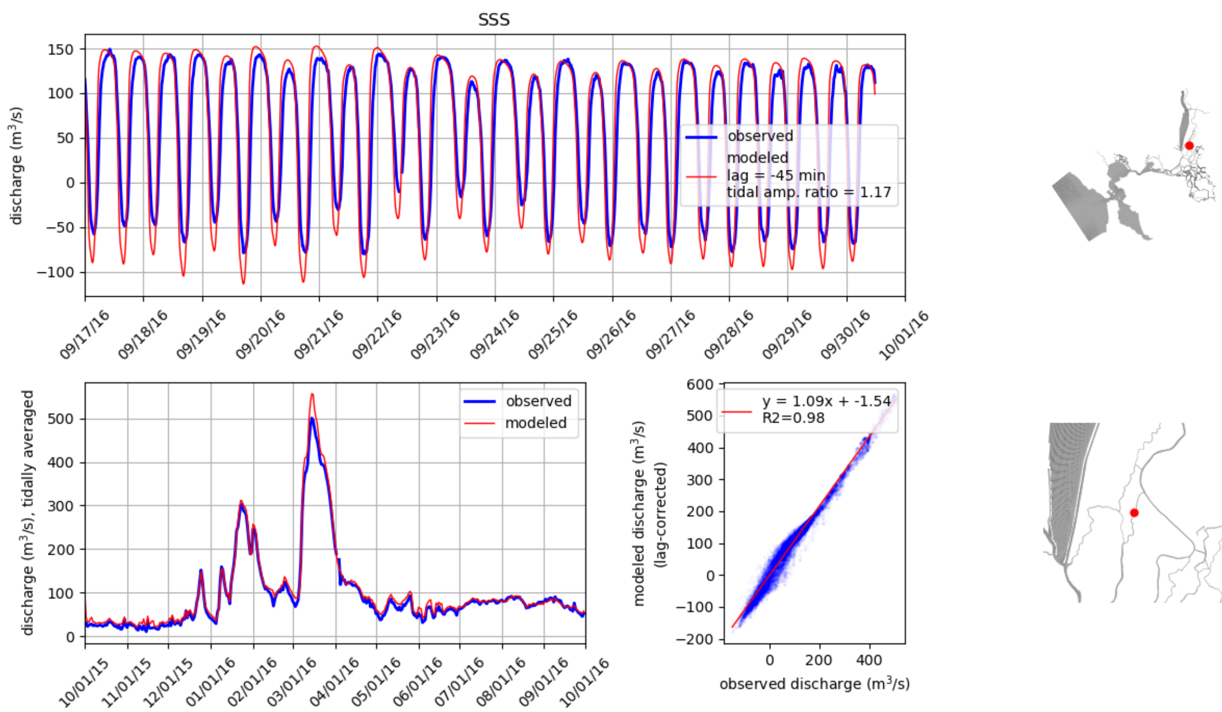

Figure 43: Comparison of modeled and observed flow rates at station SSS. Tidally averaged signals are compared over the water year in lower left panel. Unfiltered signals are compared over a two-week period in the upper panel. Lower right panel compares unfiltered signals where modeled signal has been corrected for lag. On the right, the station location is shown on the model grid.

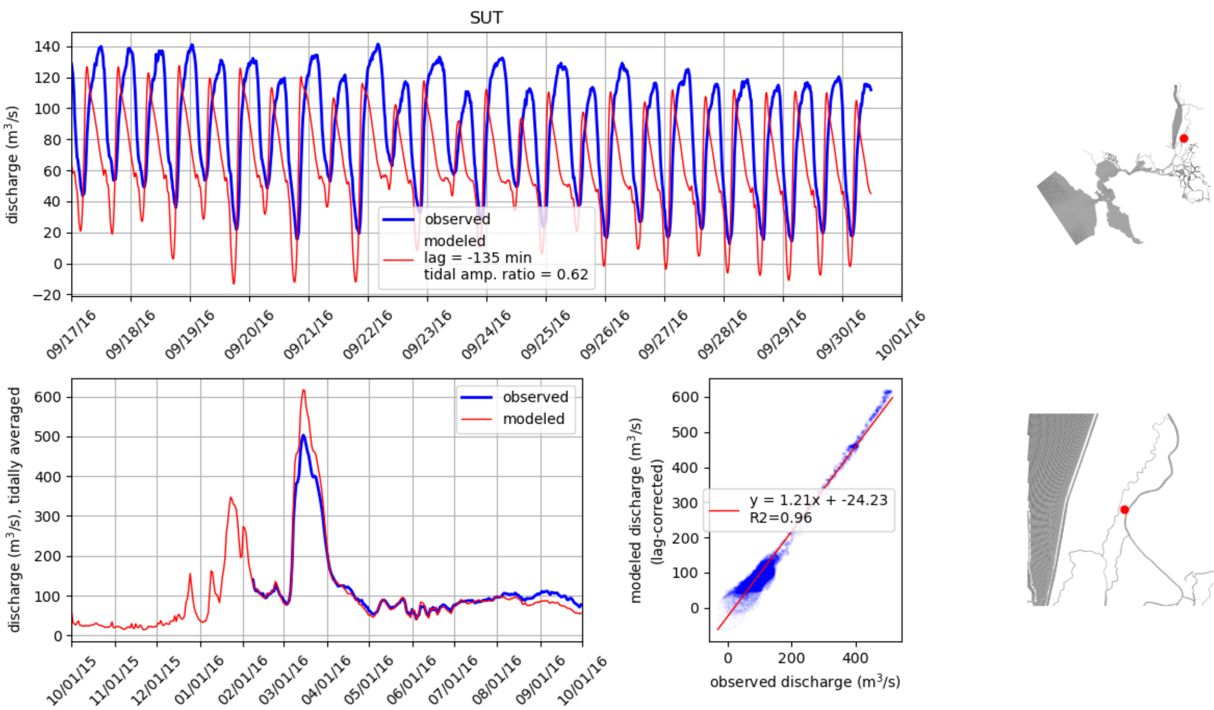

Figure 44: Comparison of modeled and observed flow rates at station SUT. Tidally averaged signals are compared over the water year in lower left panel. Unfiltered signals are compared over a two-week period in the upper panel. Lower right panel compares unfiltered signals where modeled signal has been corrected for lag. On the right, the station location is shown on the model grid.

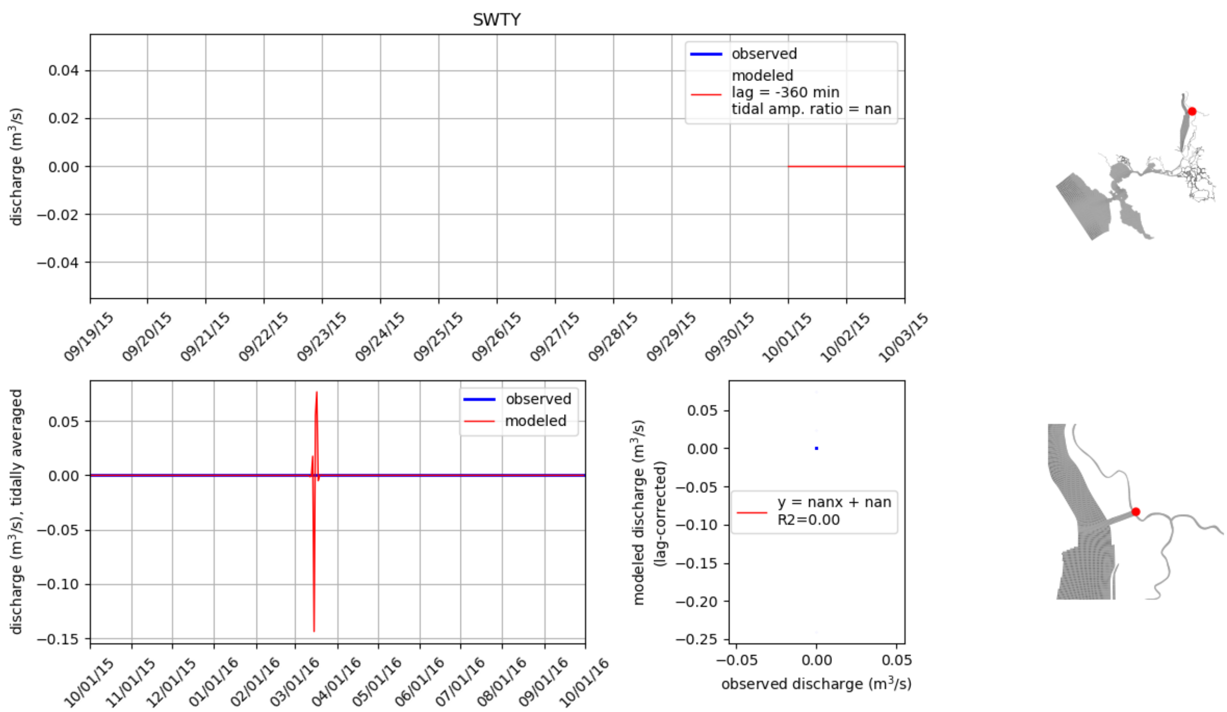

Figure 45: Comparison of modeled and observed flow rates at station SWTY. Tidally averaged signals are compared over the water year in lower left panel. Unfiltered signals are compared over a two-week period in the upper panel. Lower right panel compares unfiltered signals where modeled signal has been corrected for lag. On the right, the station location is shown on the model grid.

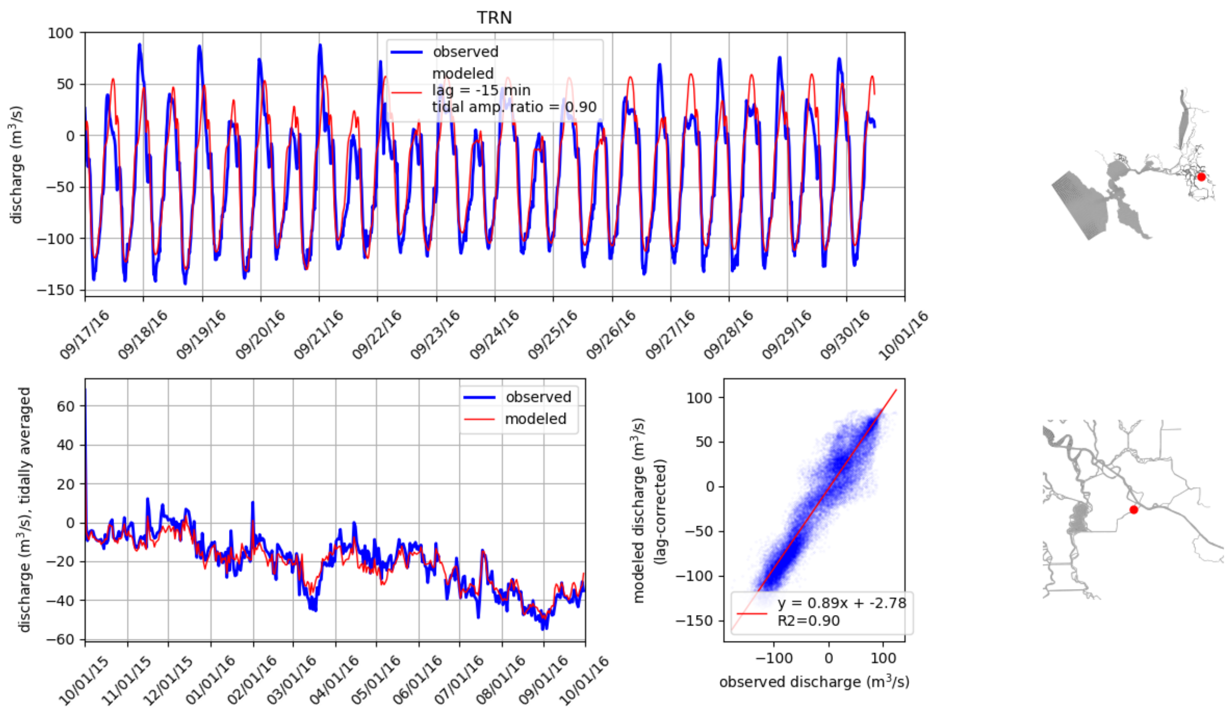

Figure 46: Comparison of modeled and observed flow rates at station TRN. Tidally averaged signals are compared over the water year in lower left panel. Unfiltered signals are compared over a two-week period in the upper panel. Lower right panel compares unfiltered signals where modeled signal has been corrected for lag. On the right, the station location is shown on the model grid.

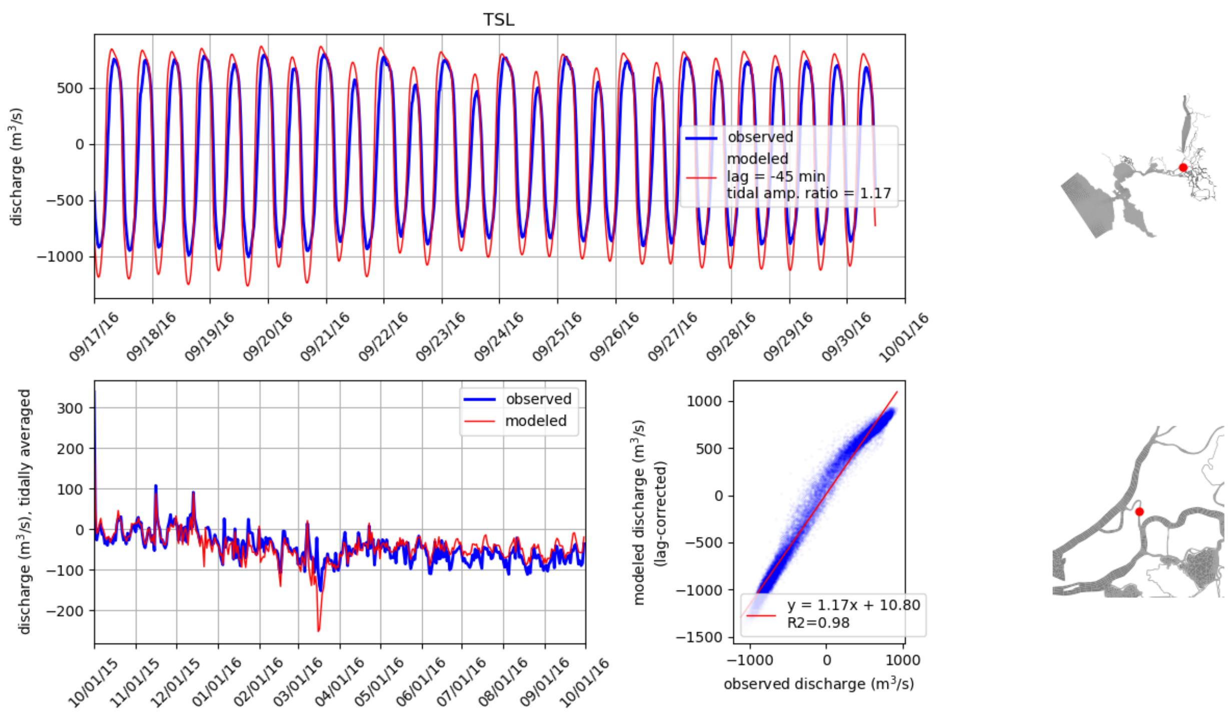

Figure 47: Comparison of modeled and observed flow rates at station TSL. Tidally averaged signals are compared over the water year in lower left panel. Unfiltered signals are compared over a two-week period in the upper panel. Lower right panel compares unfiltered signals where modeled signal has been corrected for lag. On the right, the station location is shown on the model grid.

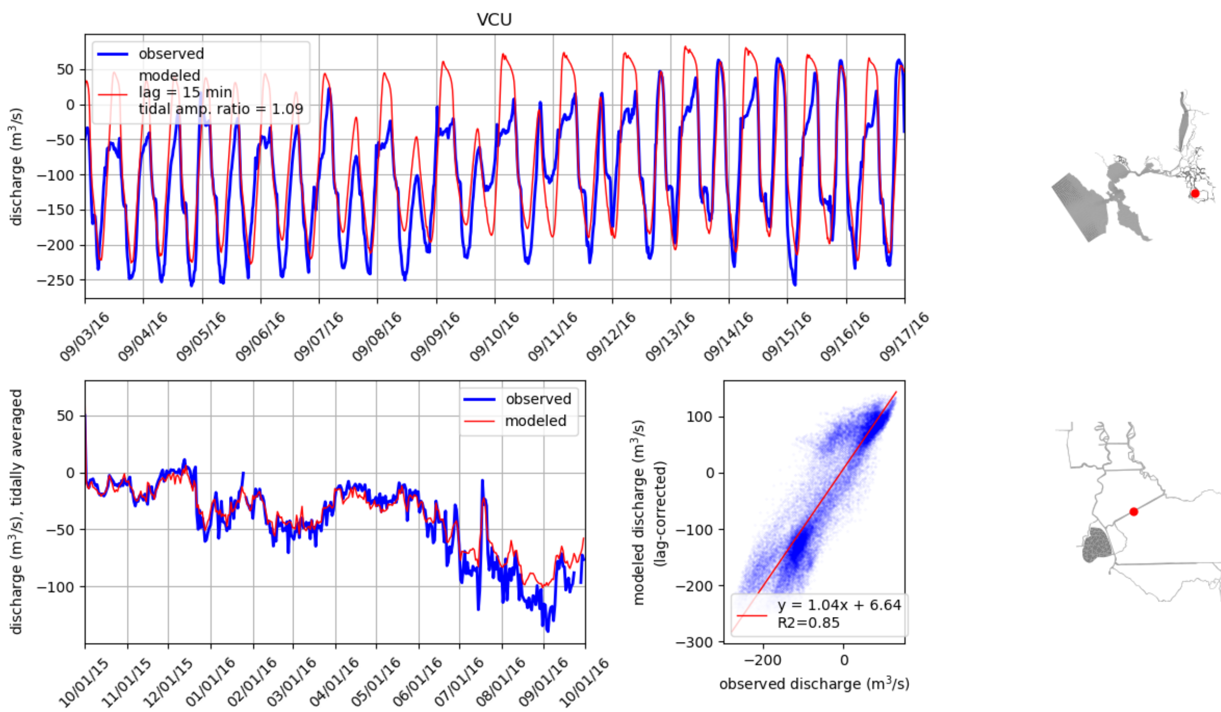

Figure 48: Comparison of modeled and observed flow rates at station VCU. Tidally averaged signals are compared over the water year in lower left panel. Unfiltered signals are compared over a two-week period in the upper panel. Lower right panel compares unfiltered signals where modeled signal has been corrected for lag. On the right, the station location is shown on the model grid.

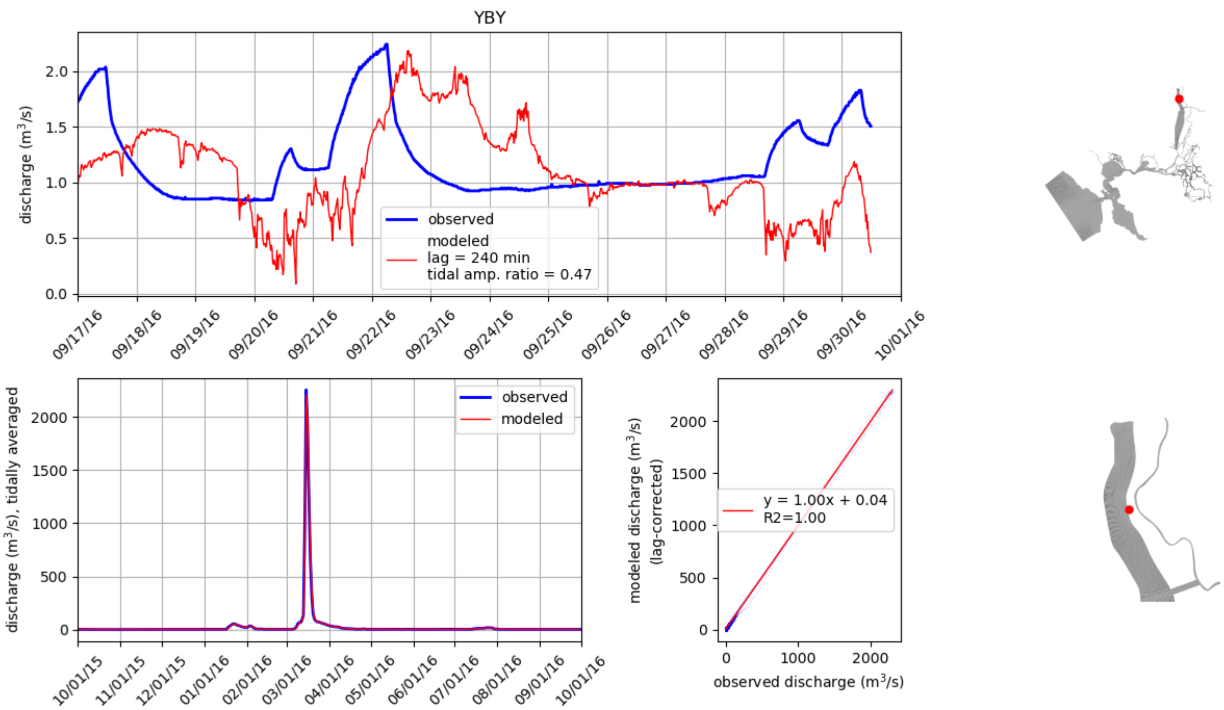

Figure 49: Comparison of modeled and observed flow rates at station YBY. Tidally averaged signals are compared over the water year in lower left panel. Unfiltered signals are compared over a two-week period in the upper panel. Lower right panel compares unfiltered signals where modeled signal has been corrected for lag. On the right, the station location is shown on the model grid.

B Validation Plots: Salinity

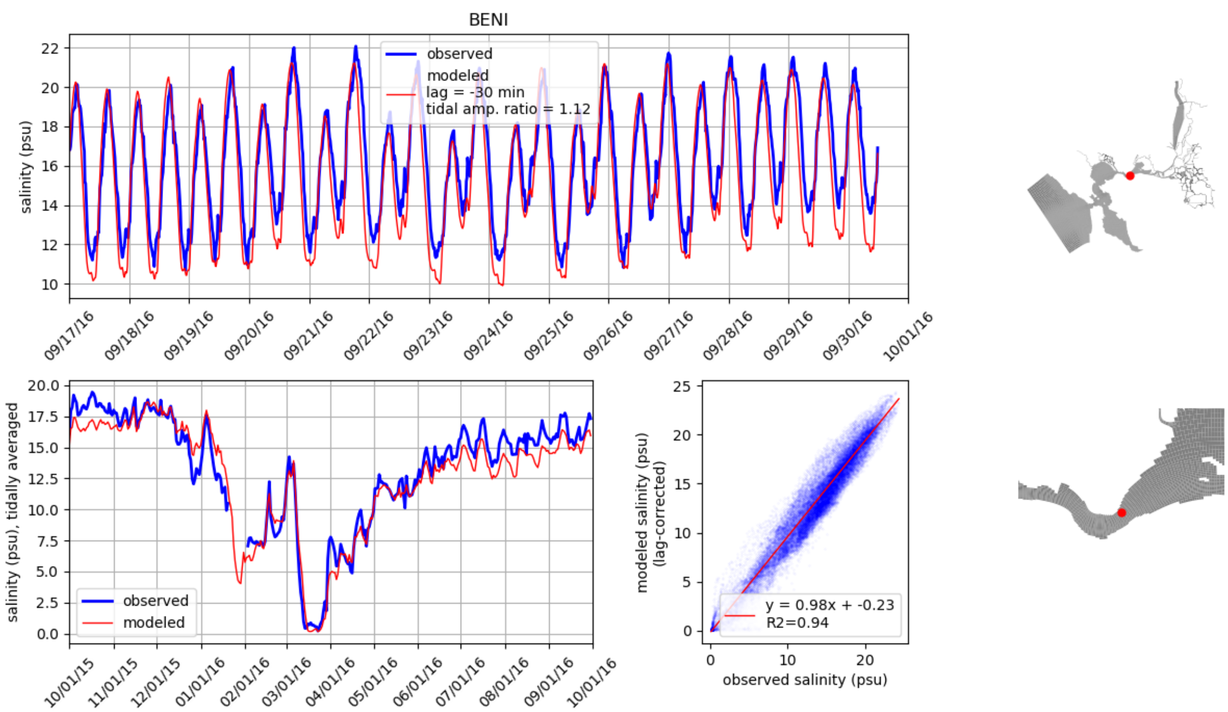

Figure 50: Comparison of modeled and observed salinity at station BENI. Tidally averaged signals are compared over the water year in lower left panel. Unfiltered signals are compared over a two-week period in the upper panel. Lower right panel compares unfiltered signals where modeled signal has been corrected for lag. On the right, the station location is shown on the model grid.

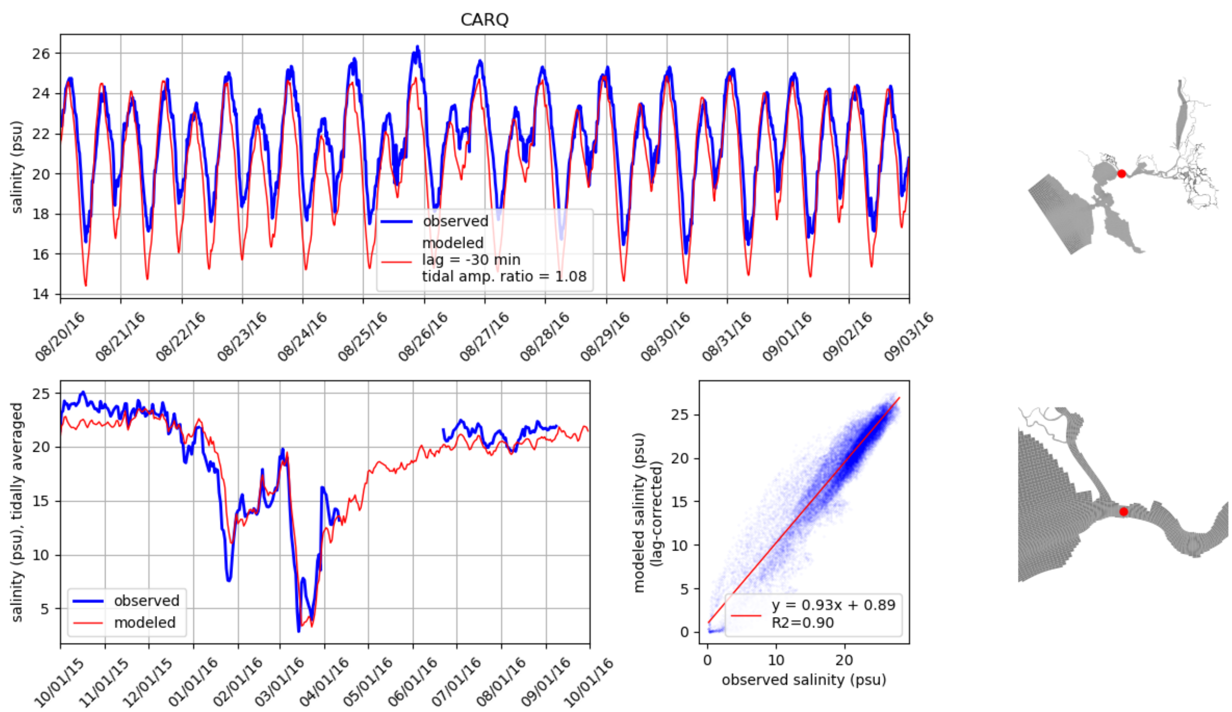

Figure 51: Comparison of modeled and observed salinity at station CARQ. Tidally averaged signals are compared over the water year in lower left panel. Unfiltered signals are compared over a two-week period in the upper panel. Lower right panel compares unfiltered signals where modeled signal has been corrected for lag. On the right, the station location is shown on the model grid.

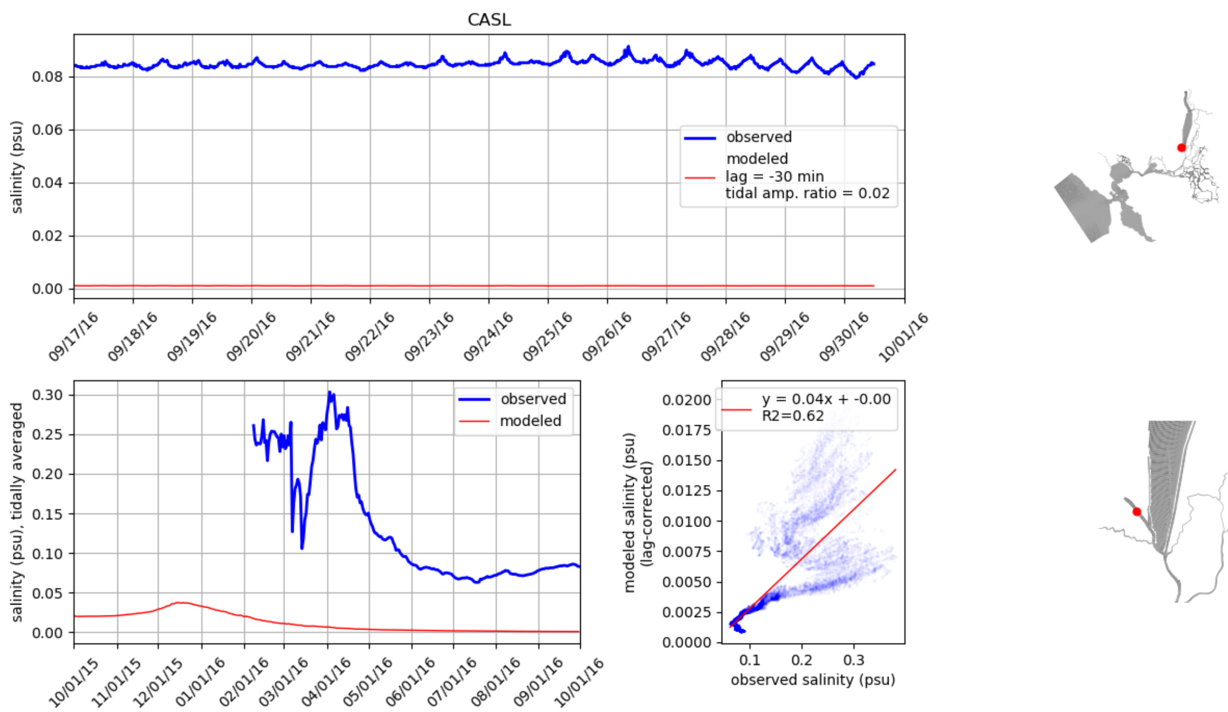

Figure 52: Comparison of modeled and observed salinity at station CASL. Tidally averaged signals are compared over the water year in lower left panel. Unfiltered signals are compared over a two-week period in the upper panel. Lower right panel compares unfiltered signals where modeled signal has been corrected for lag. On the right, the station location is shown on the model grid.

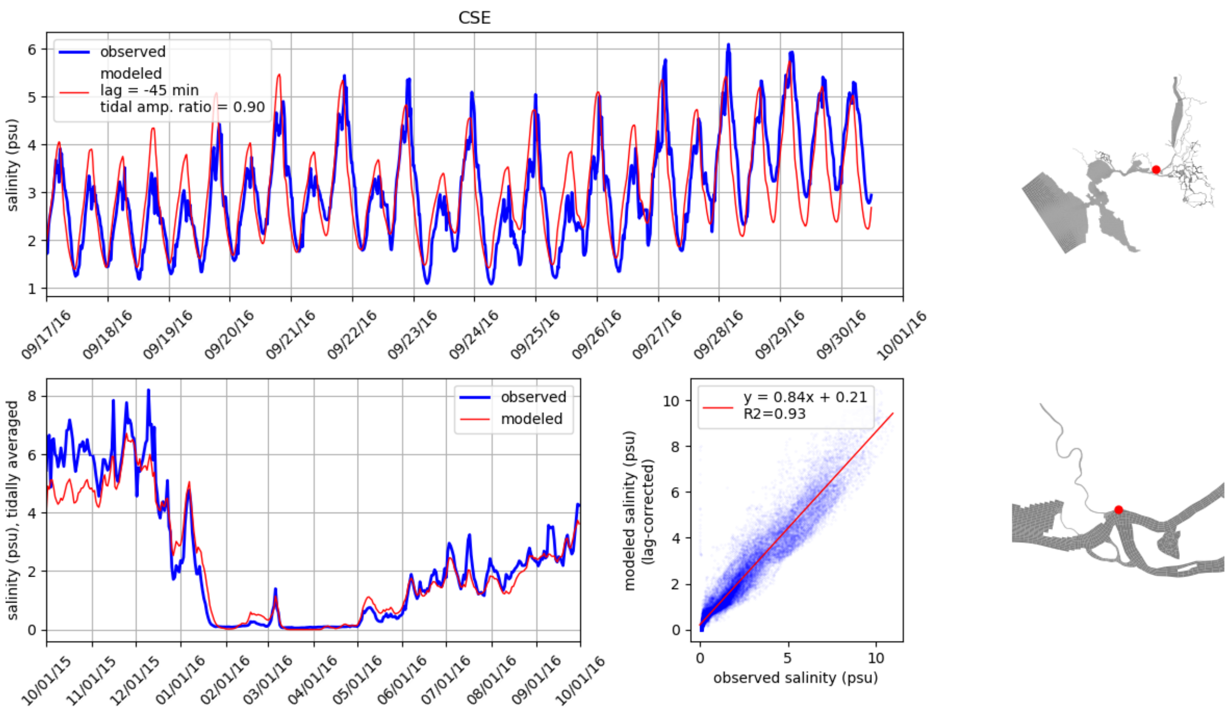

Figure 53: Comparison of modeled and observed salinity at station CSE. Tidally averaged signals are compared over the water year in lower left panel. Unfiltered signals are compared over a two-week period in the upper panel. Lower right panel compares unfiltered signals where modeled signal has been corrected for lag. On the right, the station location is shown on the model grid.

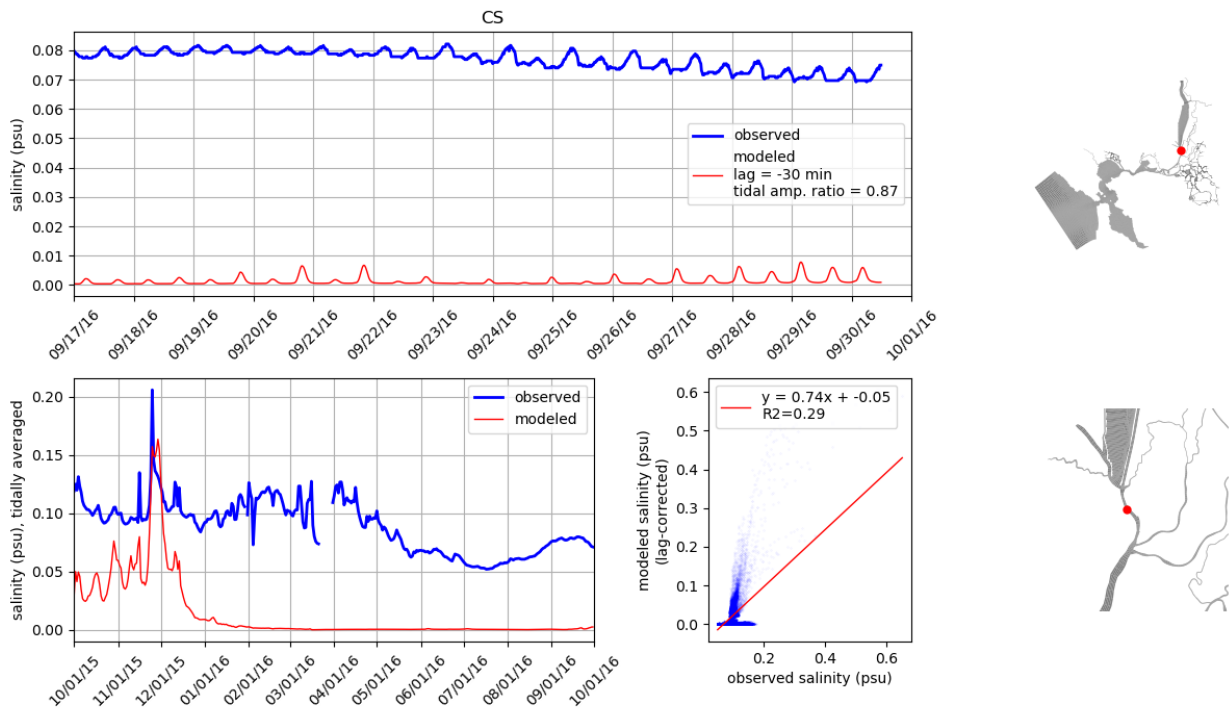

Figure 54: Comparison of modeled and observed salinity at station CS. Tidally averaged signals are compared over the water year in lower left panel. Unfiltered signals are compared over a two-week period in the upper panel. Lower right panel compares unfiltered signals where modeled signal has been corrected for lag. On the right, the station location is shown on the model grid.

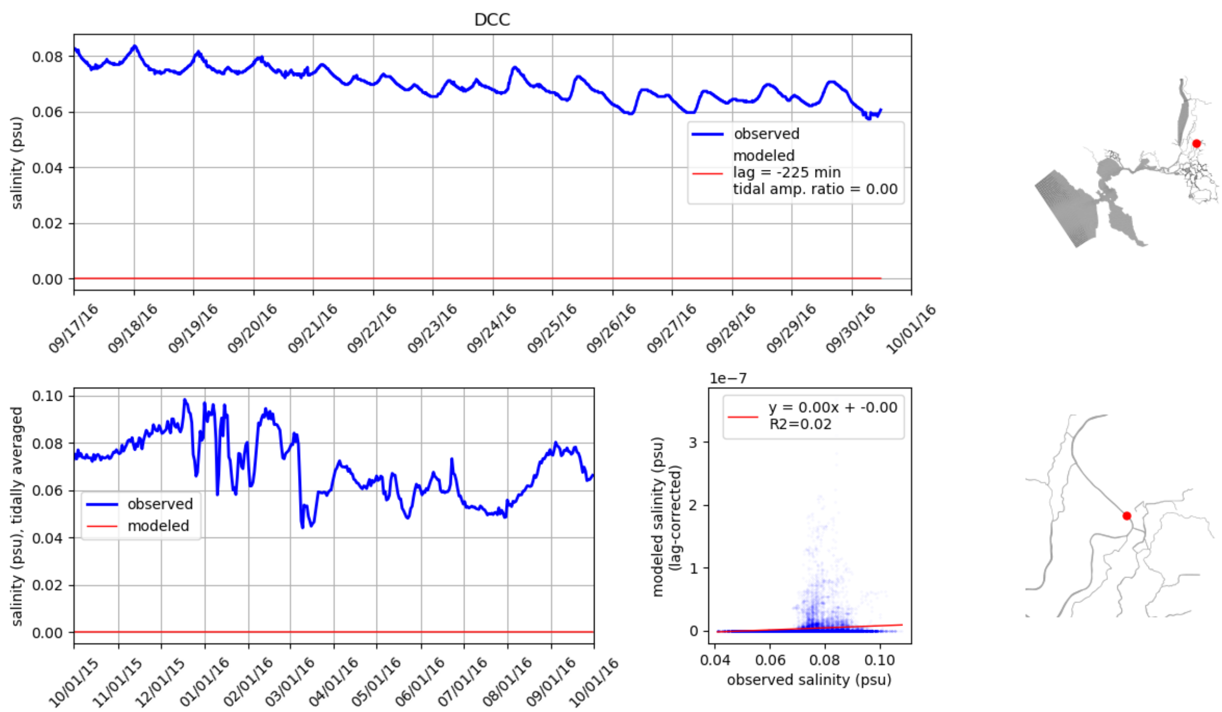

Figure 55: Comparison of modeled and observed salinity at station DCC. Tidally averaged signals are compared over the water year in lower left panel. Unfiltered signals are compared over a two-week period in the upper panel. Lower right panel compares unfiltered signals where modeled signal has been corrected for lag. On the right, the station location is shown on the model grid.

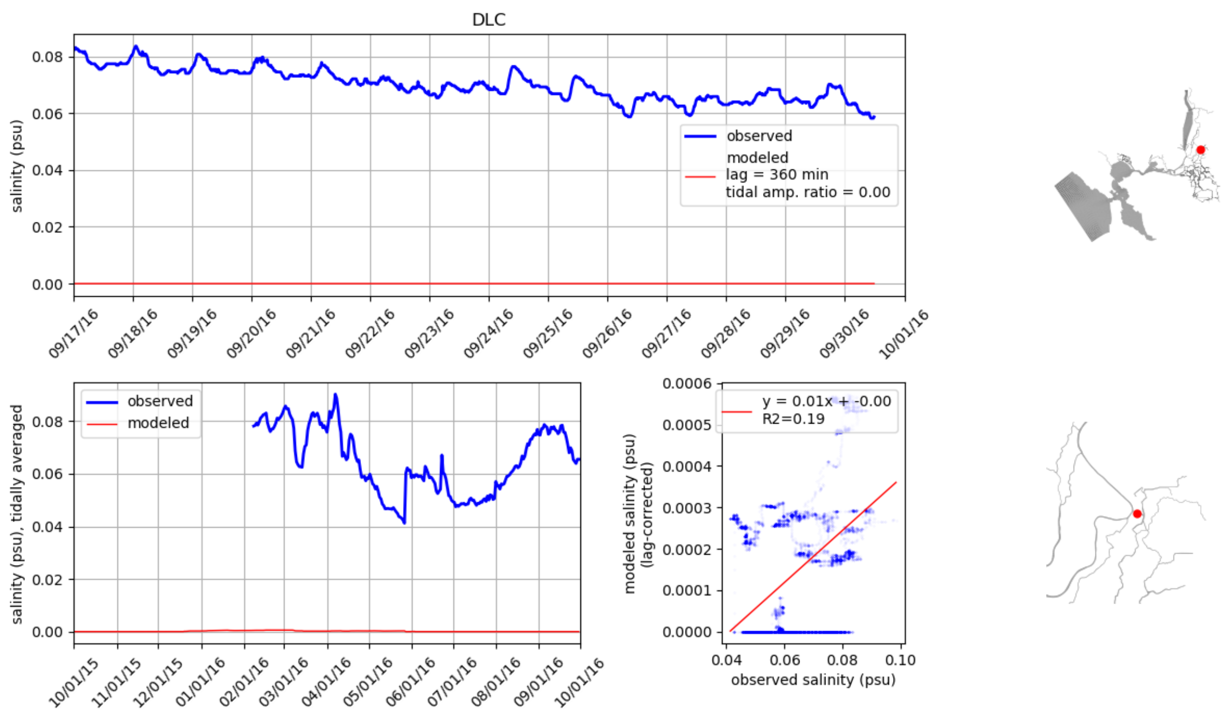

Figure 56: Comparison of modeled and observed salinity at station DLC. Tidally averaged signals are compared over the water year in lower left panel. Unfiltered signals are compared over a two-week period in the upper panel. Lower right panel compares unfiltered signals where modeled signal has been corrected for lag. On the right, the station location is shown on the model grid.

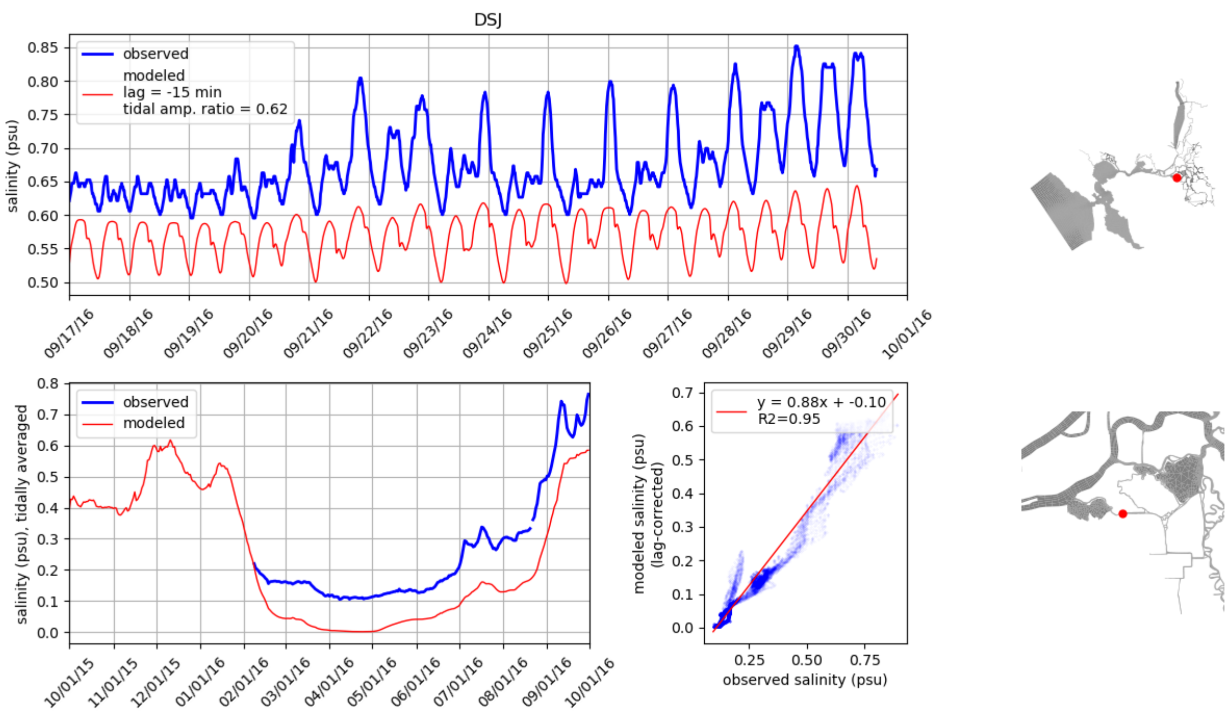

Figure 57: Comparison of modeled and observed salinity at station DSJ. Tidally averaged signals are compared over the water year in lower left panel. Unfiltered signals are compared over a two-week period in the upper panel. Lower right panel compares unfiltered signals where modeled signal has been corrected for lag. On the right, the station location is shown on the model grid.

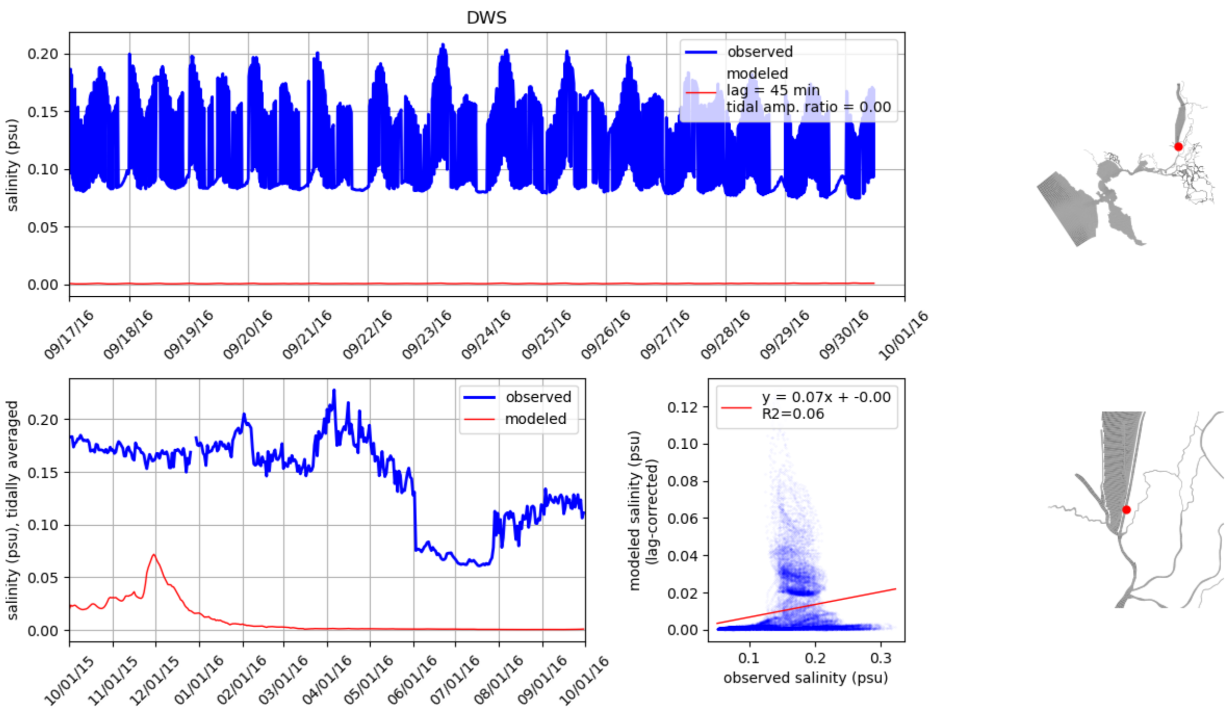

Figure 58: Comparison of modeled and observed salinity at station DWS. Tidally averaged signals are compared over the water year in lower left panel. Unfiltered signals are compared over a two-week period in the upper panel. Lower right panel compares unfiltered signals where modeled signal has been corrected for lag. On the right, the station location is shown on the model grid.

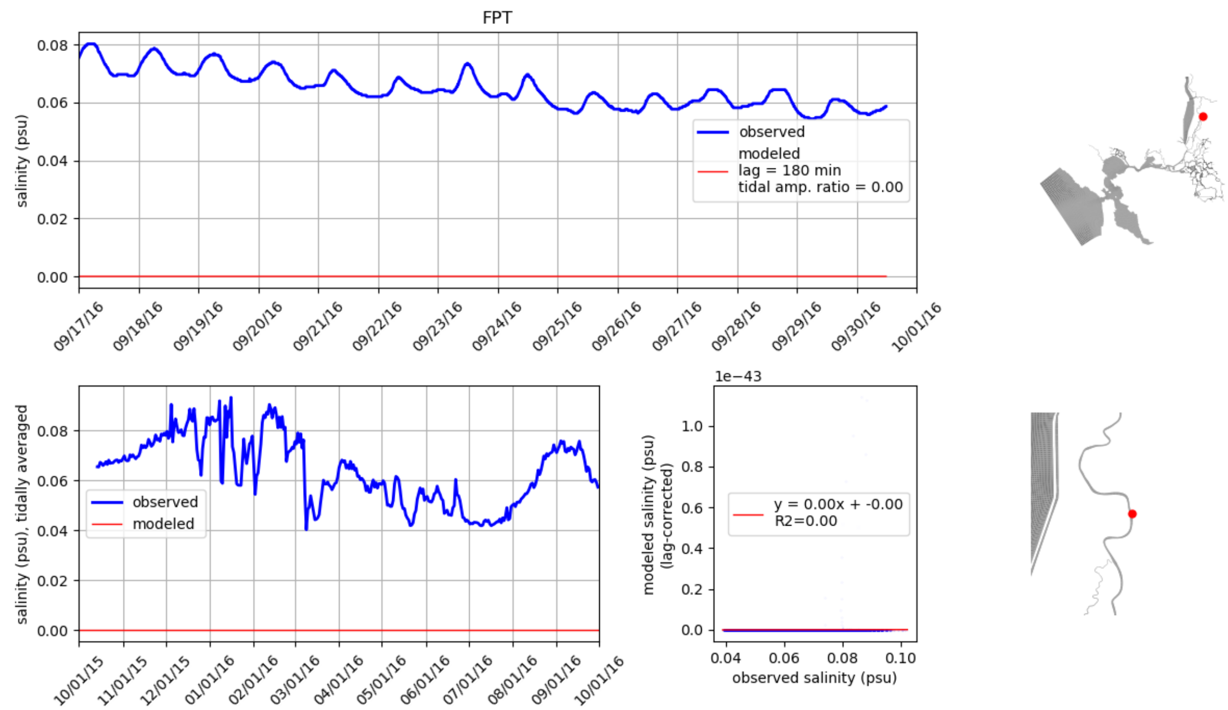

Figure 59: Comparison of modeled and observed salinity at station FPT. Tidally averaged signals are compared over the water year in lower left panel. Unfiltered signals are compared over a two-week period in the upper panel. Lower right panel compares unfiltered signals where modeled signal has been corrected for lag. On the right, the station location is shown on the model grid.

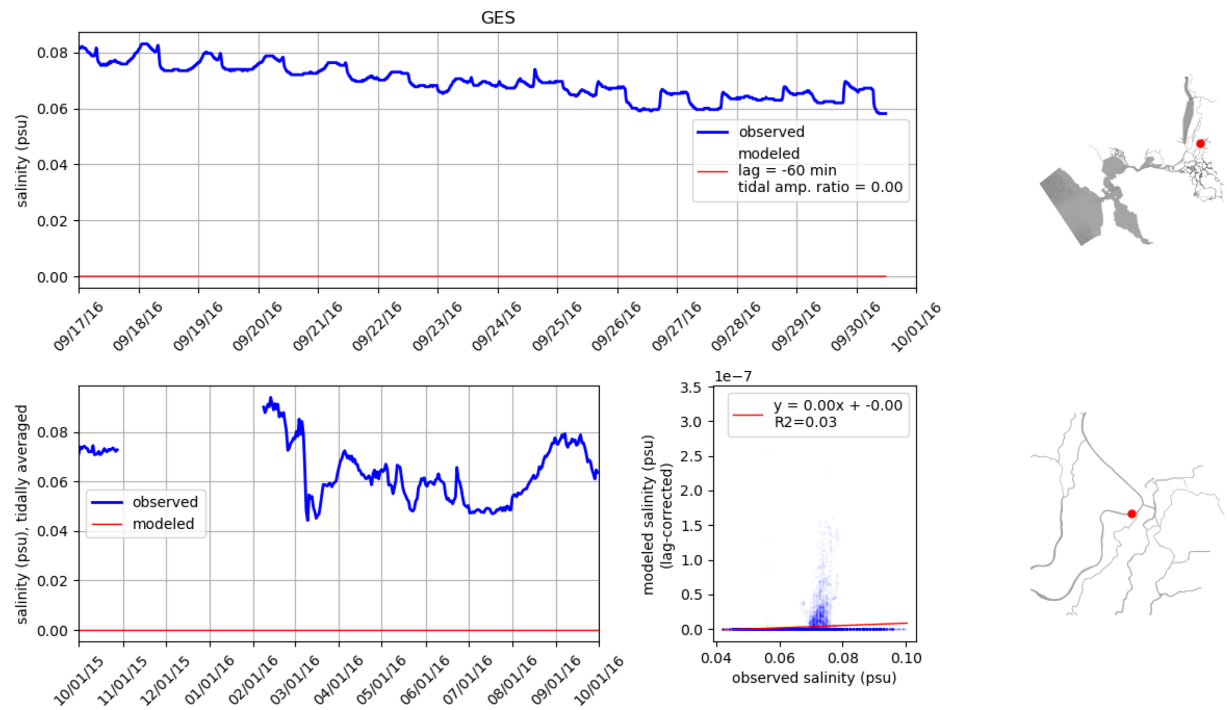

Figure 60: Comparison of modeled and observed salinity at station GES. Tidally averaged signals are compared over the water year in lower left panel. Unfiltered signals are compared over a two-week period in the upper panel. Lower right panel compares unfiltered signals where modeled signal has been corrected for lag. On the right, the station location is shown on the model grid.

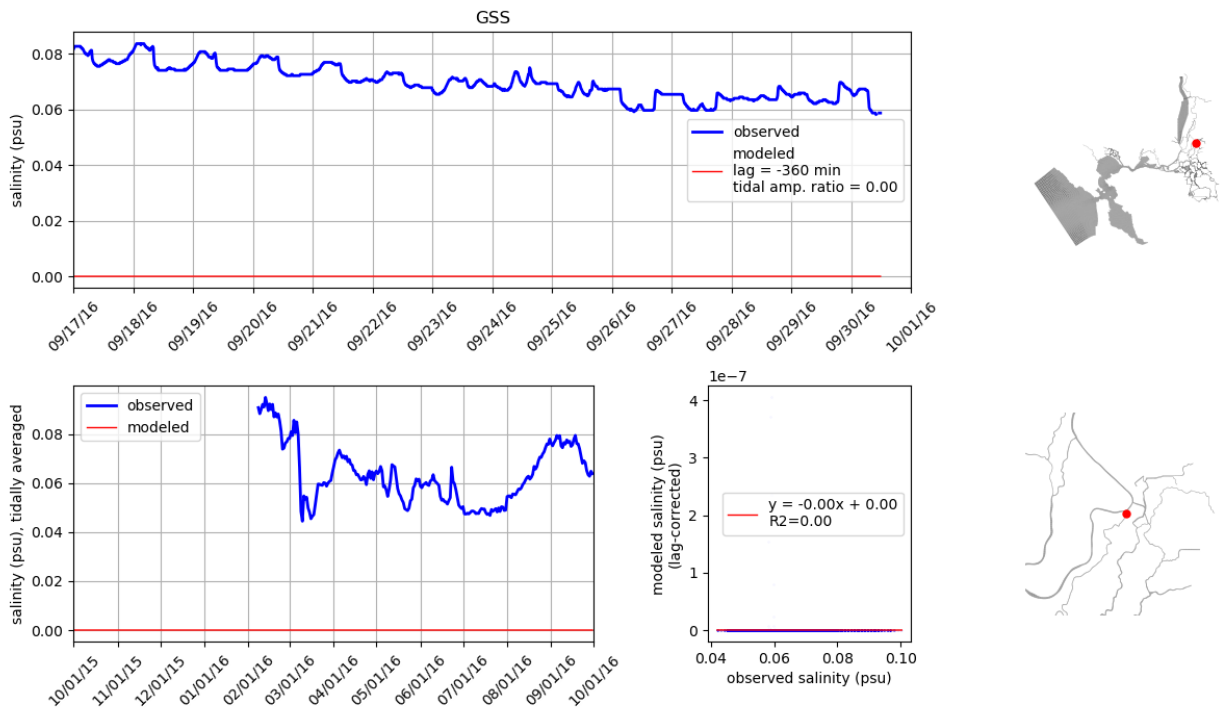

Figure 61: Comparison of modeled and observed salinity at station GSS. Tidally averaged signals are compared over the water year in lower left panel. Unfiltered signals are compared over a two-week period in the upper panel. Lower right panel compares unfiltered signals where modeled signal has been corrected for lag. On the right, the station location is shown on the model grid.

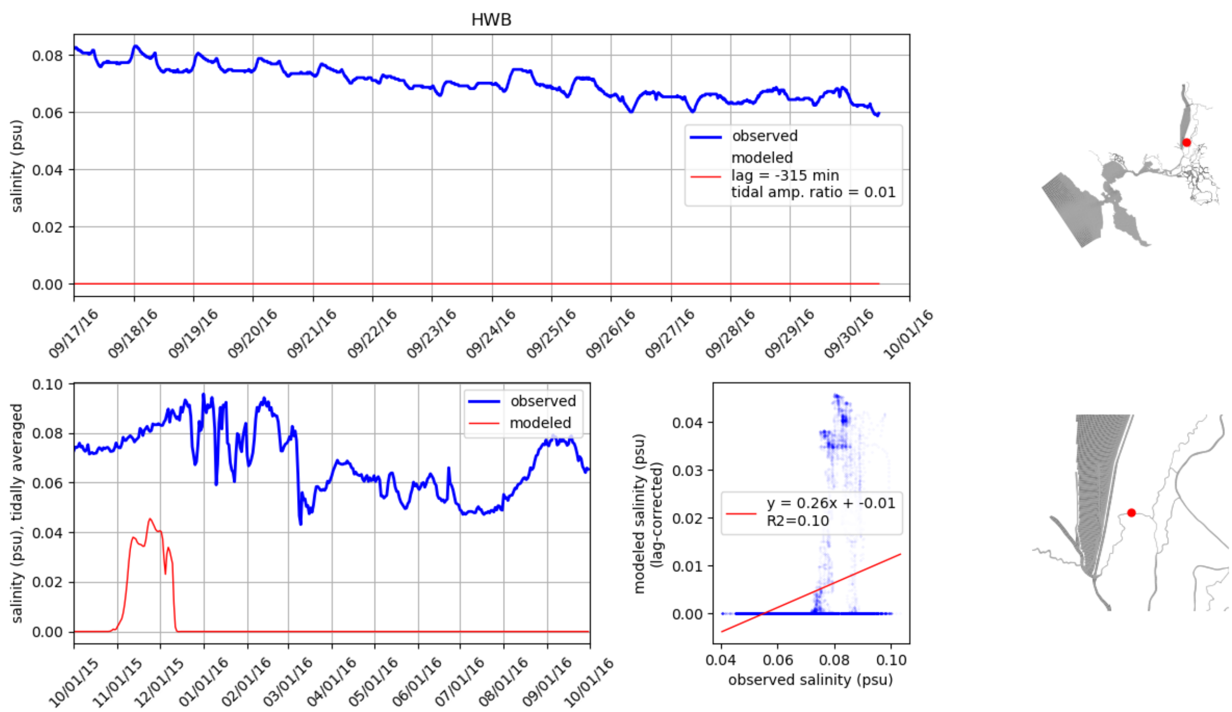

Figure 62: Comparison of modeled and observed salinity at station HWB. Tidally averaged signals are compared over the water year in lower left panel. Unfiltered signals are compared over a two-week period in the upper panel. Lower right panel compares unfiltered signals where modeled signal has been corrected for lag. On the right, the station location is shown on the model grid.

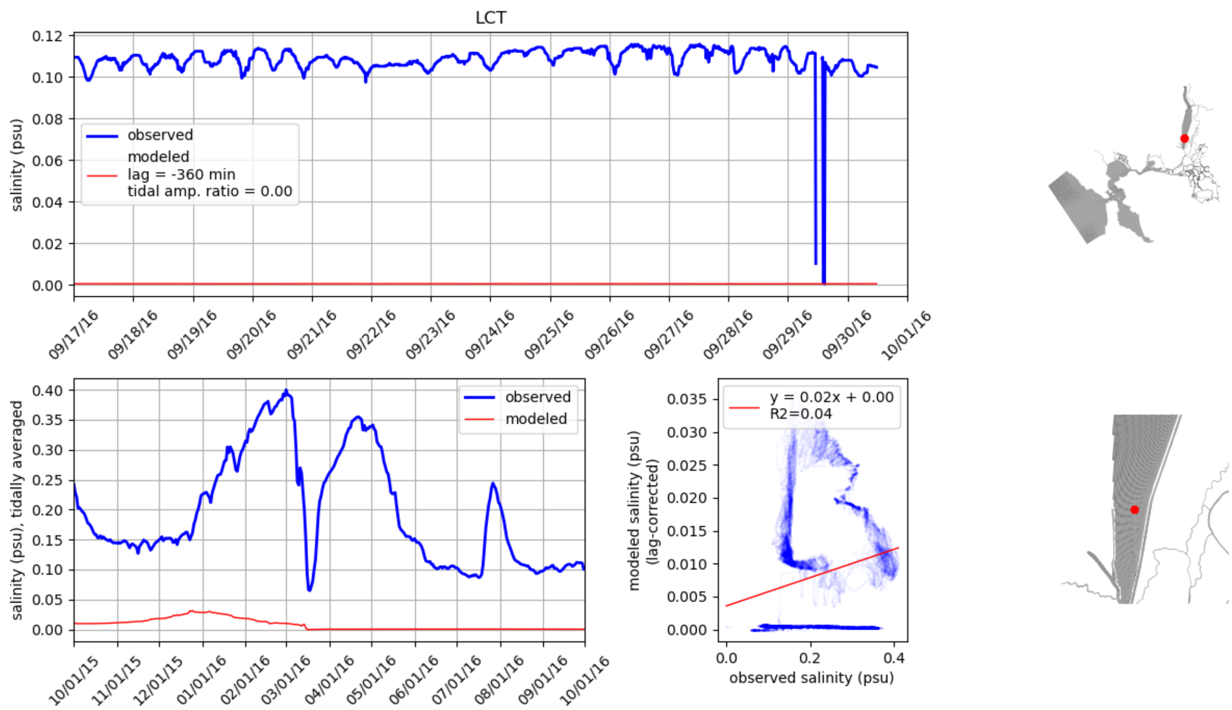

Figure 63: Comparison of modeled and observed salinity at station LCT. Tidally averaged signals are compared over the water year in lower left panel. Unfiltered signals are compared over a two-week period in the upper panel. Lower right panel compares unfiltered signals where modeled signal has been corrected for lag. On the right, the station location is shown on the model grid.

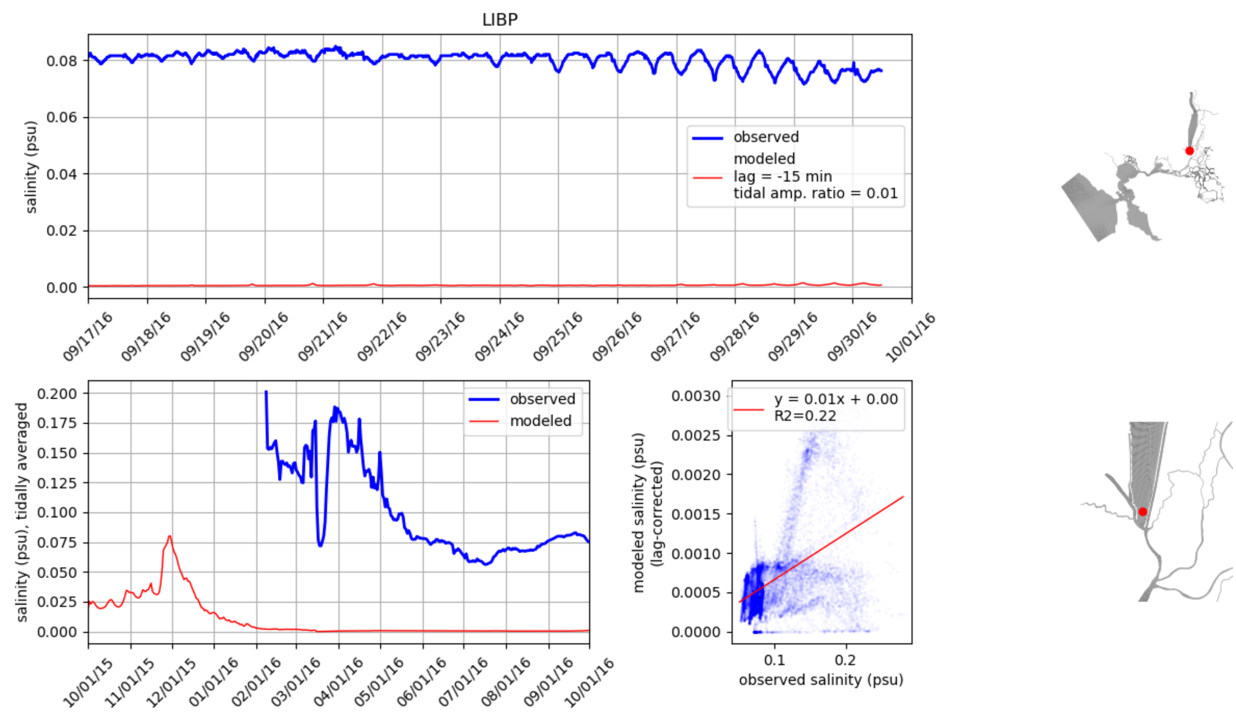

Figure 64: Comparison of modeled and observed salinity at station LIBP. Tidally averaged signals are compared over the water year in lower left panel. Unfiltered signals are compared over a two-week period in the upper panel. Lower right panel compares unfiltered signals where modeled signal has been corrected for lag. On the right, the station location is shown on the model grid.

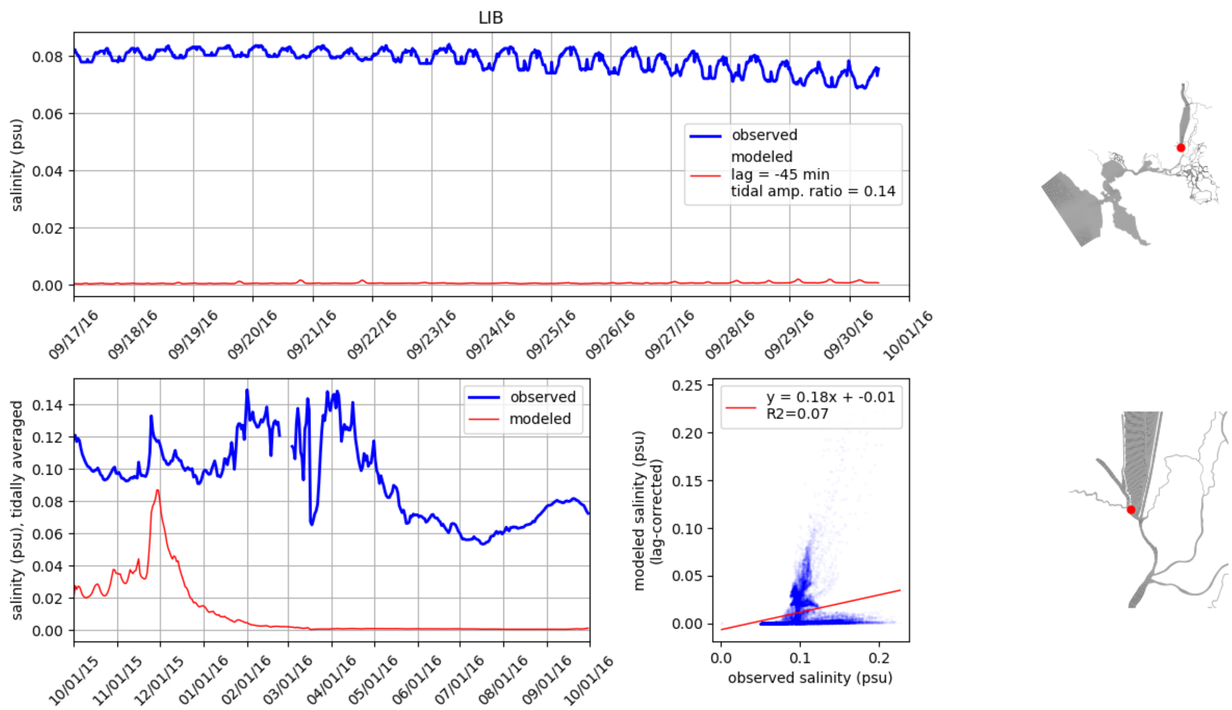

Figure 65: Comparison of modeled and observed salinity at station LIB. Tidally averaged signals are compared over the water year in lower left panel. Unfiltered signals are compared over a two-week period in the upper panel. Lower right panel compares unfiltered signals where modeled signal has been corrected for lag. On the right, the station location is shown on the model grid.

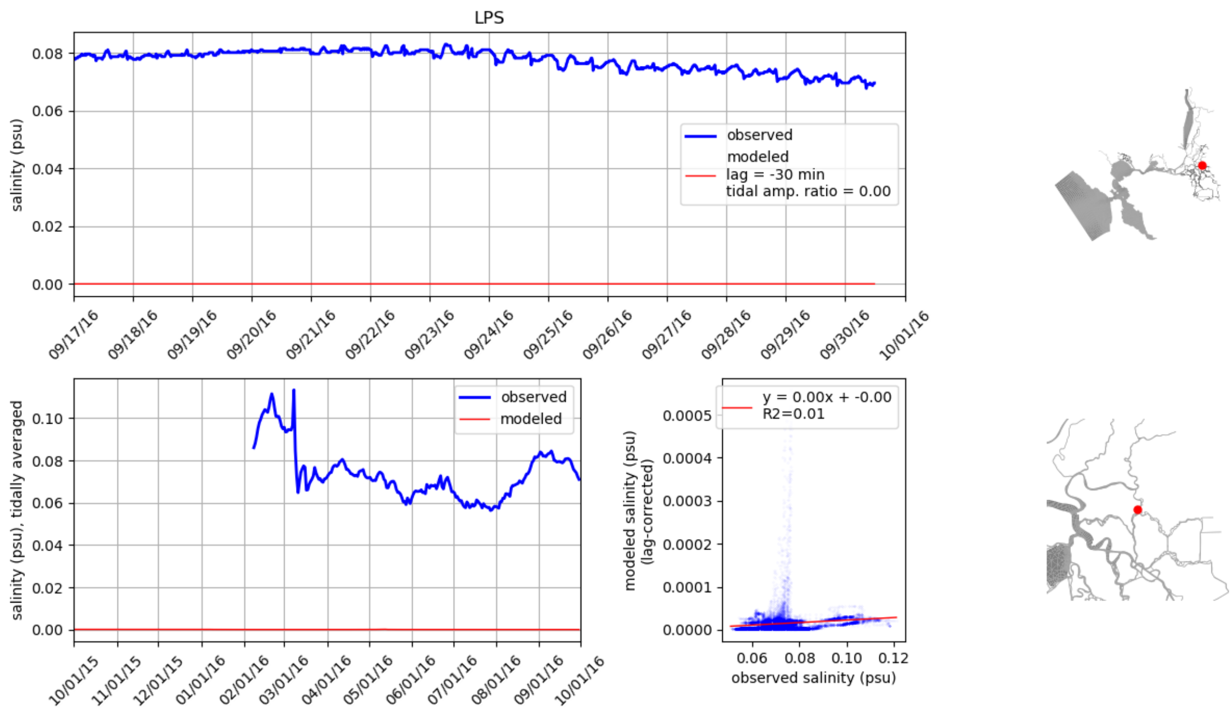

Figure 66: Comparison of modeled and observed salinity at station LPS. Tidally averaged signals are compared over the water year in lower left panel. Unfiltered signals are compared over a two-week period in the upper panel. Lower right panel compares unfiltered signals where modeled signal has been corrected for lag. On the right, the station location is shown on the model grid.

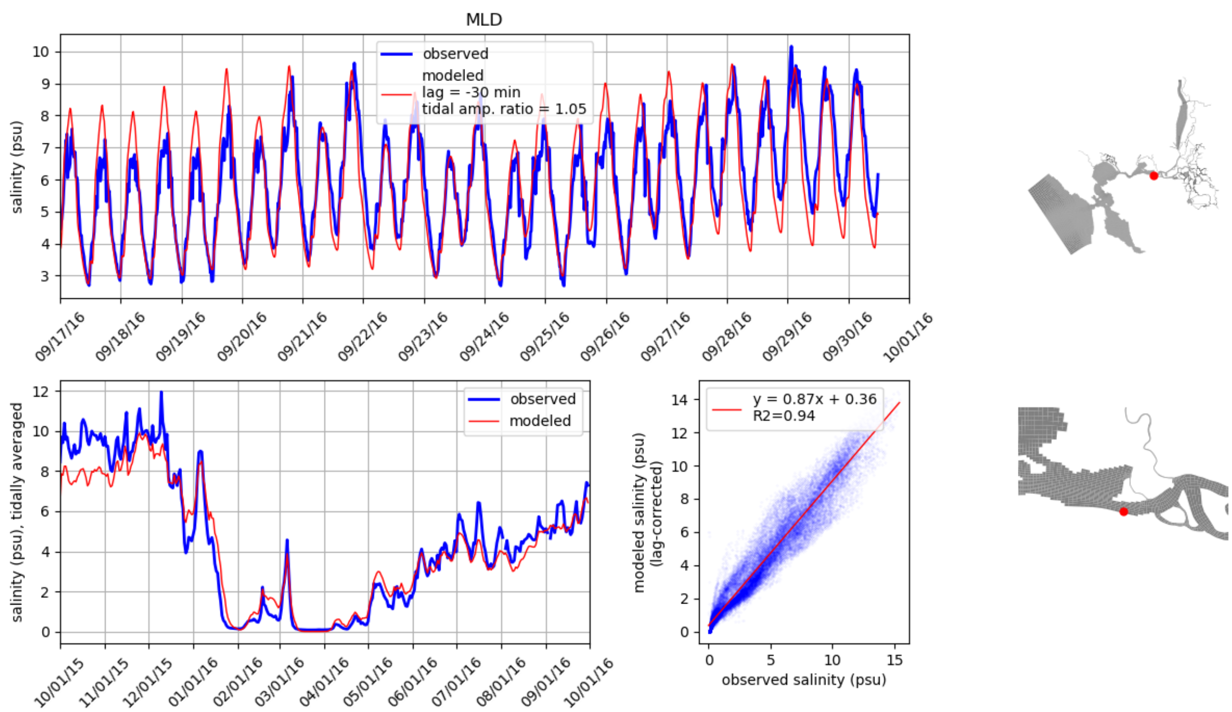

Figure 67: Comparison of modeled and observed salinity at station MLD. Tidally averaged signals are compared over the water year in lower left panel. Unfiltered signals are compared over a two-week period in the upper panel. Lower right panel compares unfiltered signals where modeled signal has been corrected for lag. On the right, the station location is shown on the model grid.

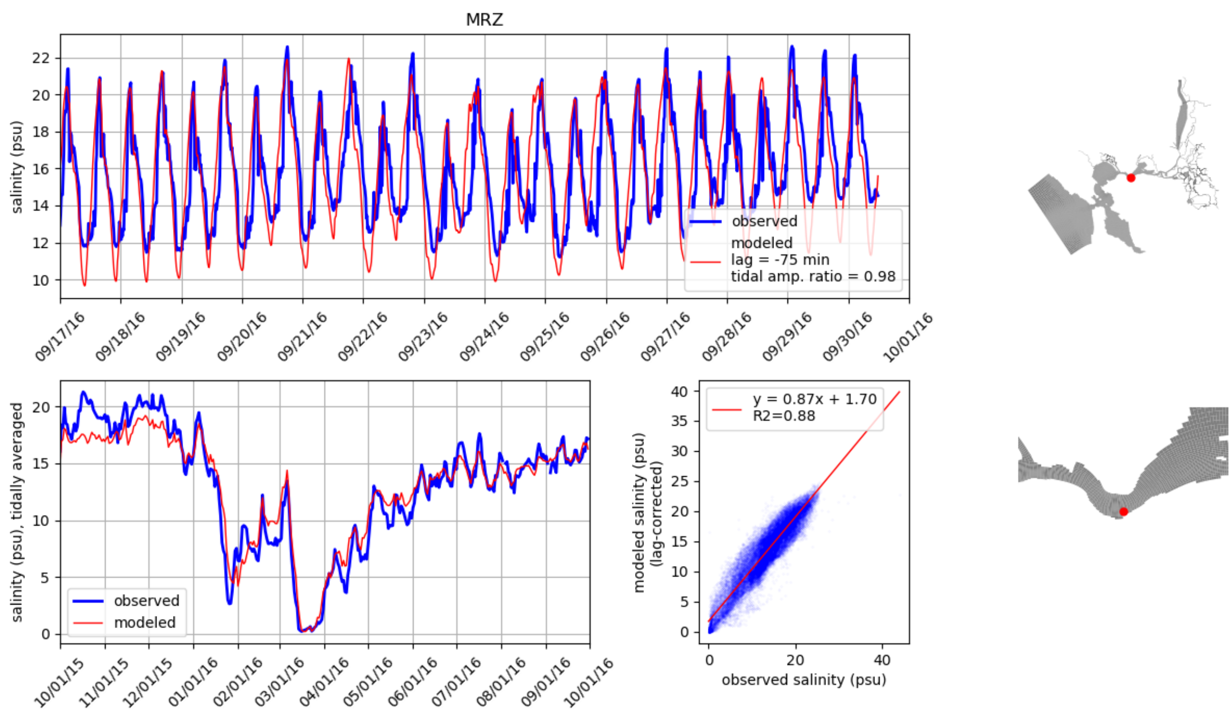

Figure 68: Comparison of modeled and observed salinity at station MRZ. Tidally averaged signals are compared over the water year in lower left panel. Unfiltered signals are compared over a two-week period in the upper panel. Lower right panel compares unfiltered signals where modeled signal has been corrected for lag. On the right, the station location is shown on the model grid.

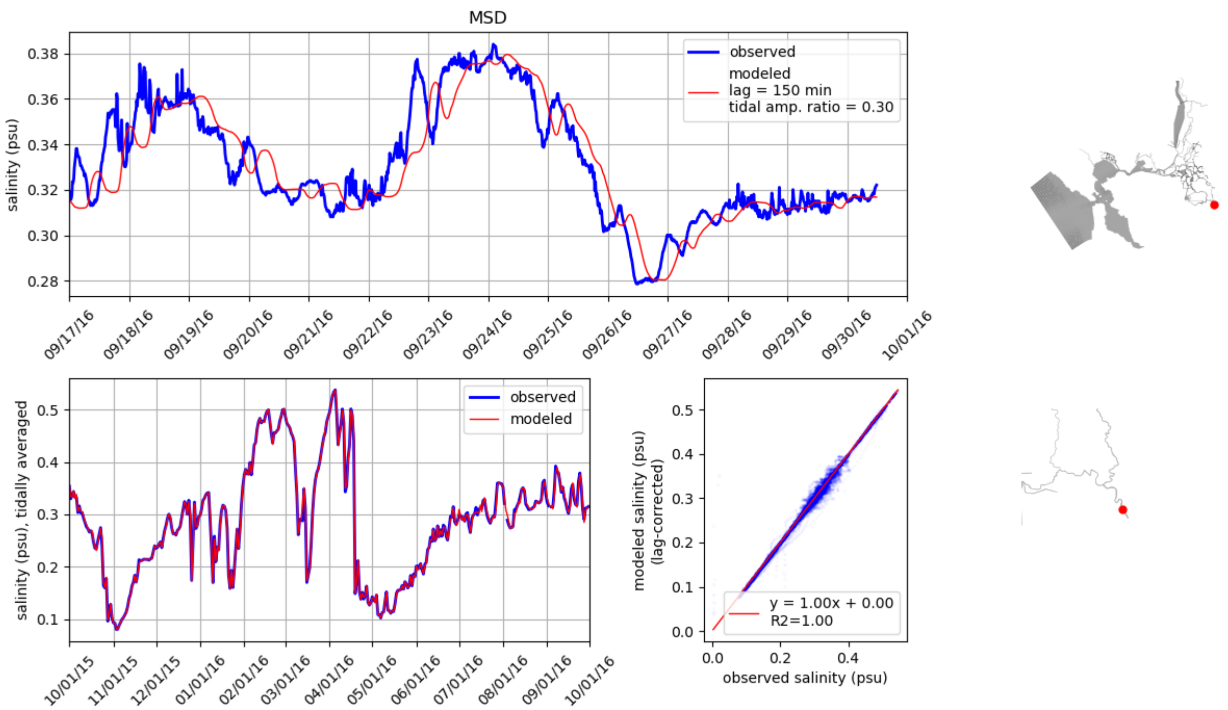

Figure 69: Comparison of modeled and observed salinity at station MSD. Tidally averaged signals are compared over the water year in lower left panel. Unfiltered signals are compared over a two-week period in the upper panel. Lower right panel compares unfiltered signals where modeled signal has been corrected for lag. On the right, the station location is shown on the model grid.

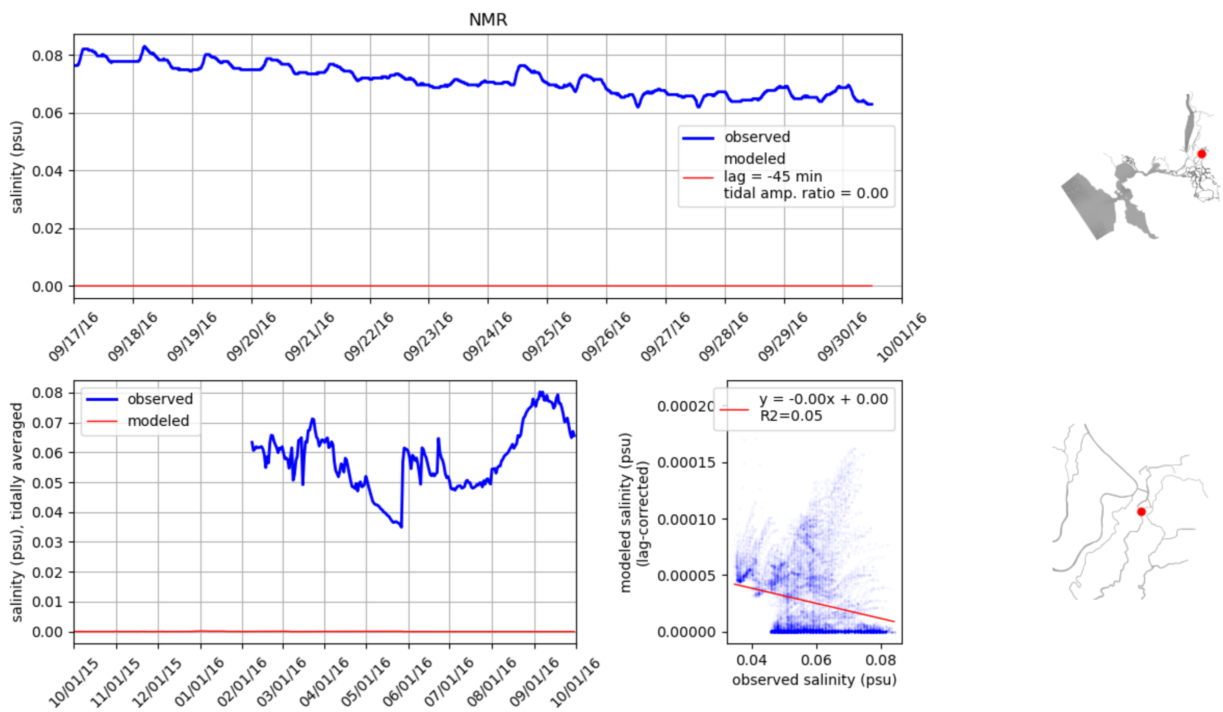

Figure 70: Comparison of modeled and observed salinity at station NMR. Tidally averaged signals are compared over the water year in lower left panel. Unfiltered signals are compared over a two-week period in the upper panel. Lower right panel compares unfiltered signals where modeled signal has been corrected for lag. On the right, the station location is shown on the model grid.

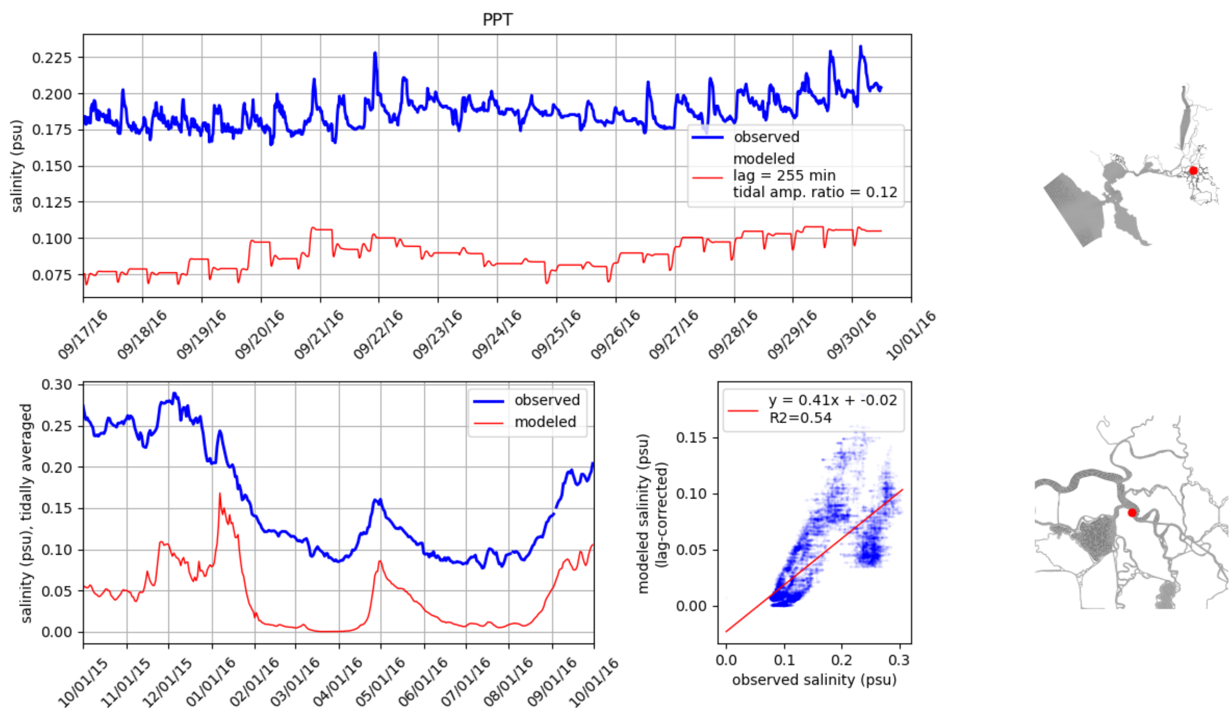

Figure 71: Comparison of modeled and observed salinity at station PPT. Tidally averaged signals are compared over the water year in lower left panel. Unfiltered signals are compared over a two-week period in the upper panel. Lower right panel compares unfiltered signals where modeled signal has been corrected for lag. On the right, the station location is shown on the model grid.

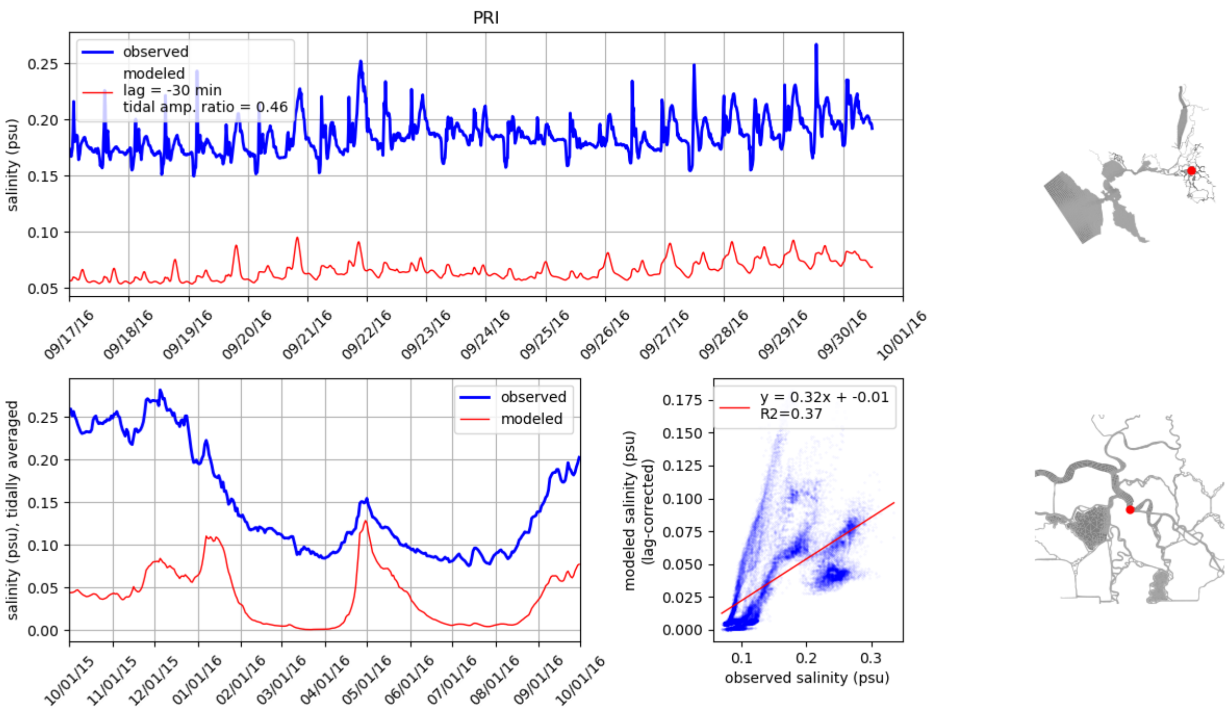

Figure 72: Comparison of modeled and observed salinity at station PRI. Tidally averaged signals are compared over the water year in lower left panel. Unfiltered signals are compared over a two-week period in the upper panel. Lower right panel compares unfiltered signals where modeled signal has been corrected for lag. On the right, the station location is shown on the model grid.

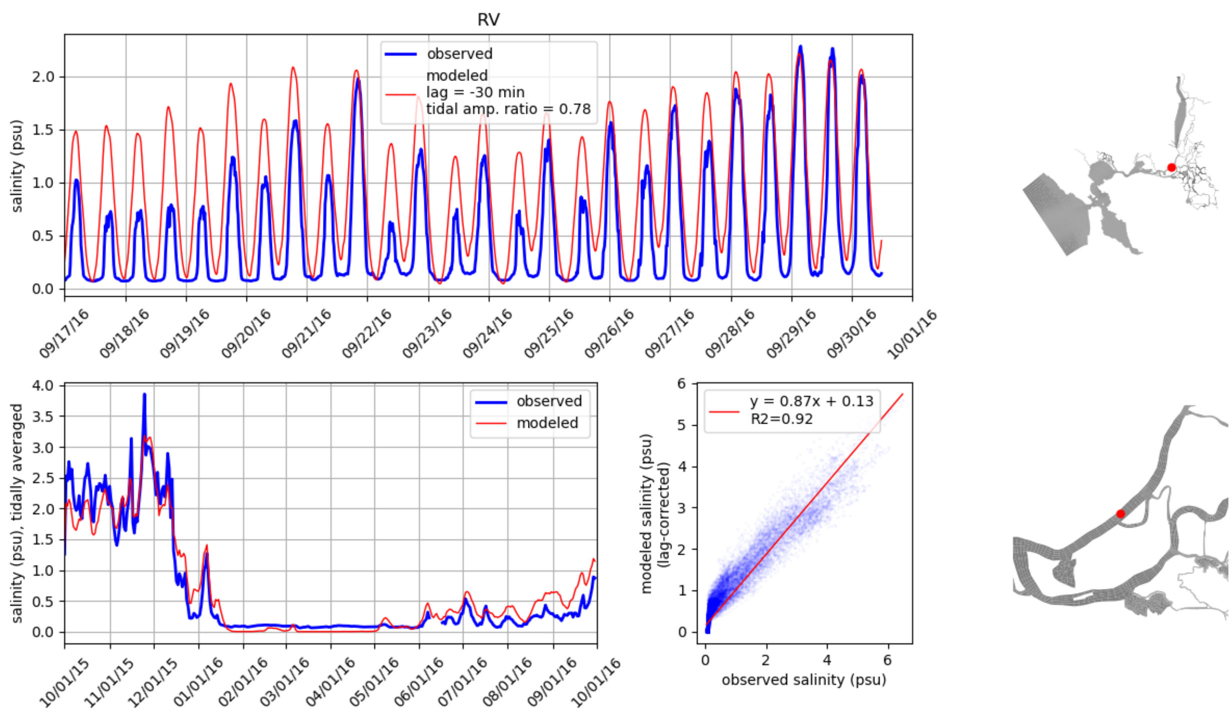

Figure 73: Comparison of modeled and observed salinity at station RV. Tidally averaged signals are compared over the water year in lower left panel. Unfiltered signals are compared over a two-week period in the upper panel. Lower right panel compares unfiltered signals where modeled signal has been corrected for lag. On the right, the station location is shown on the model grid.

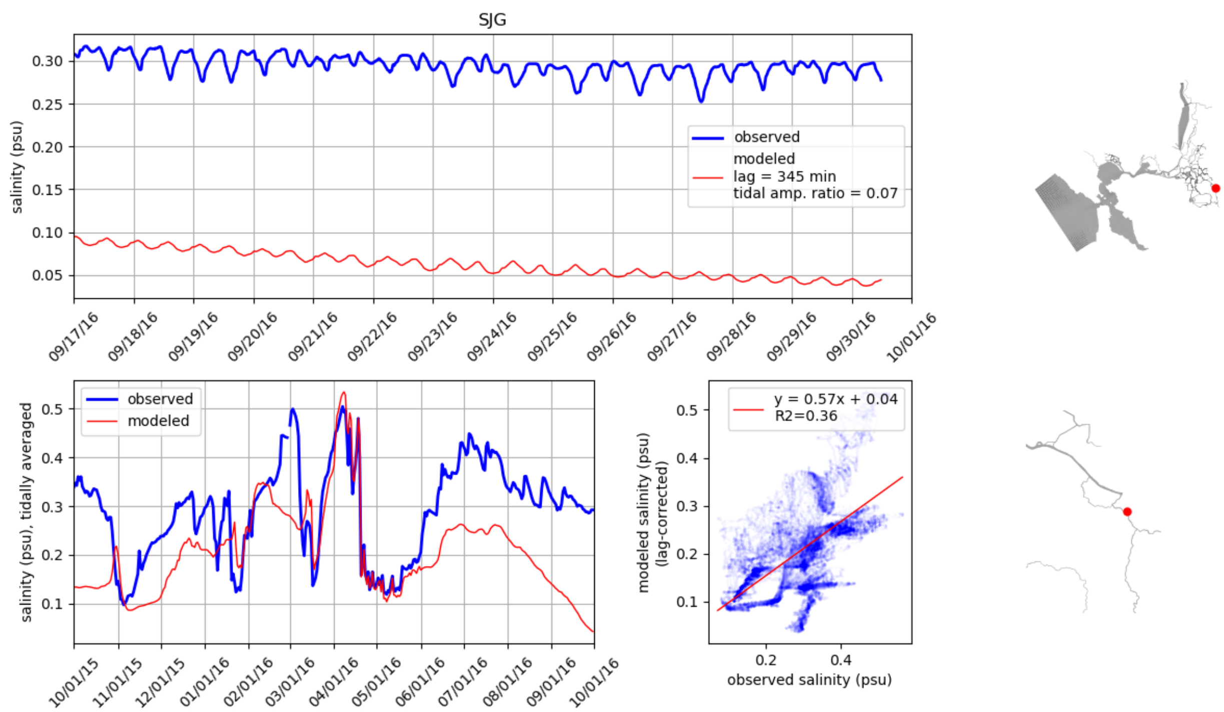

Figure 74: Comparison of modeled and observed salinity at station SJG. Tidally averaged signals are compared over the water year in lower left panel. Unfiltered signals are compared over a two-week period in the upper panel. Lower right panel compares unfiltered signals where modeled signal has been corrected for lag. On the right, the station location is shown on the model grid.

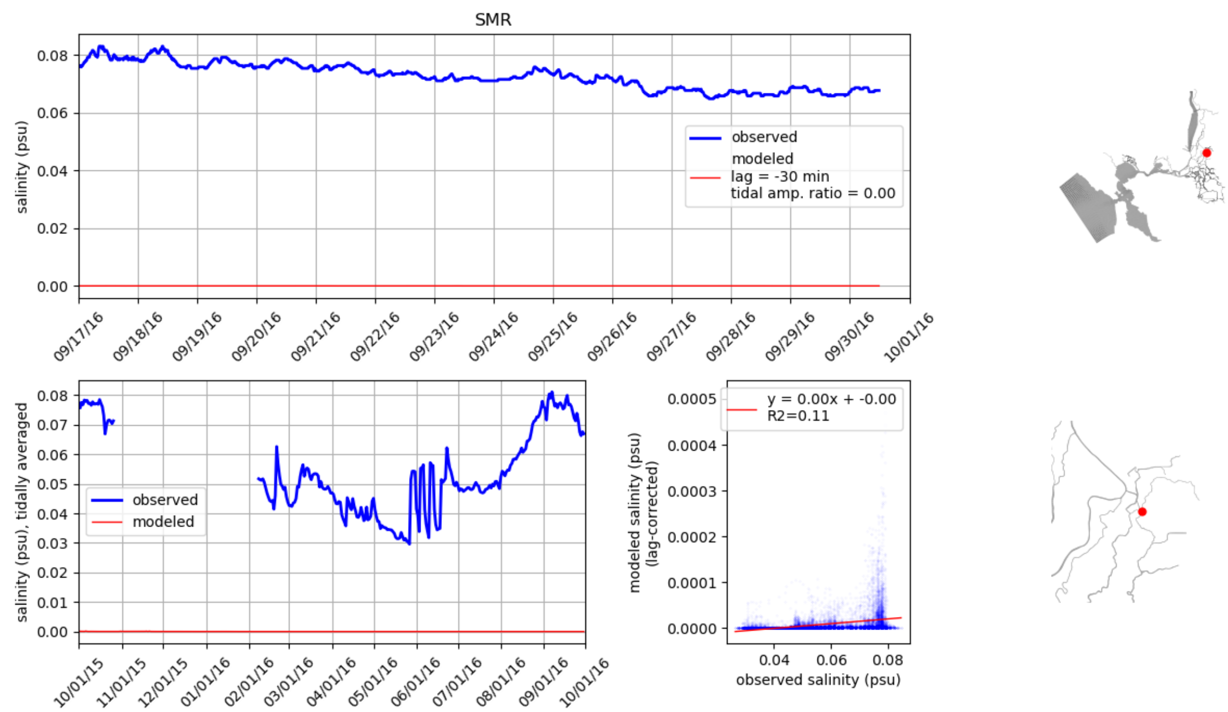

Figure 75: Comparison of modeled and observed salinity at station SMR. Tidally averaged signals are compared over the water year in lower left panel. Unfiltered signals are compared over a two-week period in the upper panel. Lower right panel compares unfiltered signals where modeled signal has been corrected for lag. On the right, the station location is shown on the model grid.

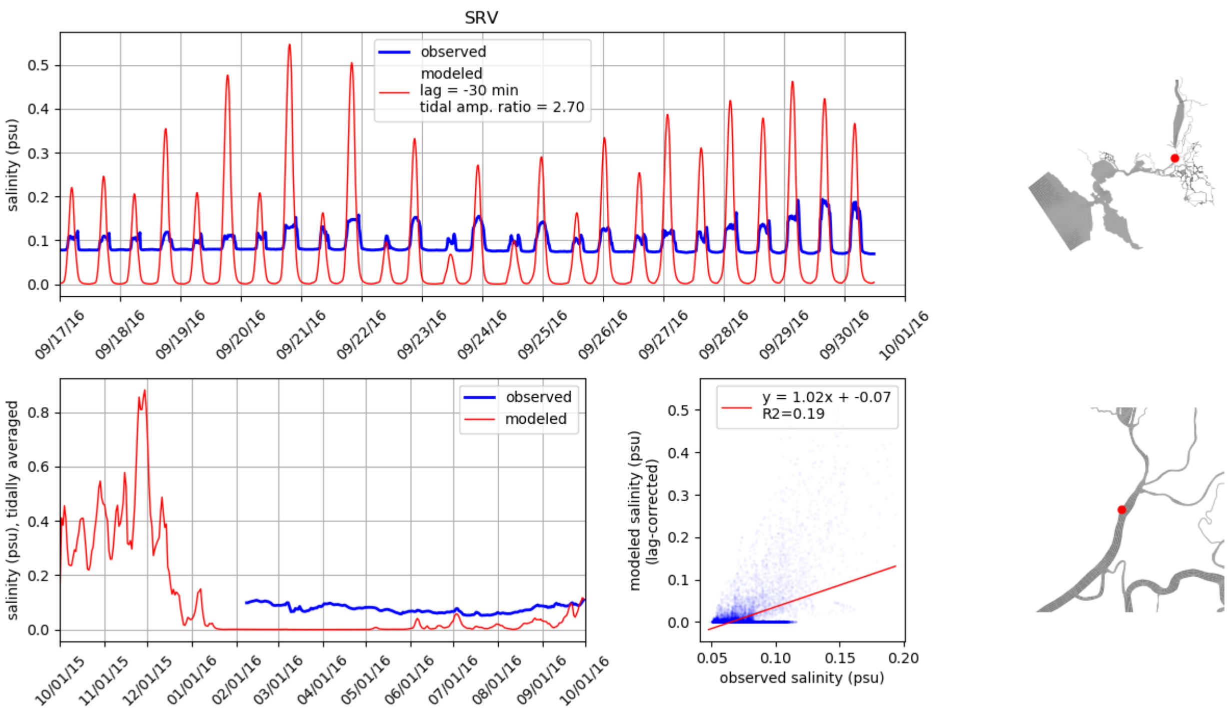

Figure 76: Comparison of modeled and observed salinity at station SRV. Tidally averaged signals are compared over the water year in lower left panel. Unfiltered signals are compared over a two-week period in the upper panel. Lower right panel compares unfiltered signals where modeled signal has been corrected for lag. On the right, the station location is shown on the model grid.

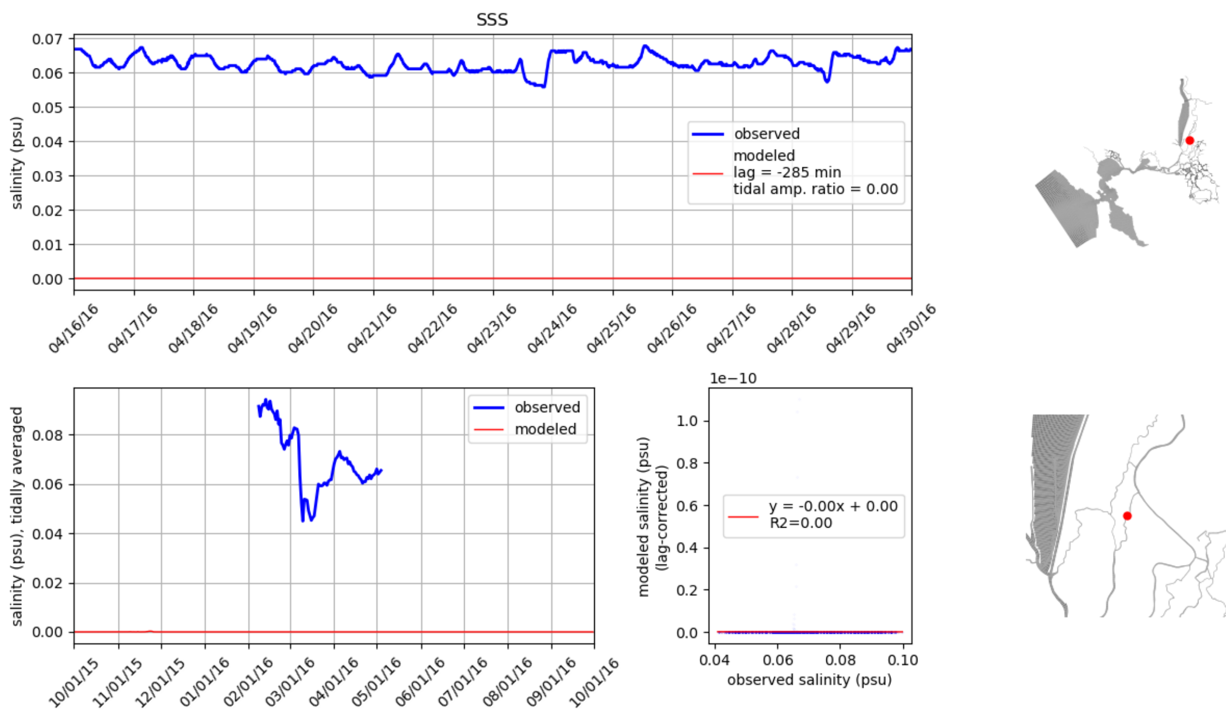

Figure 77: Comparison of modeled and observed salinity at station SSS. Tidally averaged signals are compared over the water year in lower left panel. Unfiltered signals are compared over a two-week period in the upper panel. Lower right panel compares unfiltered signals where modeled signal has been corrected for lag. On the right, the station location is shown on the model grid.

C Validation Plots: Temperature

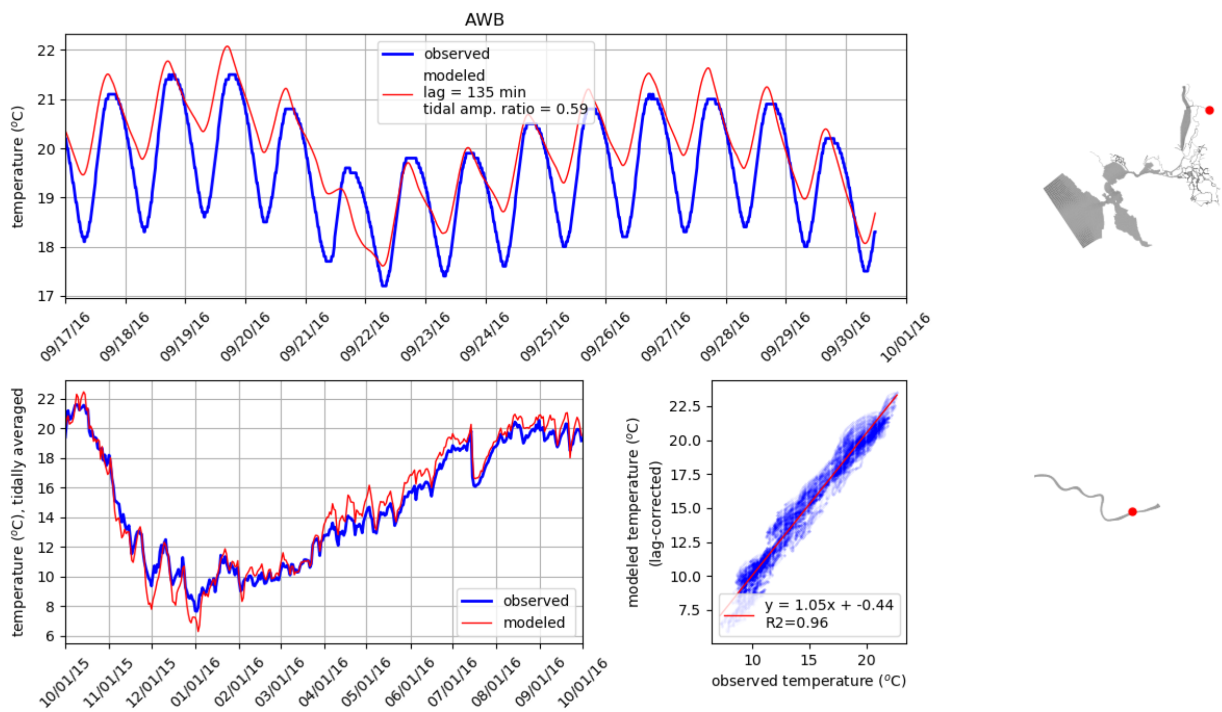

Figure 78: Comparison of modeled and observed temperatures at station AWB. Tidally averaged signals are compared over the water year in lower left panel. Unfiltered signals are compared over a two-week period in the upper panel. Lower right panel compares unfiltered signals where modeled signal has been corrected for lag. On the right, the station location is shown on the model grid.

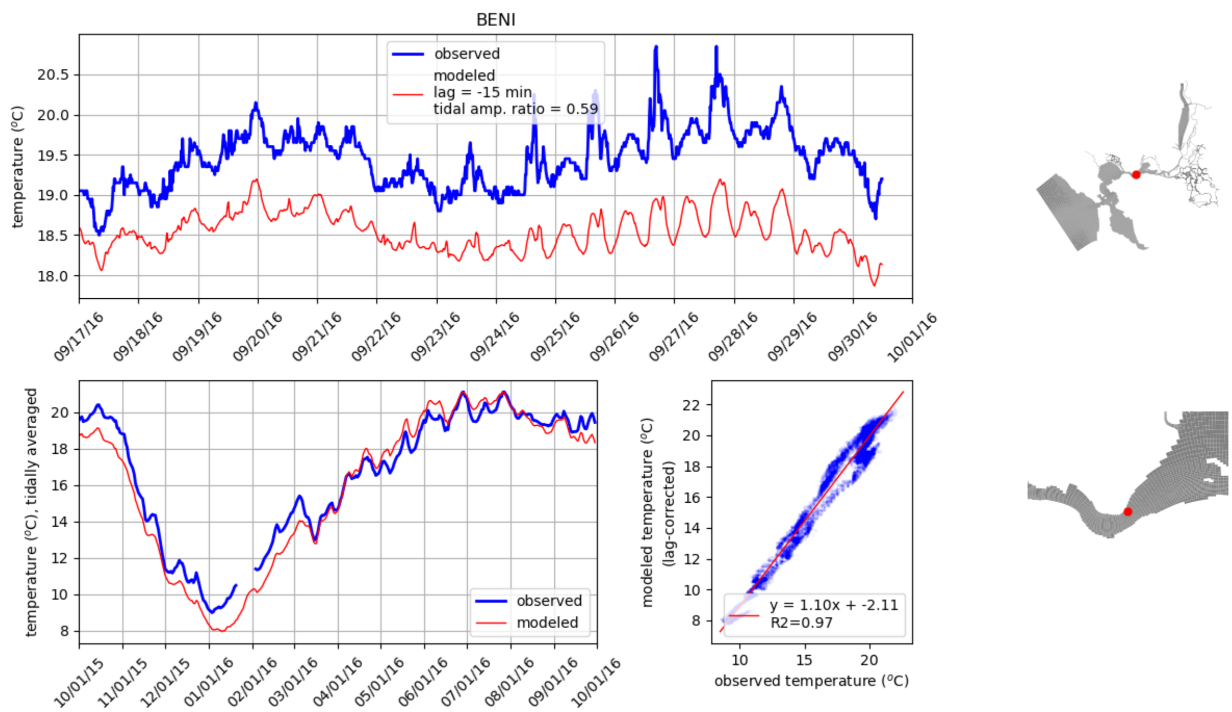

Figure 79: Comparison of modeled and observed temperatures at station BENI. Tidally averaged signals are compared over the water year in lower left panel. Unfiltered signals are compared over a two-week period in the upper panel. Lower right panel compares unfiltered signals where modeled signal has been corrected for lag. On the right, the station location is shown on the model grid.

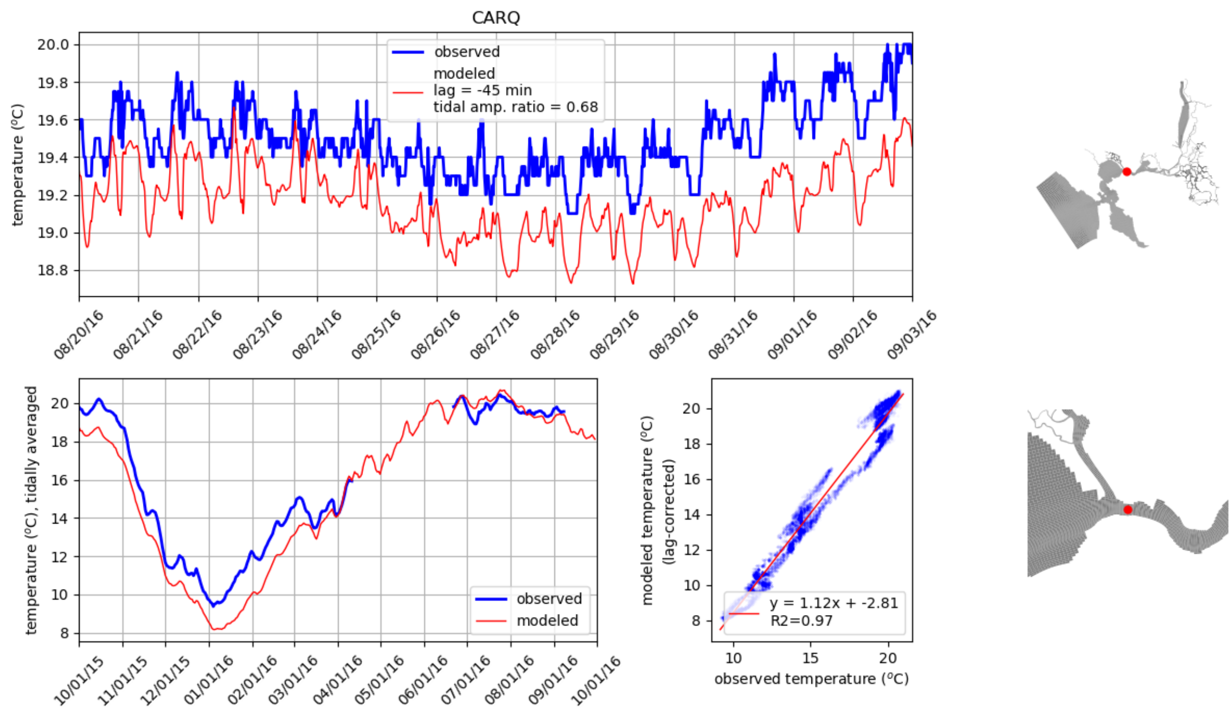

Figure 80: Comparison of modeled and observed temperatures at station CARQ. Tidally averaged signals are compared over the water year in lower left panel. Unfiltered signals are compared over a two-week period in the upper panel. Lower right panel compares unfiltered signals where modeled signal has been corrected for lag. On the right, the station location is shown on the model grid.

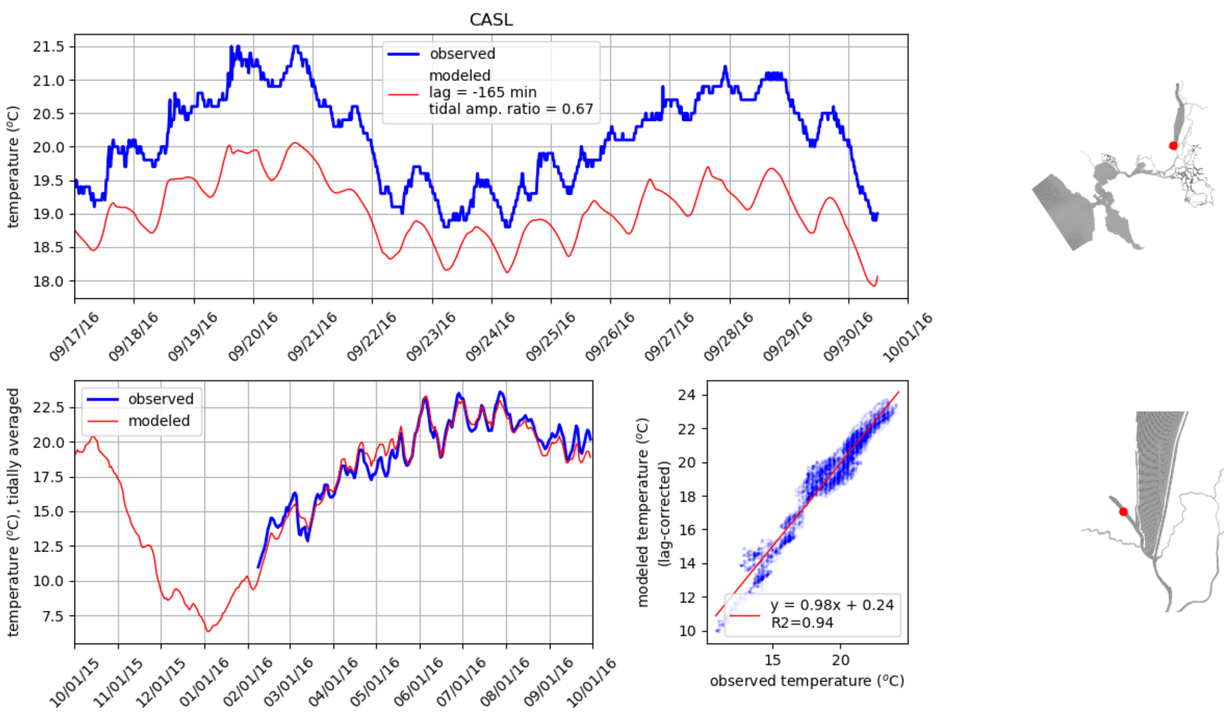

Figure 81: Comparison of modeled and observed temperatures at station CASL. Tidally averaged signals are compared over the water year in lower left panel. Unfiltered signals are compared over a two-week period in the upper panel. Lower right panel compares unfiltered signals where modeled signal has been corrected for lag. On the right, the station location is shown on the model grid.

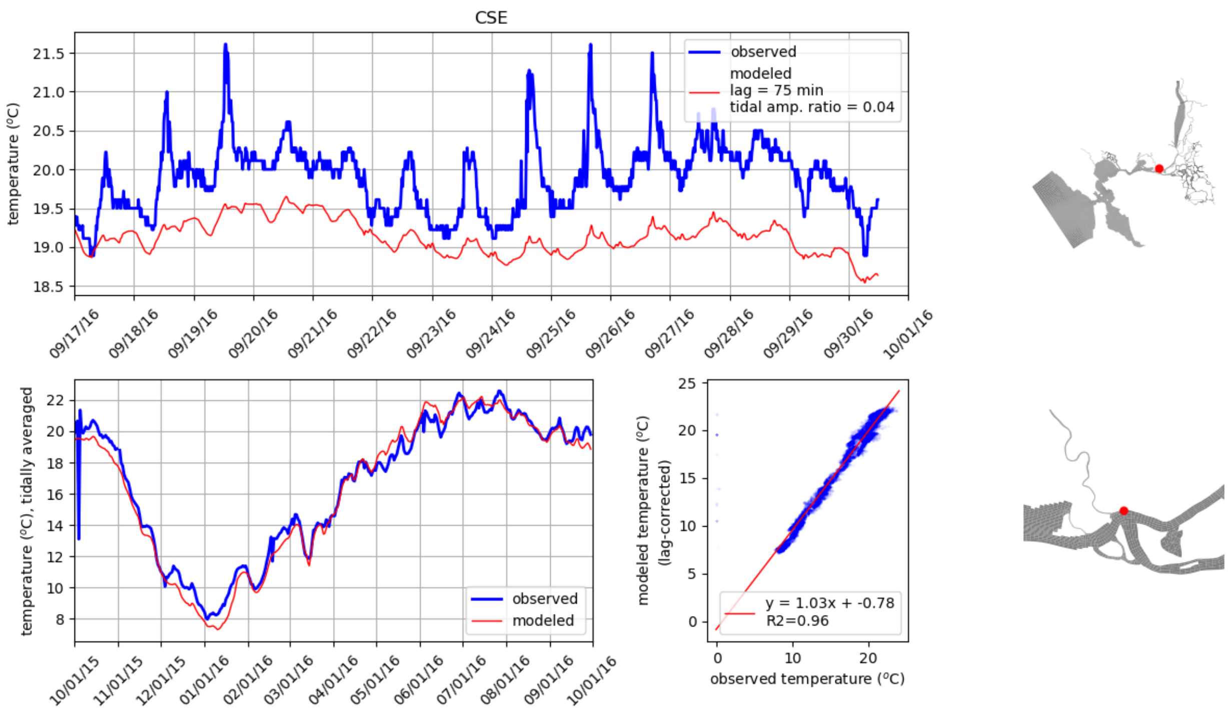

Figure 82: Comparison of modeled and observed temperatures at station CSE. Tidally averaged signals are compared over the water year in lower left panel. Unfiltered signals are compared over a two-week period in the upper panel. Lower right panel compares unfiltered signals where modeled signal has been corrected for lag. On the right, the station location is shown on the model grid.

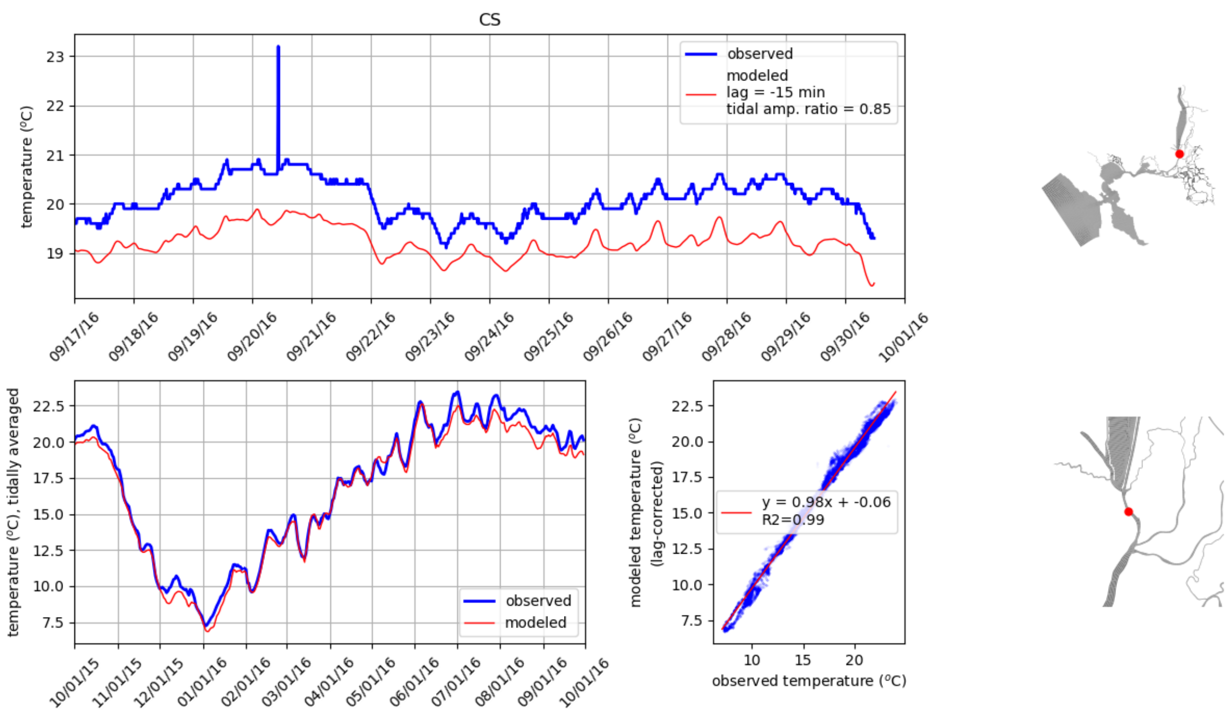

Figure 83: Comparison of modeled and observed temperatures at station CS. Tidally averaged signals are compared over the water year in lower left panel. Unfiltered signals are compared over a two-week period in the upper panel. Lower right panel compares unfiltered signals where modeled signal has been corrected for lag. On the right, the station location is shown on the model grid.

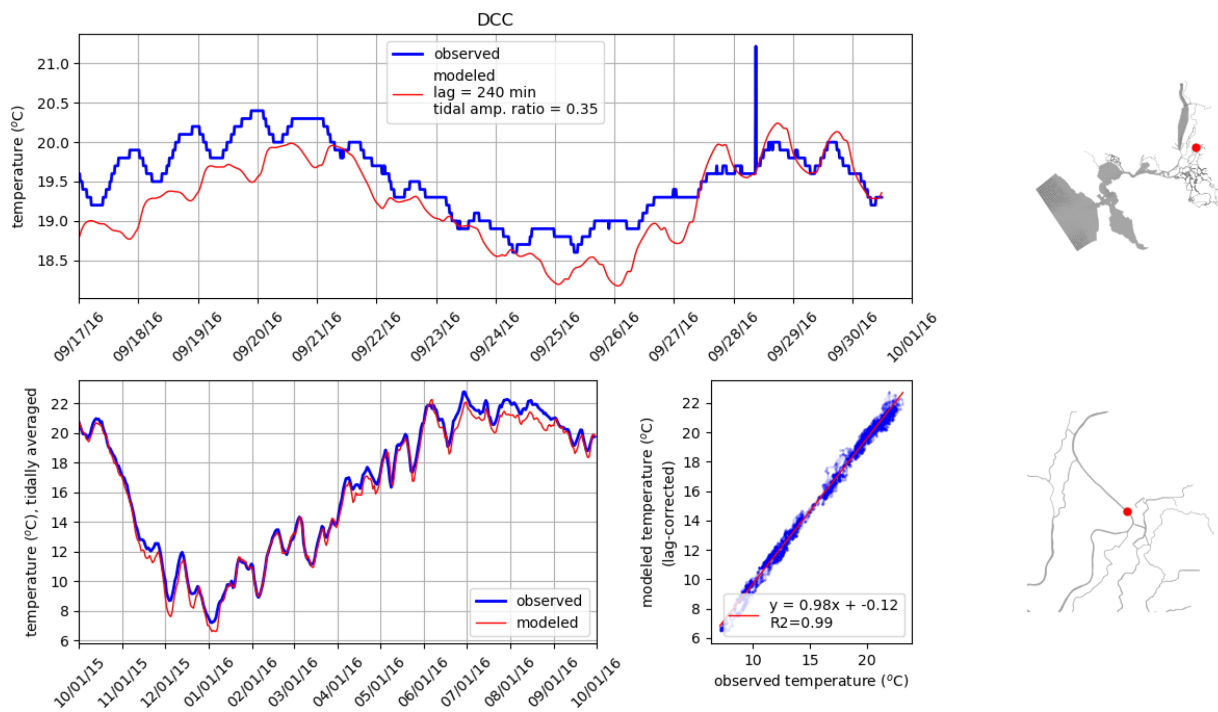

Figure 84: Comparison of modeled and observed temperatures at station DCC. Tidally averaged signals are compared over the water year in lower left panel. Unfiltered signals are compared over a two-week period in the upper panel. Lower right panel compares unfiltered signals where modeled signal has been corrected for lag. On the right, the station location is shown on the model grid.

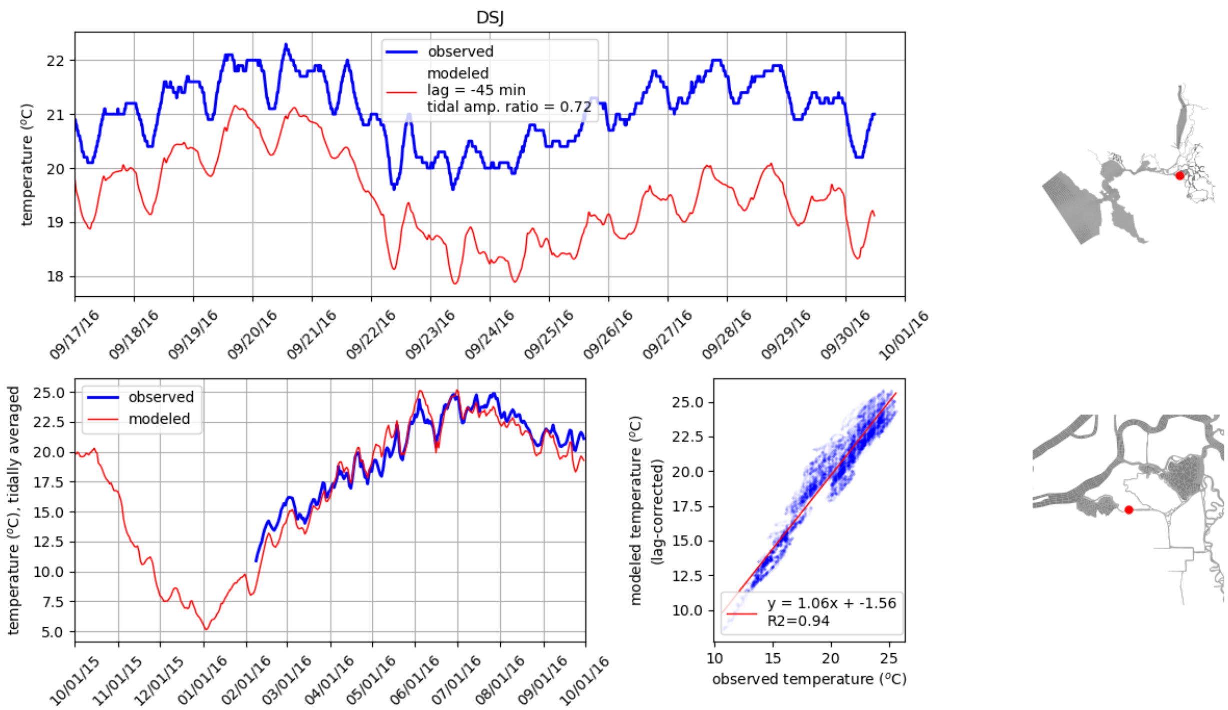

Figure 85: Comparison of modeled and observed temperatures at station DSJ. Tidally averaged signals are compared over the water year in lower left panel. Unfiltered signals are compared over a two-week period in the upper panel. Lower right panel compares unfiltered signals where modeled signal has been corrected for lag. On the right, the station location is shown on the model grid.

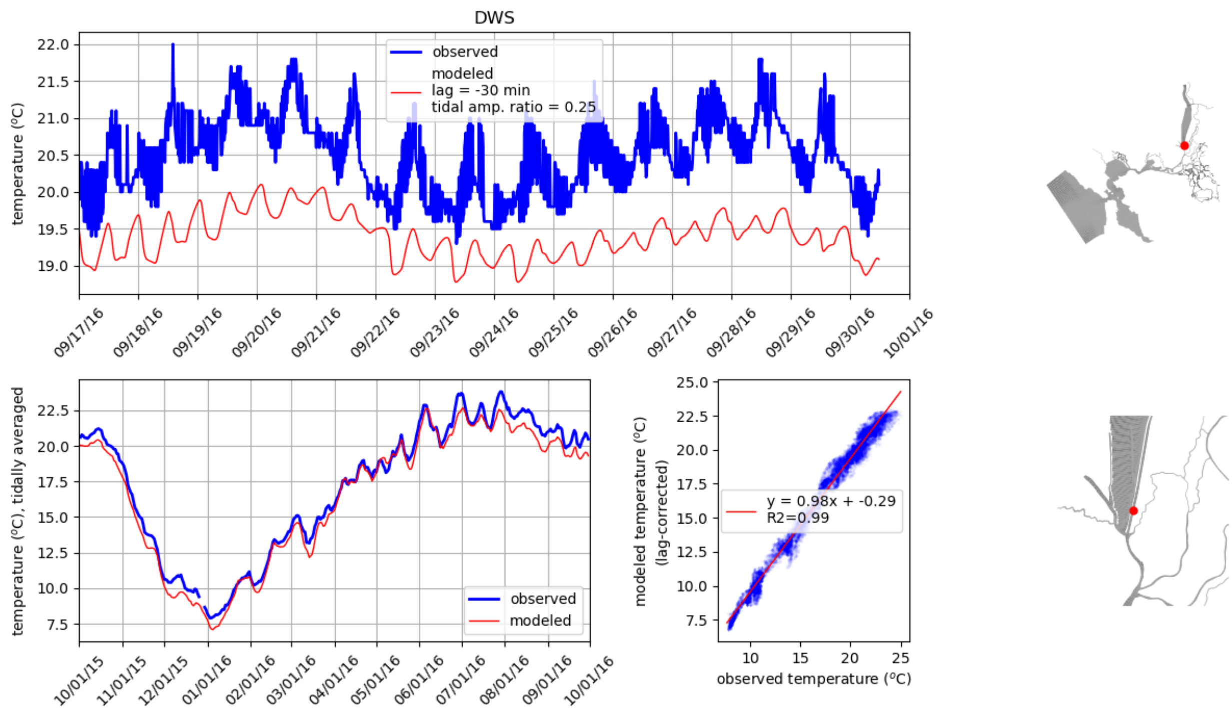

Figure 86: Comparison of modeled and observed temperatures at station DWS. Tidally averaged signals are compared over the water year in lower left panel. Unfiltered signals are compared over a two-week period in the upper panel. Lower right panel compares unfiltered signals where modeled signal has been corrected for lag. On the right, the station location is shown on the model grid.

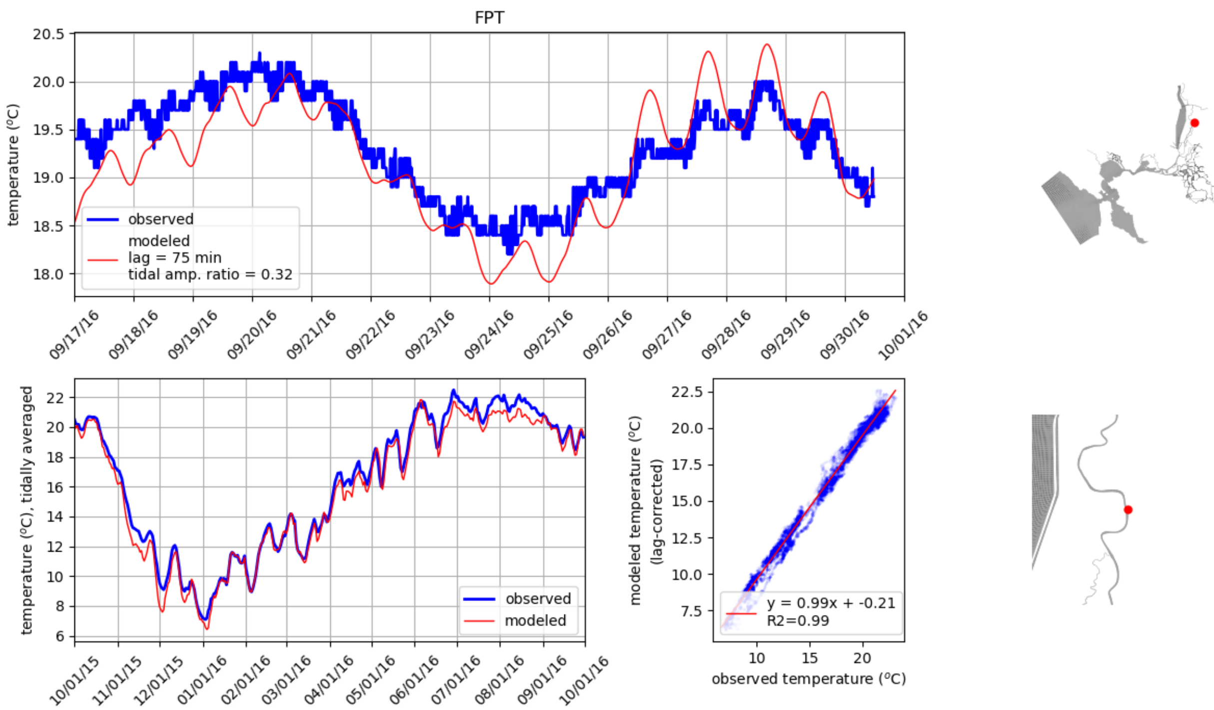

Figure 87: Comparison of modeled and observed temperatures at station FPT. Tidally averaged signals are compared over the water year in lower left panel. Unfiltered signals are compared over a two-week period in the upper panel. Lower right panel compares unfiltered signals where modeled signal has been corrected for lag. On the right, the station location is shown on the model grid.

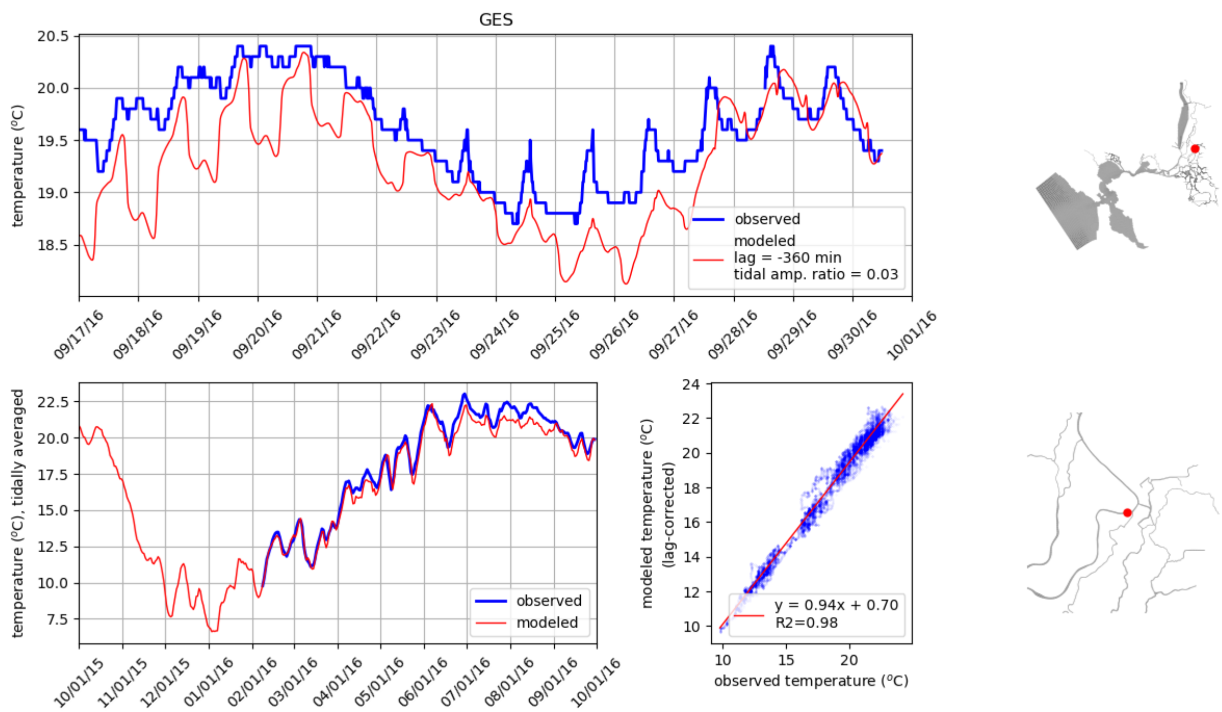

Figure 88: Comparison of modeled and observed temperatures at station GES. Tidally averaged signals are compared over the water year in lower left panel. Unfiltered signals are compared over a two-week period in the upper panel. Lower right panel compares unfiltered signals where modeled signal has been corrected for lag. On the right, the station location is shown on the model grid.

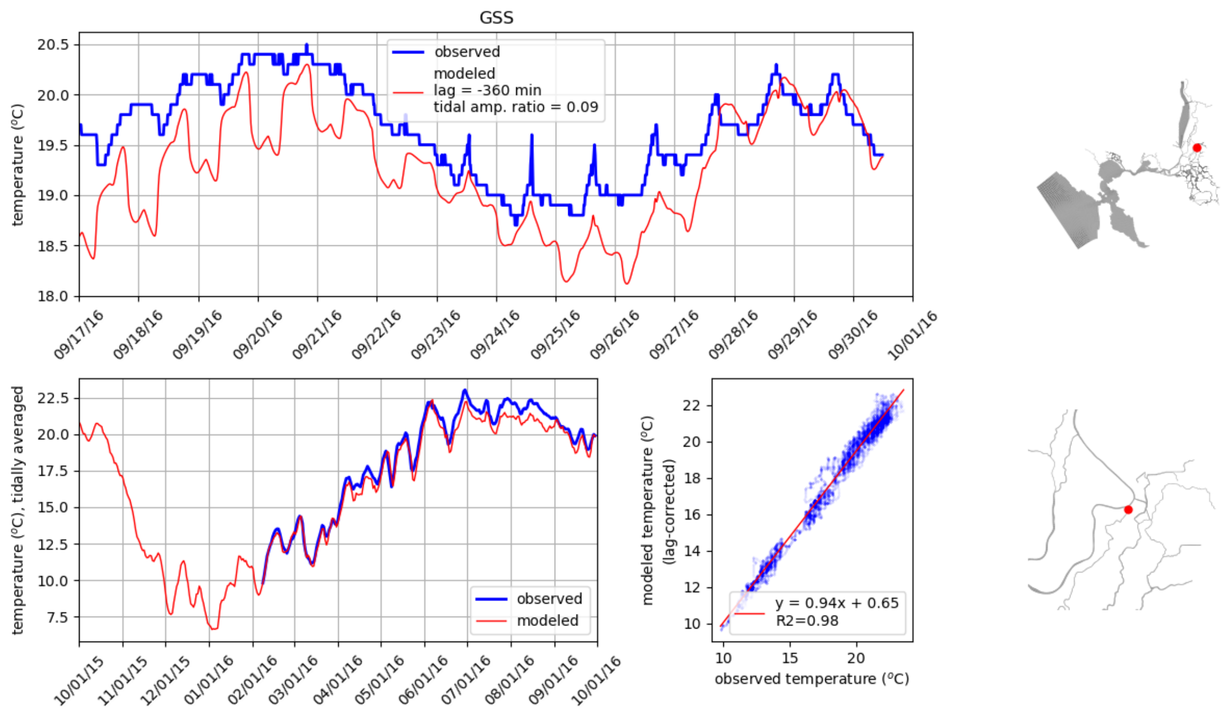

Figure 89: Comparison of modeled and observed temperatures at station GSS. Tidally averaged signals are compared over the water year in lower left panel. Unfiltered signals are compared over a two-week period in the upper panel. Lower right panel compares unfiltered signals where modeled signal has been corrected for lag. On the right, the station location is shown on the model grid.

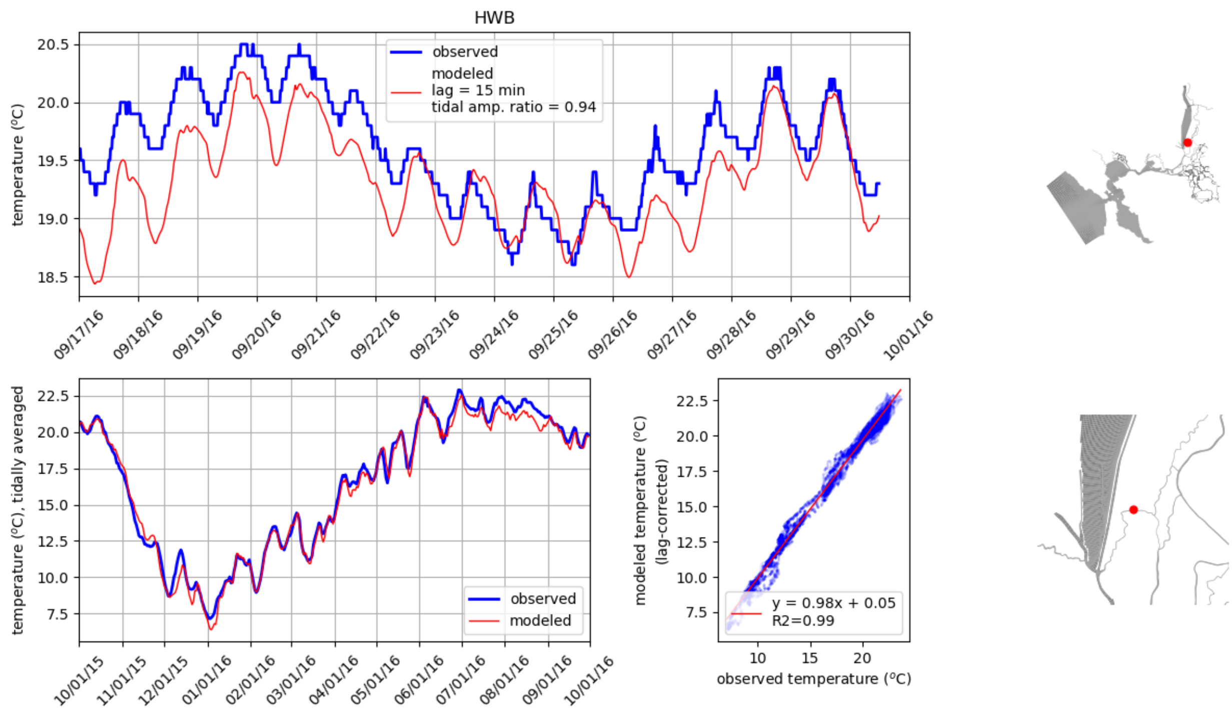

Figure 90: Comparison of modeled and observed temperatures at station HWB. Tidally averaged signals are compared over the water year in lower left panel. Unfiltered signals are compared over a two-week period in the upper panel. Lower right panel compares unfiltered signals where modeled signal has been corrected for lag. On the right, the station location is shown on the model grid.

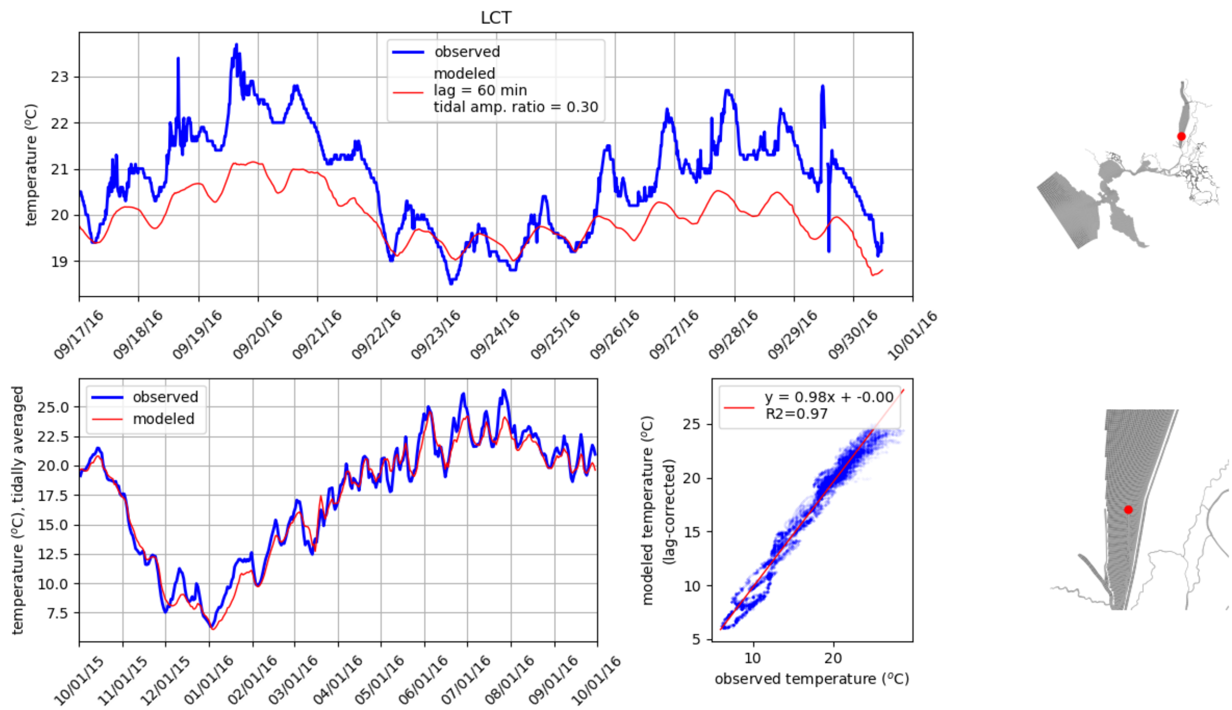

Figure 91: Comparison of modeled and observed temperatures at station LCT. Tidally averaged signals are compared over the water year in lower left panel. Unfiltered signals are compared over a two-week period in the upper panel. Lower right panel compares unfiltered signals where modeled signal has been corrected for lag. On the right, the station location is shown on the model grid.

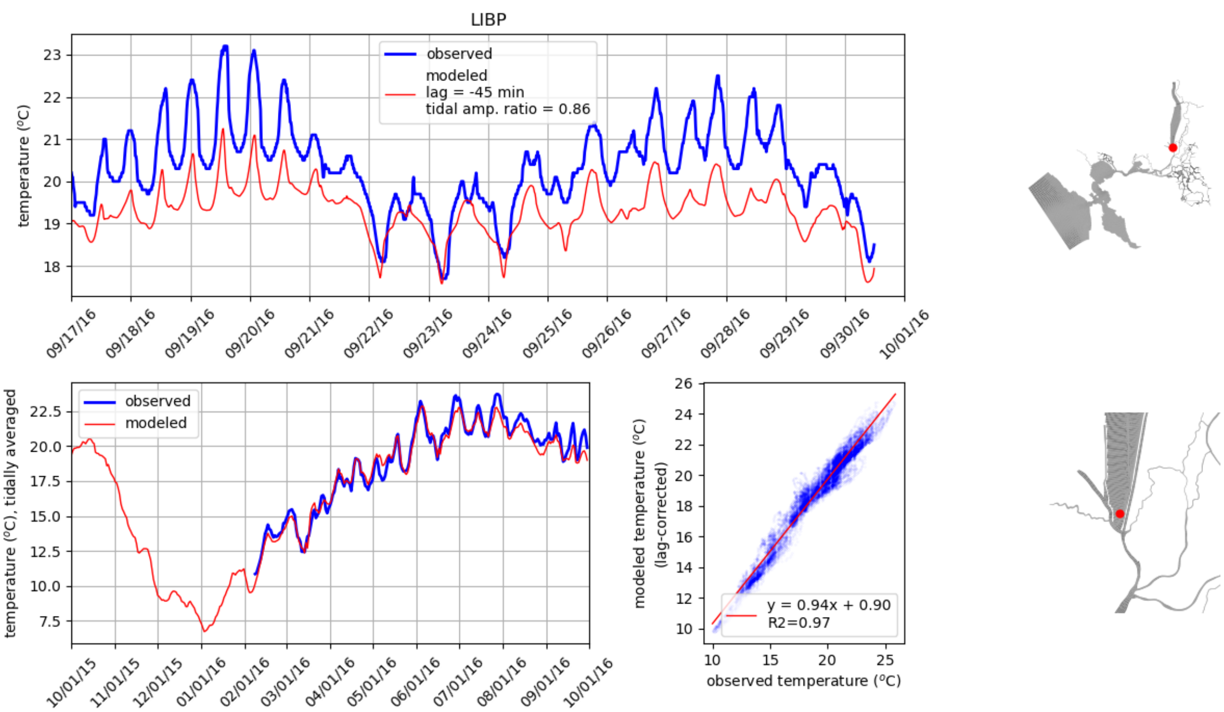

Figure 92: Comparison of modeled and observed temperatures at station LIBP. Tidally averaged signals are compared over the water year in lower left panel. Unfiltered signals are compared over a two-week period in the upper panel. Lower right panel compares unfiltered signals where modeled signal has been corrected for lag. On the right, the station location is shown on the model grid.

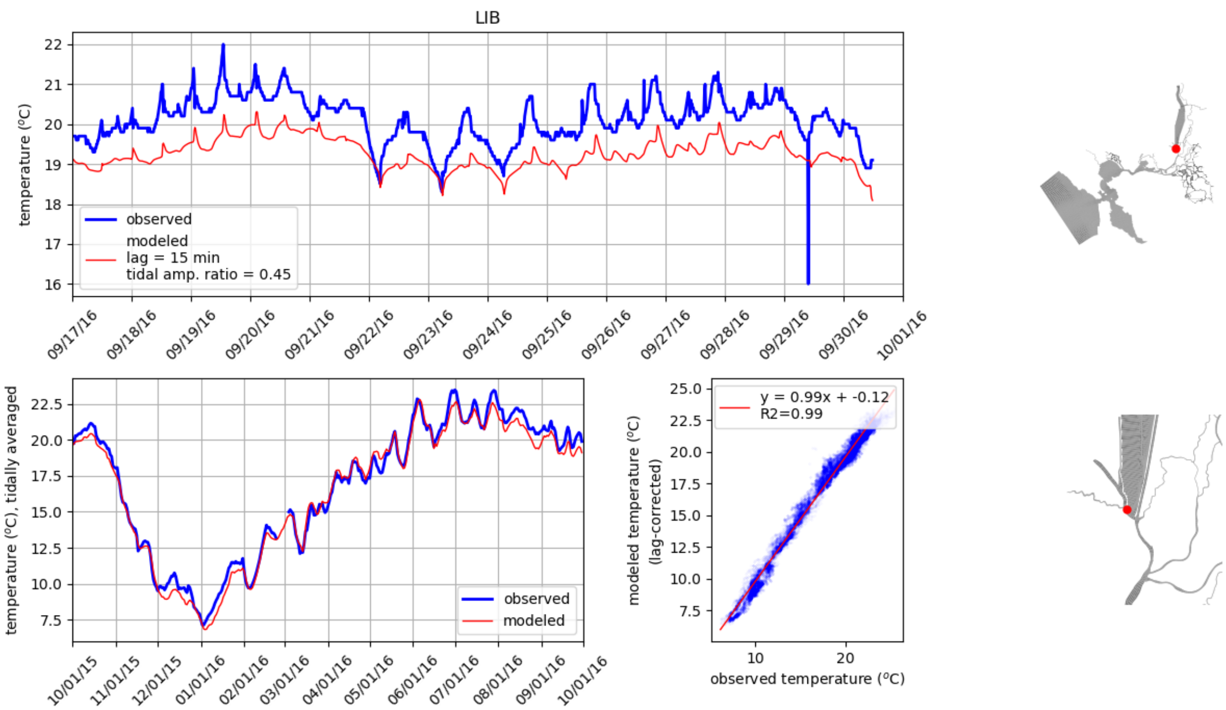

Figure 93: Comparison of modeled and observed temperatures at station LIB. Tidally averaged signals are compared over the water year in lower left panel. Unfiltered signals are compared over a two-week period in the upper panel. Lower right panel compares unfiltered signals where modeled signal has been corrected for lag. On the right, the station location is shown on the model grid.

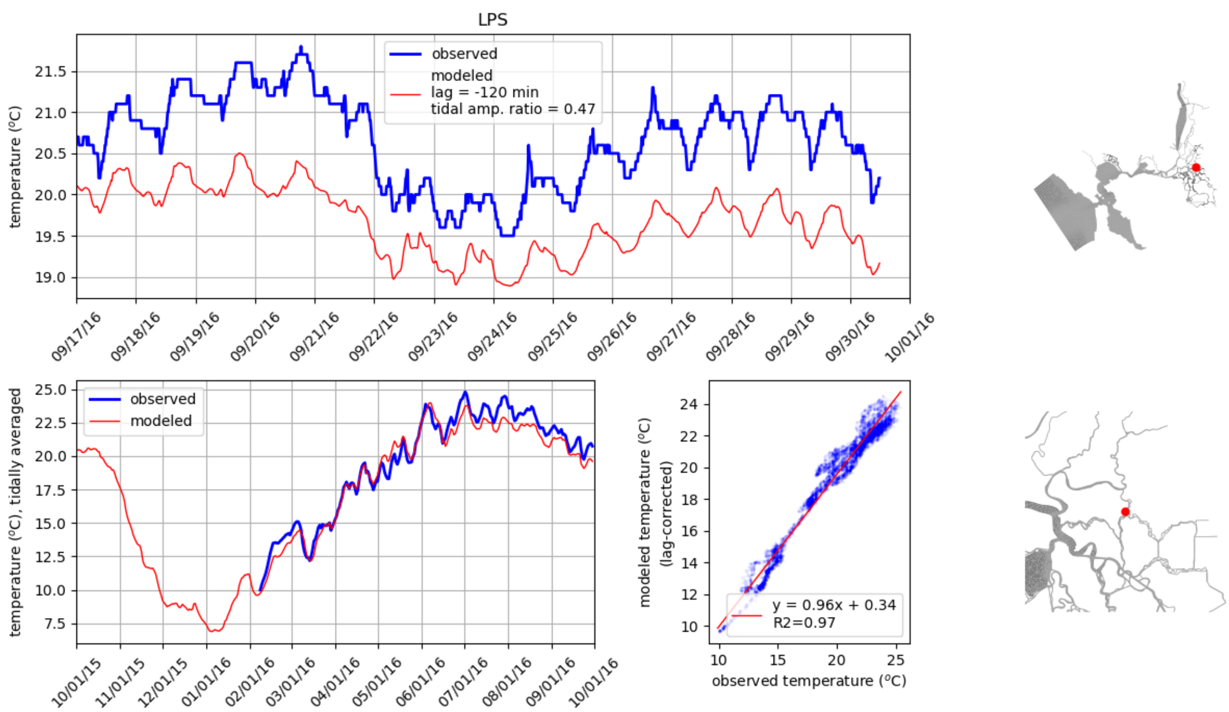

Figure 94: Comparison of modeled and observed temperatures at station LPS. Tidally averaged signals are compared over the water year in lower left panel. Unfiltered signals are compared over a two-week period in the upper panel. Lower right panel compares unfiltered signals where modeled signal has been corrected for lag. On the right, the station location is shown on the model grid.

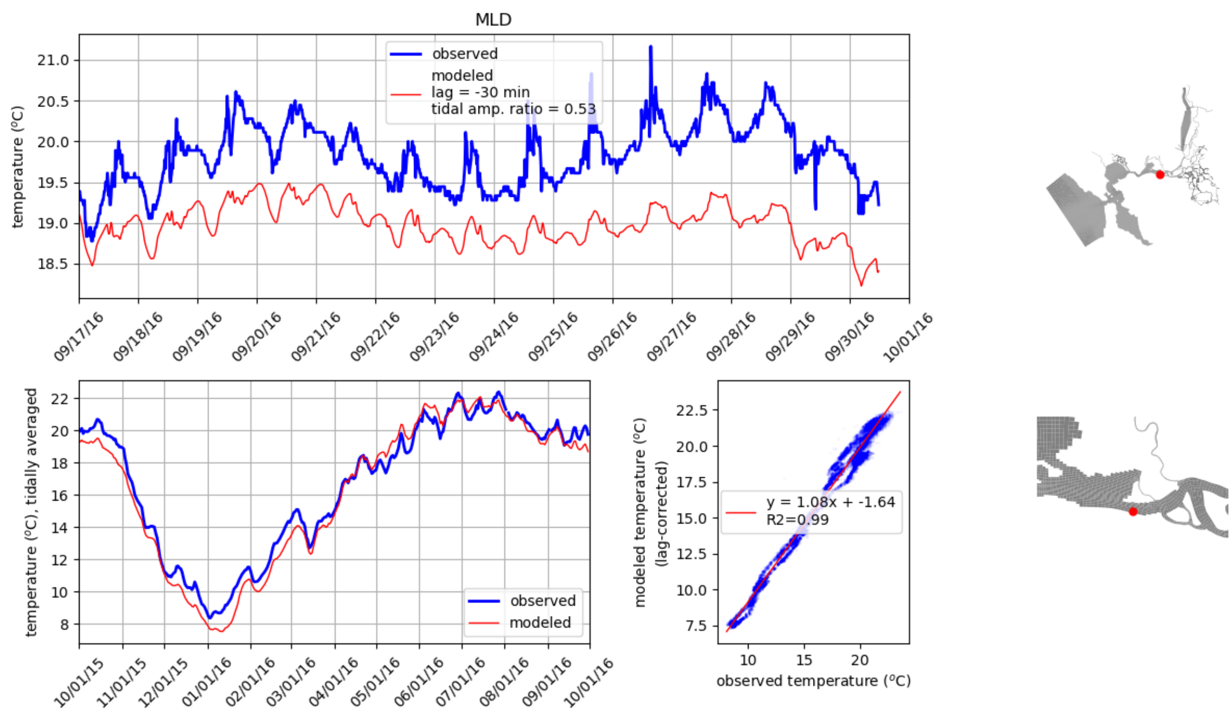

Figure 95: Comparison of modeled and observed temperatures at station MLD. Tidally averaged signals are compared over the water year in lower left panel. Unfiltered signals are compared over a two-week period in the upper panel. Lower right panel compares unfiltered signals where modeled signal has been corrected for lag. On the right, the station location is shown on the model grid.

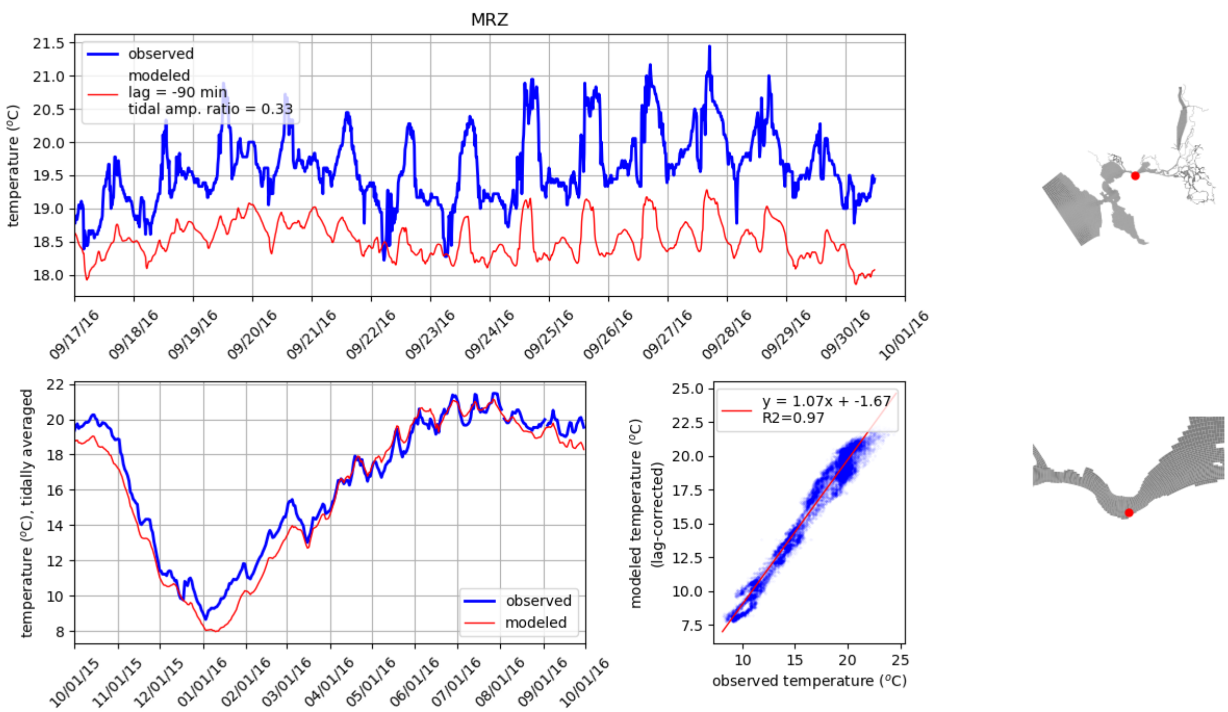

Figure 96: Comparison of modeled and observed temperatures at station MRZ. Tidally averaged signals are compared over the water year in lower left panel. Unfiltered signals are compared over a two-week period in the upper panel. Lower right panel compares unfiltered signals where modeled signal has been corrected for lag. On the right, the station location is shown on the model grid.

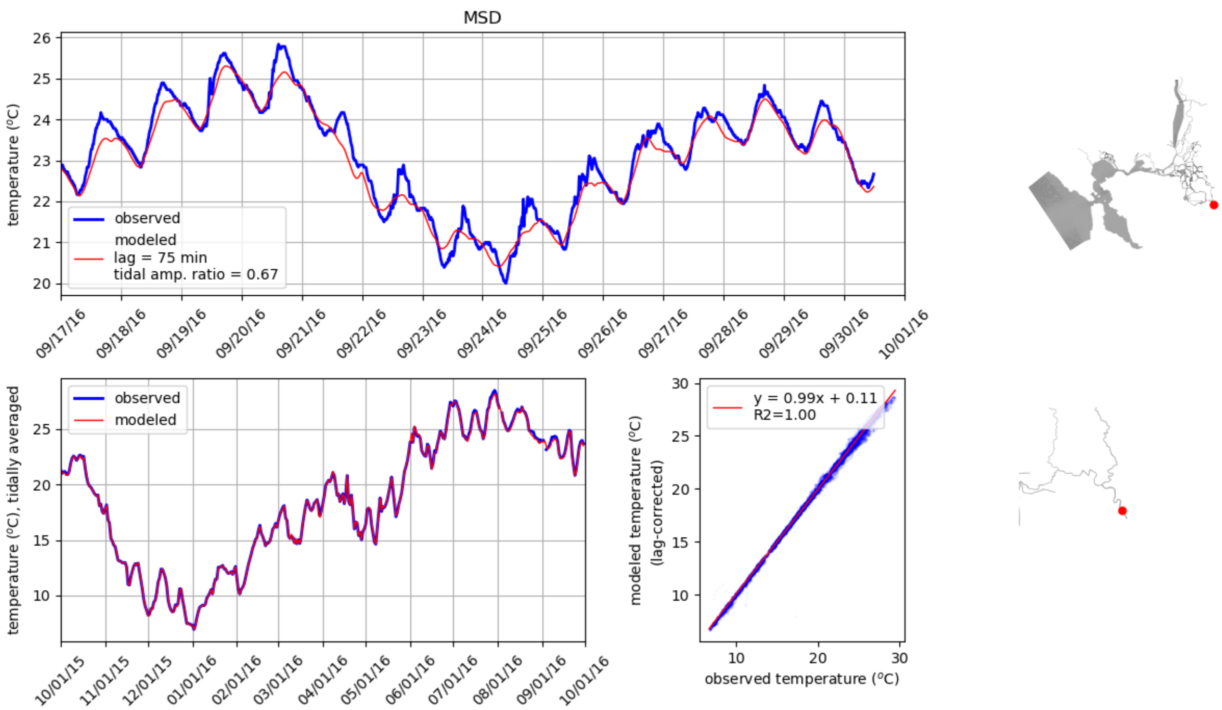

Figure 97: Comparison of modeled and observed temperatures at station MSD. Tidally averaged signals are compared over the water year in lower left panel. Unfiltered signals are compared over a two-week period in the upper panel. Lower right panel compares unfiltered signals where modeled signal has been corrected for lag. On the right, the station location is shown on the model grid.

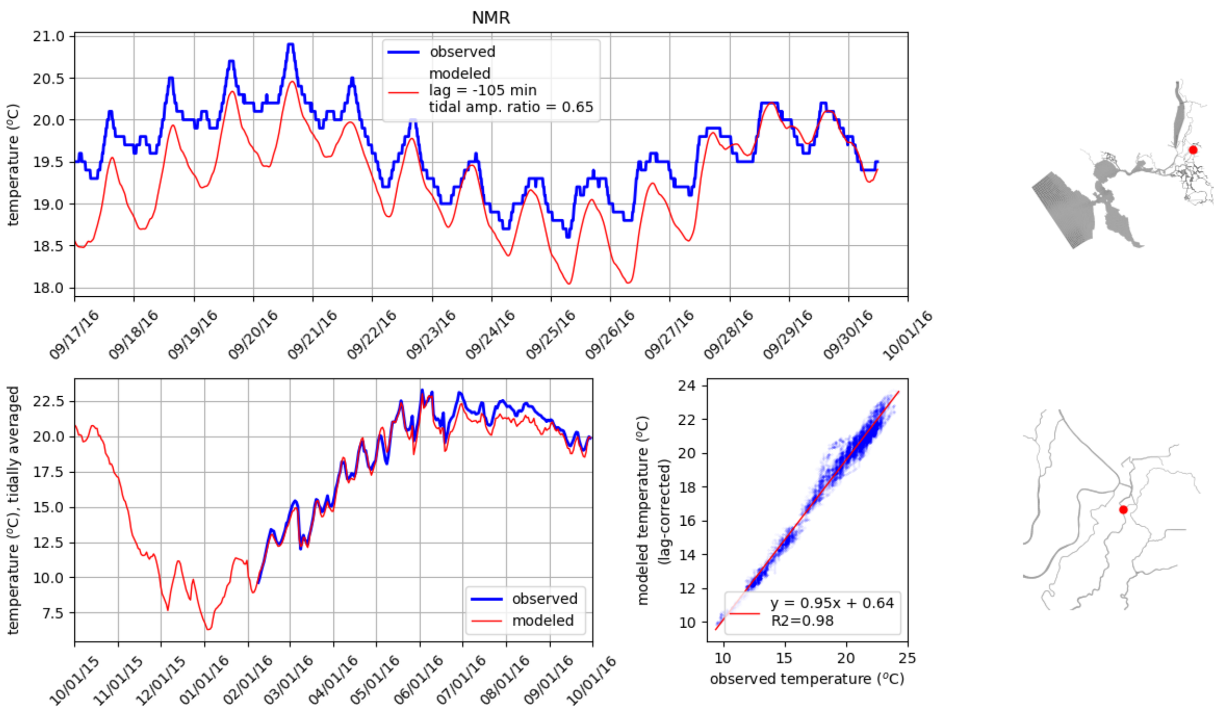

Figure 98: Comparison of modeled and observed temperatures at station NMR. Tidally averaged signals are compared over the water year in lower left panel. Unfiltered signals are compared over a two-week period in the upper panel. Lower right panel compares unfiltered signals where modeled signal has been corrected for lag. On the right, the station location is shown on the model grid.

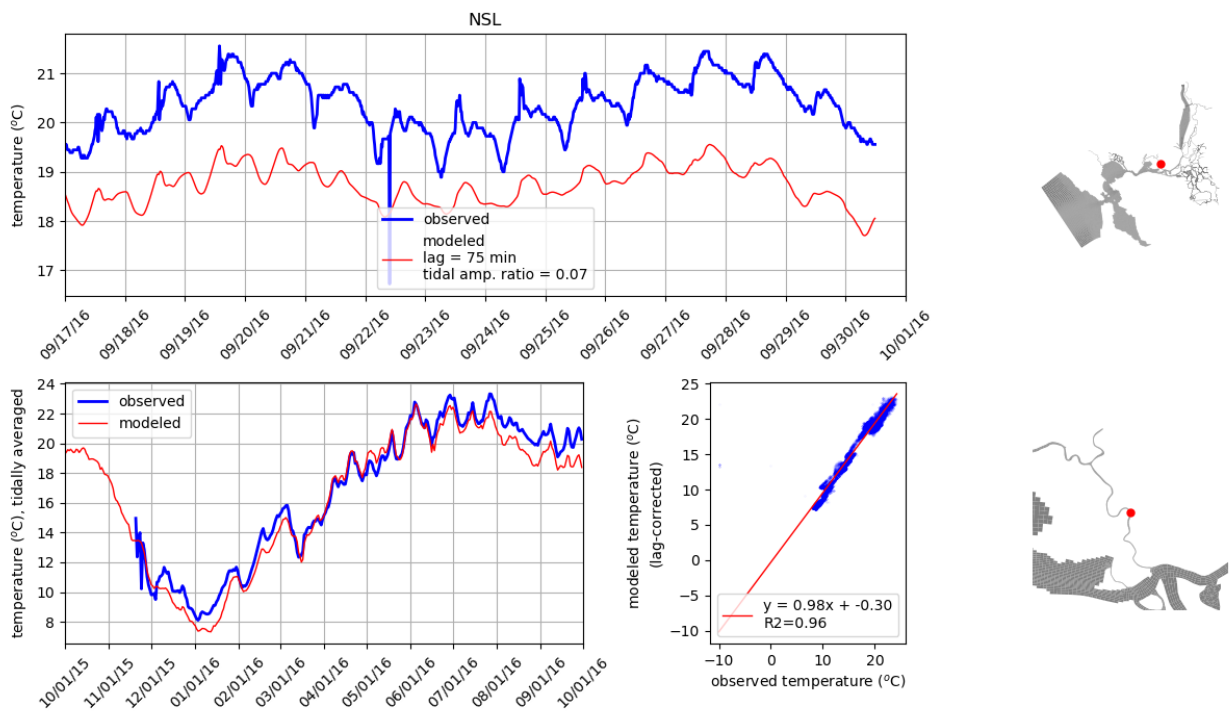

Figure 99: Comparison of modeled and observed temperatures at station NSL. Tidally averaged signals are compared over the water year in lower left panel. Unfiltered signals are compared over a two-week period in the upper panel. Lower right panel compares unfiltered signals where modeled signal has been corrected for lag. On the right, the station location is shown on the model grid.

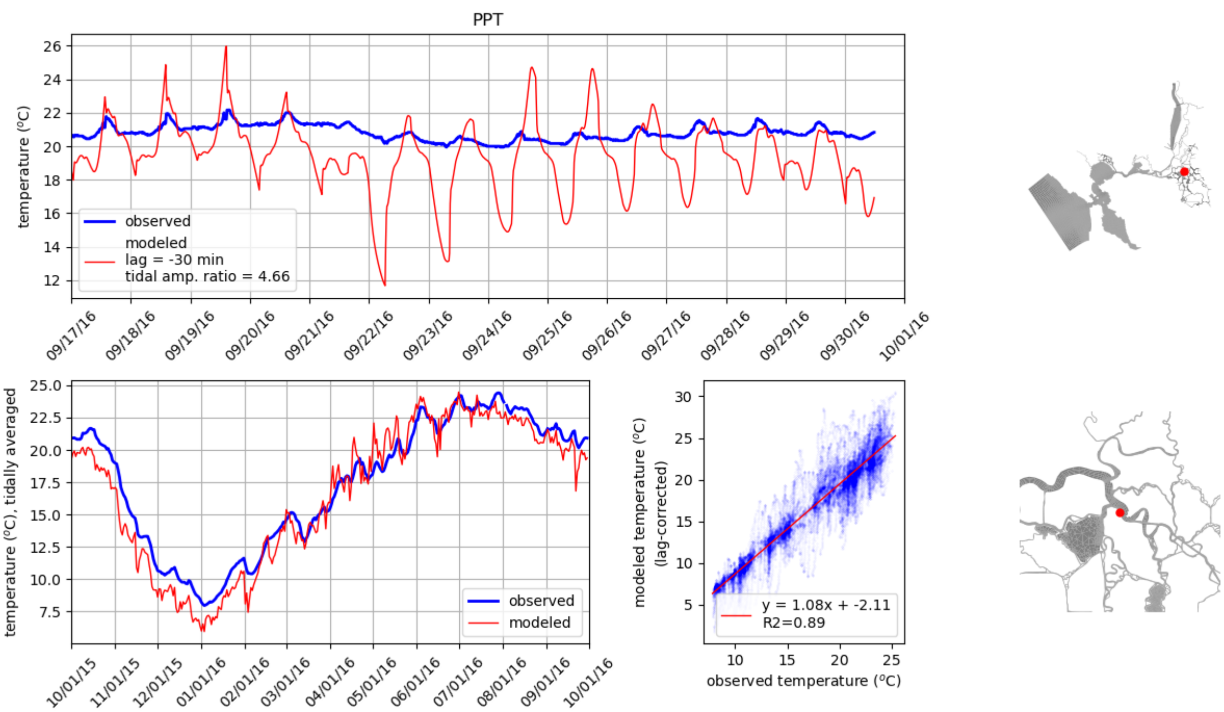

Figure 100: Comparison of modeled and observed temperatures at station PPT. Tidally averaged signals are compared over the water year in lower left panel. Unfiltered signals are compared over a two-week period in the upper panel. Lower right panel compares unfiltered signals where modeled signal has been corrected for lag. On the right, the station location is shown on the model grid.

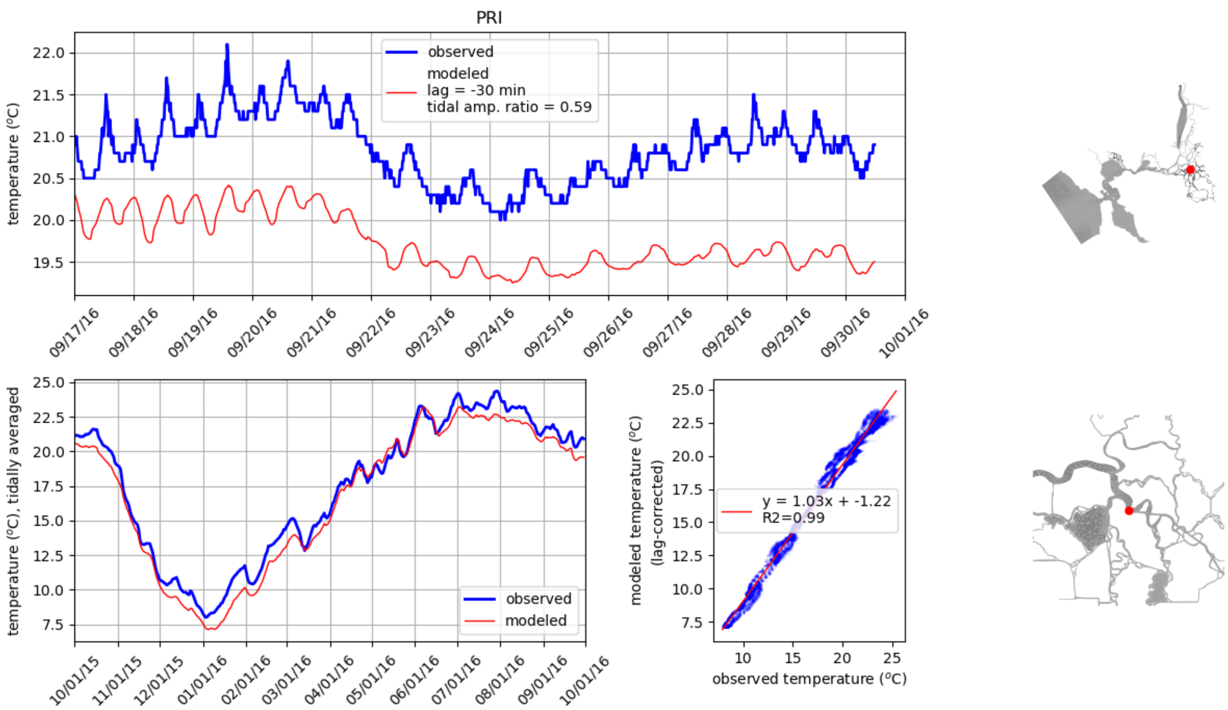

Figure 101: Comparison of modeled and observed temperatures at station PRI. Tidally averaged signals are compared over the water year in lower left panel. Unfiltered signals are compared over a two-week period in the upper panel. Lower right panel compares unfiltered signals where modeled signal has been corrected for lag. On the right, the station location is shown on the model grid.

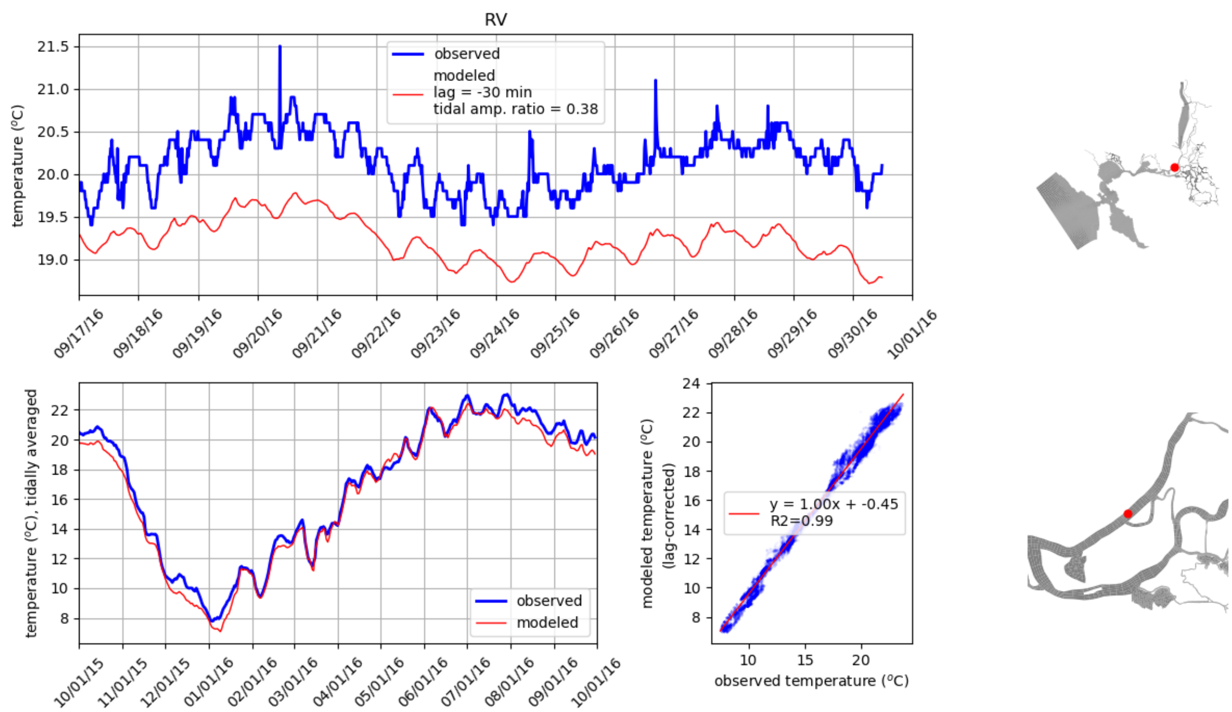

Figure 102: Comparison of modeled and observed temperatures at station RV. Tidally averaged signals are compared over the water year in lower left panel. Unfiltered signals are compared over a two-week period in the upper panel. Lower right panel compares unfiltered signals where modeled signal has been corrected for lag. On the right, the station location is shown on the model grid.

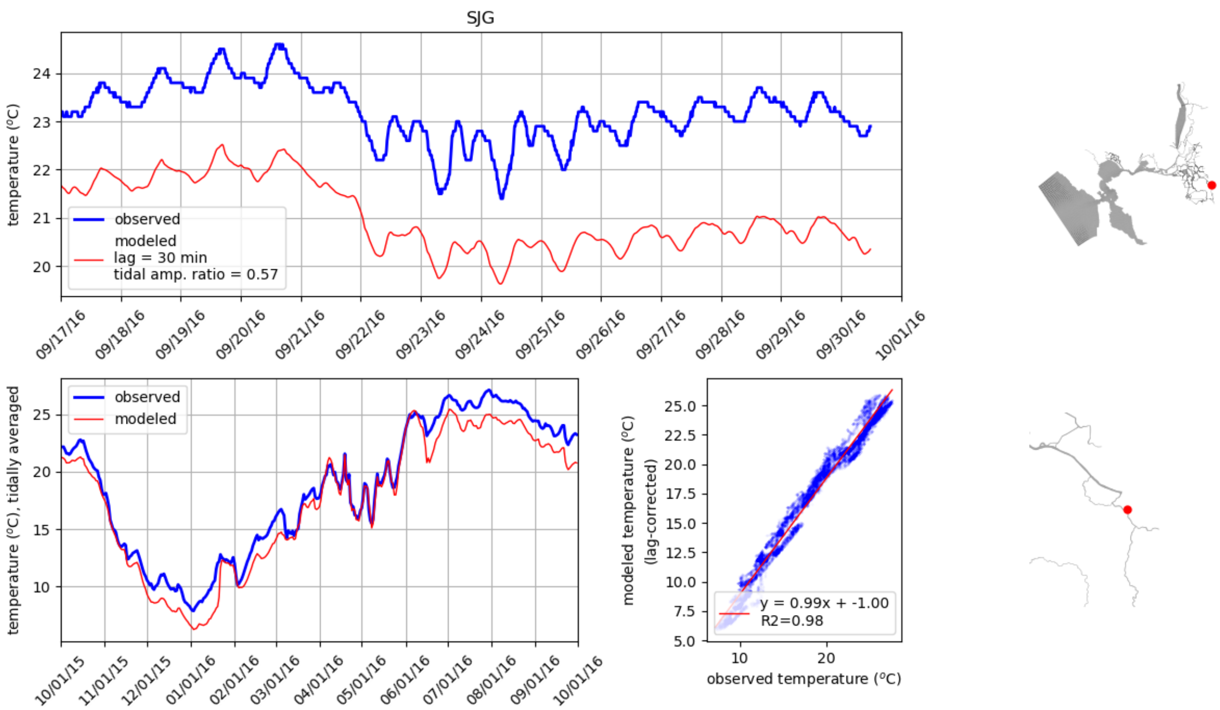

Figure 103: Comparison of modeled and observed temperatures at station SJG. Tidally averaged signals are compared over the water year in lower left panel. Unfiltered signals are compared over a two-week period in the upper panel. Lower right panel compares unfiltered signals where modeled signal has been corrected for lag. On the right, the station location is shown on the model grid.

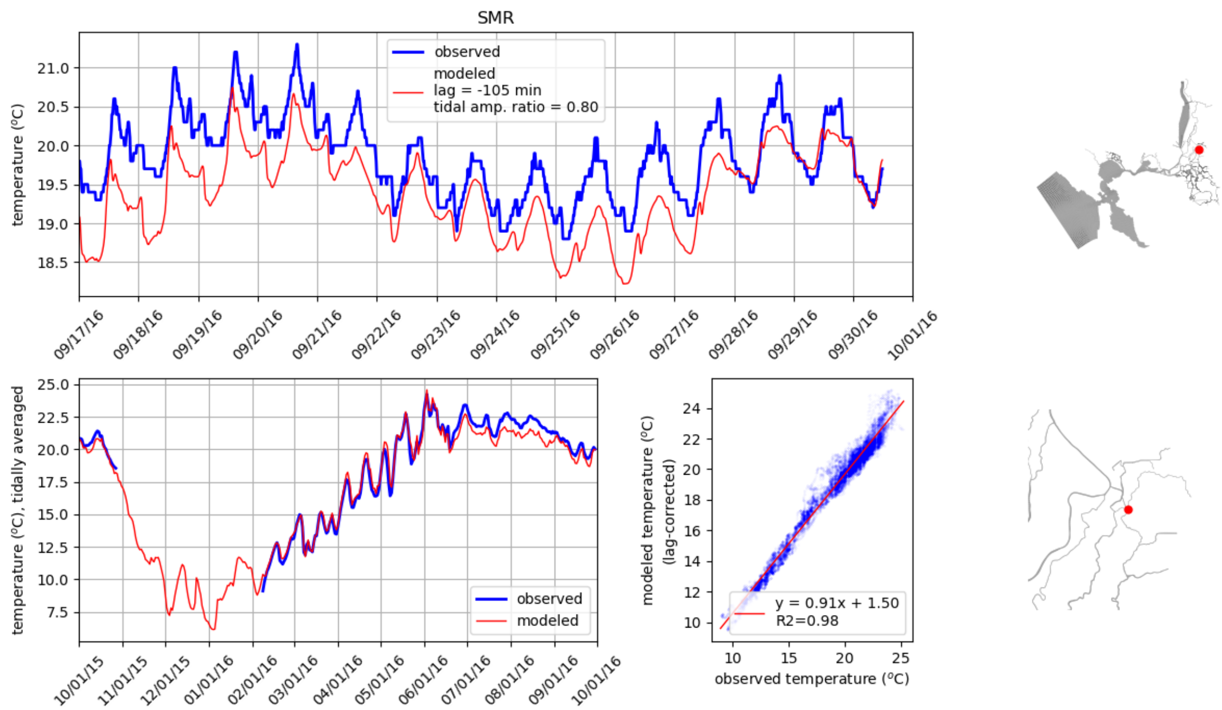

Figure 104: Comparison of modeled and observed temperatures at station SMR. Tidally averaged signals are compared over the water year in lower left panel. Unfiltered signals are compared over a two-week period in the upper panel. Lower right panel compares unfiltered signals where modeled signal has been corrected for lag. On the right, the station location is shown on the model grid.

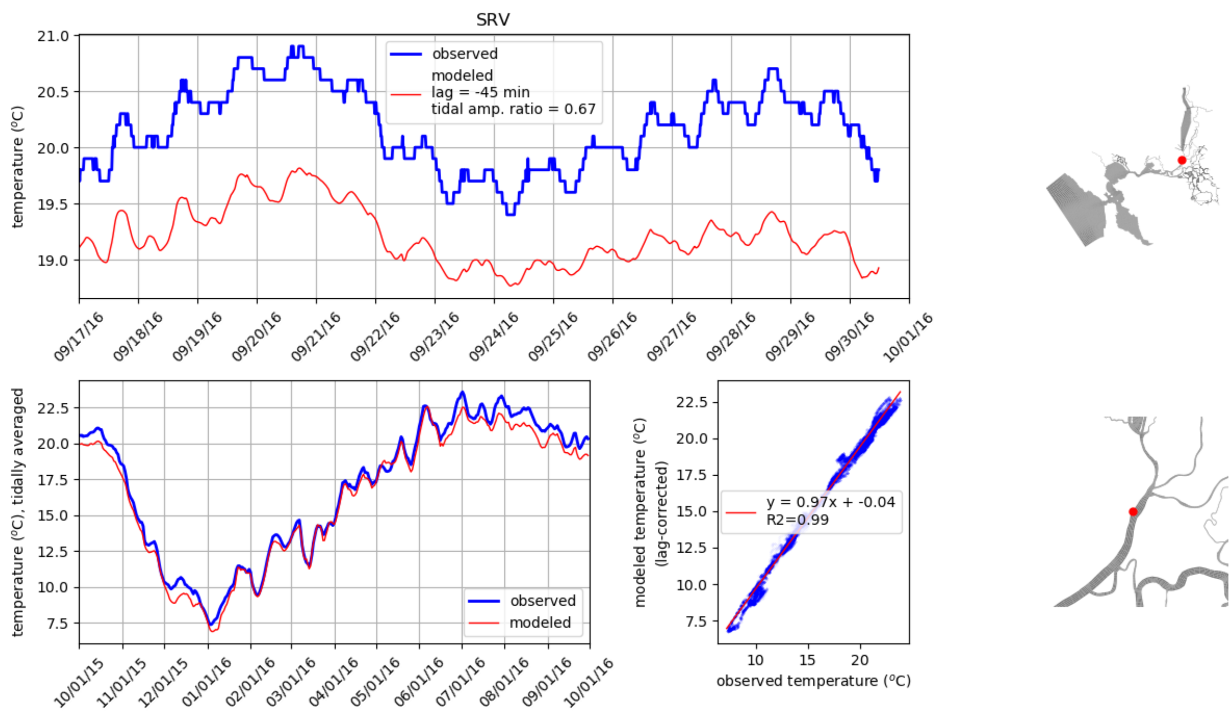

Figure 105: Comparison of modeled and observed temperatures at station SRV. Tidally averaged signals are compared over the water year in lower left panel. Unfiltered signals are compared over a two-week period in the upper panel. Lower right panel compares unfiltered signals where modeled signal has been corrected for lag. On the right, the station location is shown on the model grid.

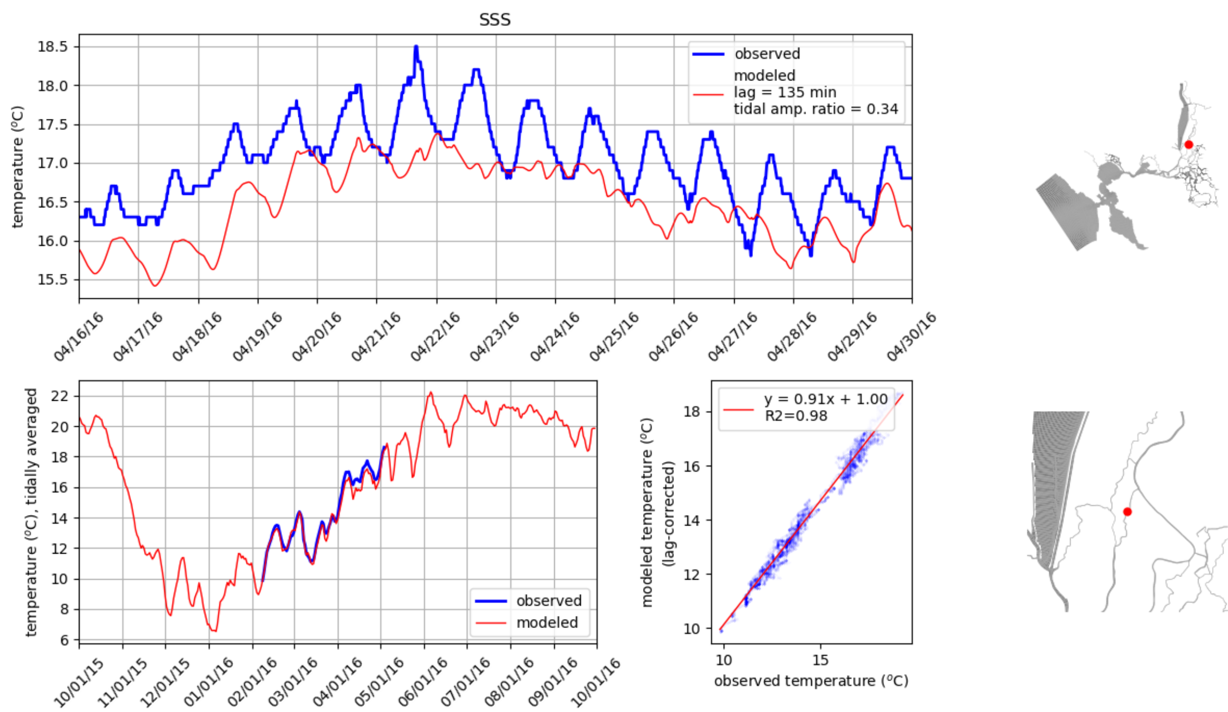

Figure 106: Comparison of modeled and observed temperatures at station SSS. Tidally averaged signals are compared over the water year in lower left panel. Unfiltered signals are compared over a two-week period in the upper panel. Lower right panel compares unfiltered signals where modeled signal has been corrected for lag. On the right, the station location is shown on the model grid.

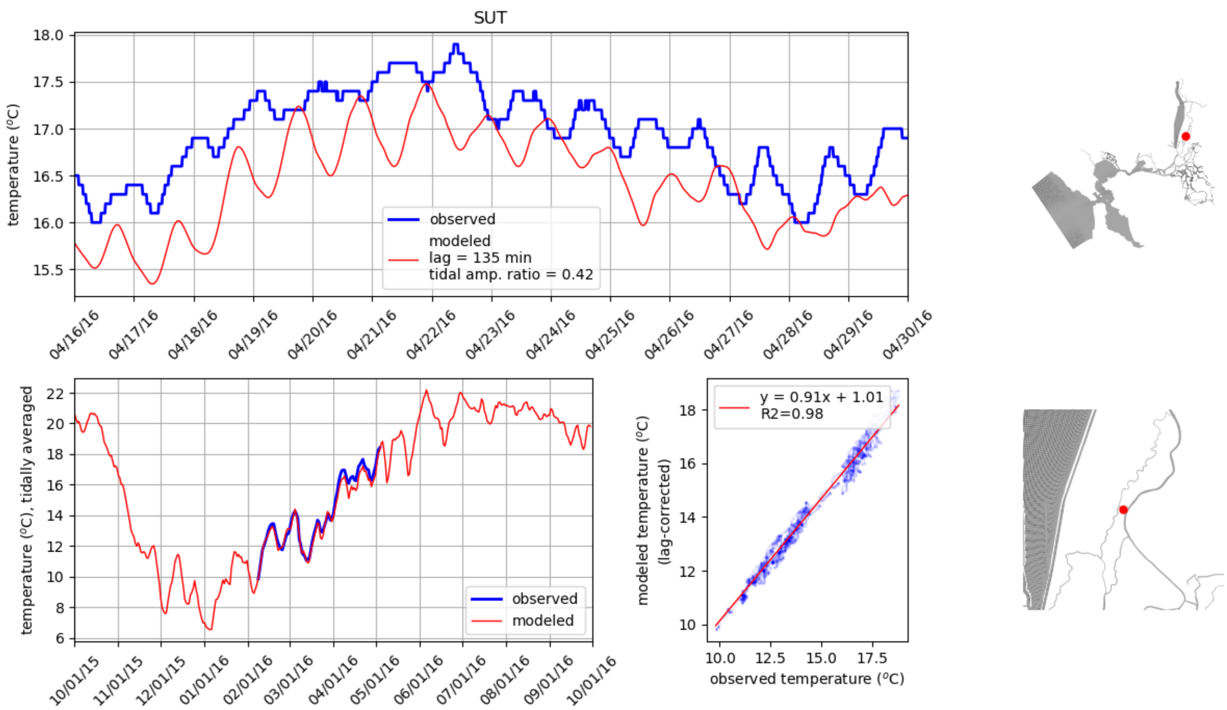

Figure 107: Comparison of modeled and observed temperatures at station SUT. Tidally averaged signals are compared over the water year in lower left panel. Unfiltered signals are compared over a two-week period in the upper panel. Lower right panel compares unfiltered signals where modeled signal has been corrected for lag. On the right, the station location is shown on the model grid.

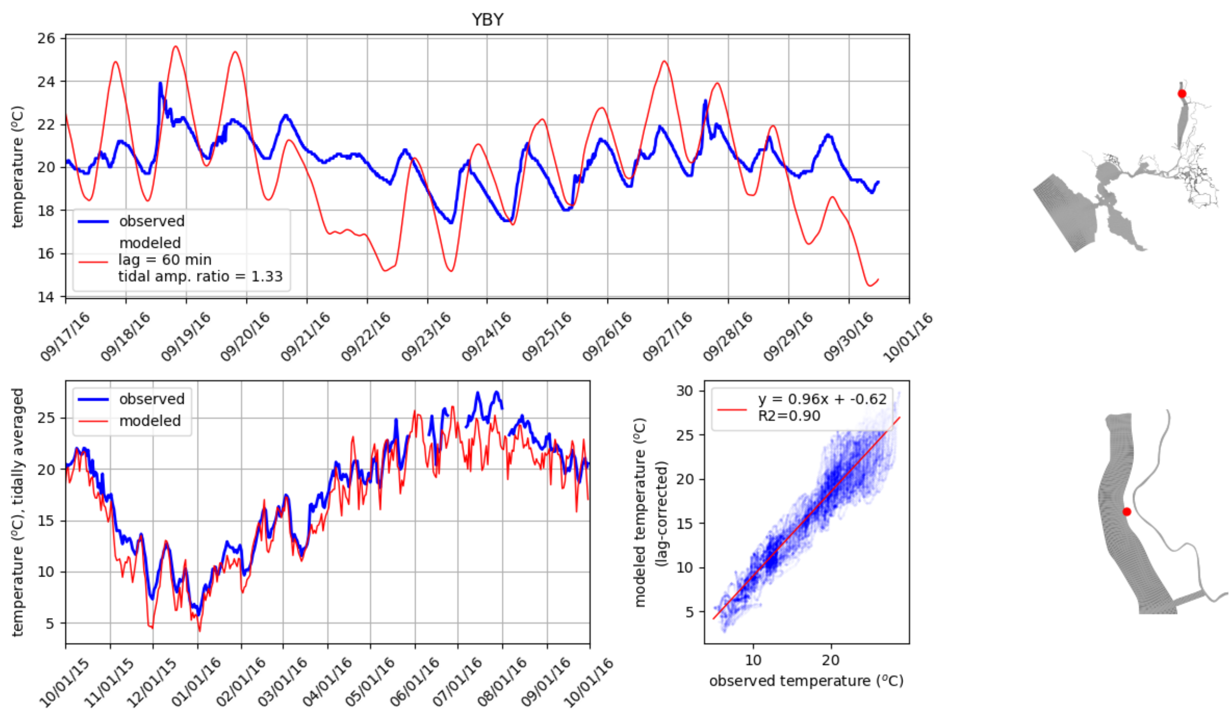

Figure 108: Comparison of modeled and observed temperatures at station YBY. Tidally averaged signals are compared over the water year in lower left panel. Unfiltered signals are compared over a two-week period in the upper panel. Lower right panel compares unfiltered signals where modeled signal has been corrected for lag. On the right, the station location is shown on the model grid.